A molecular mechanism for root thermomorphogenesis in *Arabidopsis thaliana* seedlings

Dissertation

zur Erlangung des

Doktorgrades der Naturwissenschaften (Dr. rer. nat.)

der

Naturwissenschaftlichen Fakultät III

Agrar- und Ernährungswissenschaften,

Geowissenschaften und Informatik

der Martin-Luther-Universität Halle Wittenberg

vorgelegt von

Herrn M. Sc Haiyue Ai

Geb. am 25.05.1994 in Hunan, China

Gutachter:

1. Prof. Dr. Marcel Quint
2. Prof. Dr. William Gray

29.09.2023

Halle (Saale)

Table of Contents

List of abbreviations

ANOVA   analysis of variance
ATS   *Arabidopsis thaliana* solution
BR   brassinosteroids
Col-0   Columbia-0
Fig.   Figure
IAA   indole-3-acetic acid
IPCC   Intergovernmental Panel on Climate Change
LD   long days
NAA   1-Naphthaleneacetic acid
OE   overexpression
PAR   photosynthetically active radiaiton
PEO-IAA   2-(1H-Indol-3-yl)-4-oxo-4-phenyl-butyric acid
PHYB   PHYTOCHROME B
PIF4   PHYTOCHROME INTERACTING FACTOR 4
qRT-PCR   quantitative real-time polymerase chain reaction
SD   short days
TIRE   temperature induced root elongation
TAA   TRYPTOPHAN AMINOTRANSFERASE OF ARABIDOPSIS
YUC   YUCCA
ZT   Zeitgeber time

List of figures

List of table

Abstract

Since the early 20th century, climate experts reached a consensus attributing increased earth surface temperature to human activity. Consequently, global warming's impact on crop yield losses has gained increasing attention. To cope with elevated ambient temperature, plants undergo thermomorphogenesis, with above-ground adjustments mainly involving temperature-sensitive cell elongation. However, temperature influence on root growth remains unclear. Roots, being highly plastic organs, play a crucial role in adapting to below-ground changes. Besides abiotic factors such as nutrients or mechanical force, plant roots also exhibit sensitivity to temperature variation. Below the heat stress threshold, *Arabidopsis thaliana* seedlings respond to elevated temperature by promoting primary root elongation, possibly enabling them to reach deeper soil layers with better water saturation. In this study, I propose that:

1. Roots possess an autonomous system that can sense and respond to temperature cues independently of the shoot.

2. An unidentified root thermosensor uses auxin as a messenger to convey temperature information, stimulating growth in the root apical meristem through local auxin biosynthesis and temperature-sensitive polar auxin transport. Thus, the main cellular response to increased ambient temperature varies significantly between root and shoot tissues, while the messenger auxin remains the same.

3. Additionally, a positive root thermotropic effect could only be observed in Maize but not in Arabidopsis.

Together, I present a comprehensive molecular mechanism for temperature-induced root growth that provides ample starting points for future research approaches.

KEYWORDS: thermomorphogenesis, root, auxin, cell cycle, cell division, Arabidopsis

Chapter 1: Introduction

The global average surface temperature of the earth has been steadily increasing since the dawn of industrialization, as evidenced by temperature records dating back to the 1880s. Among the past decade, 2016 stands out as the hottest year, and in 2020, it equaled the temperature record set in 2016 (Data source: NASA's Goddard Institute for Space Studies, GISS). In the 2018 report by the Intergovernmental Panel on Climate Change (IPCC), it was highlighted that if the current rate continues, the world could reach a temperature 1.5 ˚C above pre-industrial levels as early as 2030 (IPCC, 2018). This underscores the need for the plant research community and breeding companies to devote more attention to understanding the potential impact of global warming on crop production in the future. It is widely recognized that global warming will lead to significant crop yield losses (Lobell *et al.*, 2011; Challinor *et al.*, 2014), thereby increasing the vulnerability of food supply chains. Particularly when coupled with seasonal drought, global warming presents a significant threat to crop production in various regions worldwide. Considering the projected 26% increase in the global population to 9.7 billion by 2050 (World Population Prospects 2019: Highlights), farmers face an exceptionally challenging task of producing more food than ever in human being history to guarantee food security. To enable informed plant breeding approaches to generate climate-resilient crops, it is imperative to understand how elevated ambient temperatures affect plant growth and development. Using model plants like *Arabidopsis thaliana* to investigate how plants acclimate to changing ambient temperatures represents an important first step in identifying future targets for crop improvement. Therefore, understanding the molecular mechanisms underlying plant responses to high temperatures in model plants serves as a fundamental stage in the pre-breeding process, with the ultimate goal of transferring this knowledge to staple crops.

1.1 Thermomorphogenesis

In line with the principles of photomorphogenesis, which refers to light-mediated plant development and growth, the term "thermomorphogenesis" was initially coined by Stoller and Woolley (Stoller & Woolley, 1983), to describe temperature effects on plant morphogenesis. Thermomorphogenesis is an acclimation strategy that enables plants to cope with elevated ambient temperatures as they are occurring for example in the course of global warming. The primary aim of thermomorphogenic responses is to modify the plant's architecture to facilitate improved cooling of photosynthetic tissues. In Arabidopsis, high ambient temperature leads to a more open rosette structure resulting in better ventilation. Consequently, plants acclimated to high temperature display lower leaf temperatures compared to those with a compact rosette structure. Presumably, this is attributed to the evaporative cooling effect facilitated by the open rosette architecture, which promotes photosynthetic efficiency (Crawford *et al.*, 2012) (Fig. 1-1).

These architectural changes are a result of temperature-induced cell elongation, as observed in Arabidopsis hypocotyls (Gray *et al.*, 1998). In petioles, this promotion of cell elongation is more prevalent at the lower side of the petiole, resulting in hyponastic growth (upward bending of leaves). Together with general petiole elongation, hyponasty contributes to the above described open rosette structure at the maturation stage (Lippmann *et al.*, 2019) (Fig. 1-2).

2
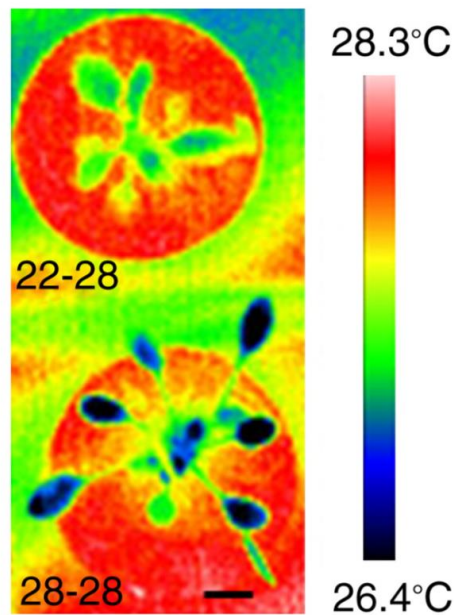
Fig. 1-1 Thermal image of 22°C–28°C (shift temperature) and 28°C–28°C (constant temperature) plants on day 3 of the transpiration experiment (Crawford *et al.*, 2012).

The upper plant acclimated for 3 weeks at 22 °C and then shifted to 28 °C, lower plant acclimated already at 28 °C.
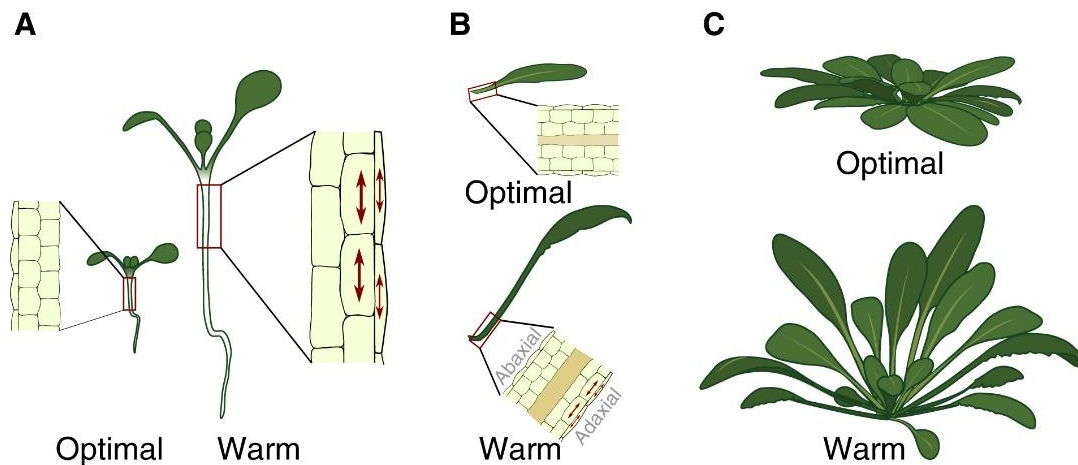
Fig. 1-2 Thermomorphogenesis during vegetative growth.

A Temperature-induced elongation of hypocotyls is caused primarily by cell elongation. **B** Thermal induction of leaf hyponasty is a result of asymmetric cell elongation in the petiole.

C Petiole elongation and leaf hyponasty result in an open rosette structure that allows efficient transpiration cooling of leaves. Red arrows symbolize cell elongation (Lippmann *et al.*, 2019).

Over the past 10-15 years, significant progress has been made by researchers in understanding temperature sensing and signaling in the shoot of plants (Quint *et al.*, 2016; Casal & Balasubramanian, 2019). Among the pathways studied, the role of phytochrome B in sensing temperature changes has emerged as the best understood and most prominent (Jung *et al.*, 2016; Legris *et al.*, 2016). At low temperatures, phytochrome B (phyB) represses the key signaling hub, a bHLH (basic helix–loop–helix) transcription factor called PHYTOCHROME INTERACTING FACTOR 4 (PIF4) (Koini *et al.*, 2009). However, this repression is relieved at high temperatures, leading to the induction of auxin biosynthesis genes by PIF4. Subsequently, auxin functions as a mobile signal, traveling from the cotyledons to the hypocotyl, where it stimulates brassinosteroid biosynthesis. Together, auxin and brassinosteroids likely contribute to cell elongation (Ibañez *et al.*, 2018; Bellstaedt *et al.*, 2019). While the signaling pathways governing shoot thermomorphogenesis have been relatively well investigated, our understanding of how roots perceive and respond to temperature stimuli remains limited.

However, similar to the shoot, roots respond to high temperature also by inducing growth (e.g., Quint *et al.*, 2005; Quint *et al.*, 2009; Hanzawa *et al.*, 2013; Wang *et al.*, 2016; Ibañez *et al.*, 2017; Martins *et al.*, 2017; Feraru *et al.*, 2019; Gaillochet *et al.*, 2020; reviewed in Fonseca de Lima *et al.*, 2021). However, unlike shoots, our understanding of the physiological basis of Temperature-Induced Root Elongation (referred to as TIRE) is relatively limited, if existent at all. TIRE may potentially coexist with drought responses, enabling plants to access water resources more effectively by exploring deeper soil layers (Martins *et al.*, 2017; Ludwig *et al.*, 2021). Nonetheless, the mechanistic understanding of TIRE is rather fragmentary. Given that roots grow

belowground, it is rather unlikely that its temperature sensitivity is, like in shoot tissues, regulated by photomorphogenesis signaling components. Root and shoot temperature sensing and signaling pathways might therefore be quite different. Several phytohormones have been postulated to play a role in temperature-responsive root growth. Although recent studies have demonstrated that auxin seems to be necessary for temperature-induced root elongation (reviewed in Fonseca de Lima *et al.*, 2021), proposed roles for brassinosteroids (Martins *et al.*, 2017), ethylene and gibberellic acid (Fei *et al.*, 2019, 2017) require additional investigation.

1.2 Molecular network of thermomorphogenic response

Shoot thermomorphogenesis is primarily mediated via PIF4, making it a central signaling hub for ambient temperature response. It functions as a key regulator in the molecular network of thermomorphogenesis resulting in several thermo-responsive phenotypes such as hyponasty, hypocotyl and petiole elongation. PIF4 plays its essential role in high temperature signaling by coordinating transcriptional changes that ultimately trigger phytohormone-induced elongation responses. In addition, *PIF4* itself is transcriptionally induced when plants are exposed to warm ambient temperature, further promoting thermomorphogenesis (Koini *et al.*, 2009; Stavang *et al.*, 2009; Sun *et al.*, 2012). Therefore, in order to avoid excessive elongation growth, precise regulation of PIF4 is necessary. This includes gene expression, epigenetic regulation, protein stability, protein sequestration, promoter acquisition, and promoter competition (Quint *et al.*, 2016) (Fig. 1-3). These intricate modifications in PIF4's activity, along with other coordinating factors, are crucial for integrating diverse environmental signals into precise growth responses.
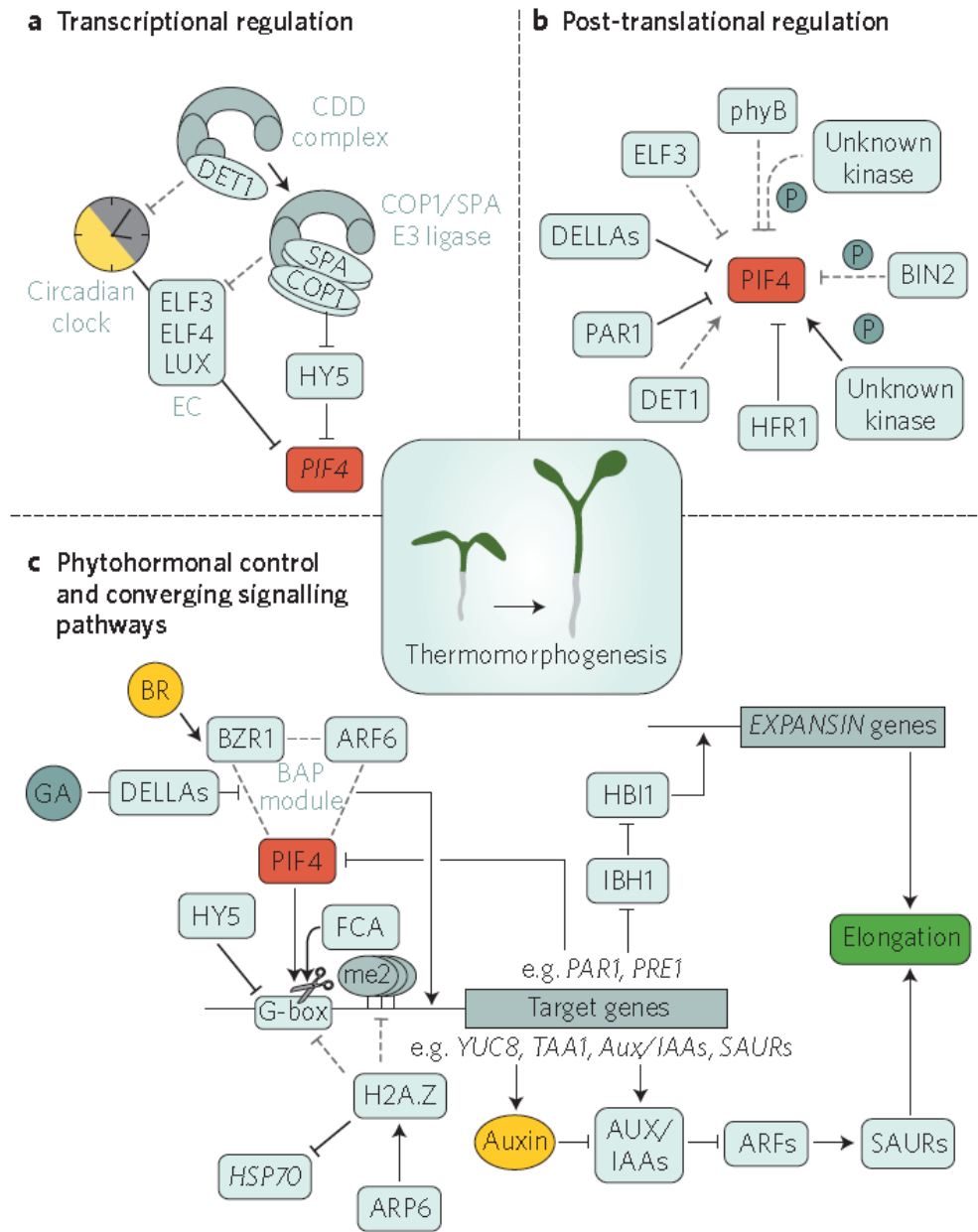
Fig. 1-3 Simplified model of the central role of PIF4 in the molecular genetic circuitries underlying thermomorphogenesis.

a, In darkness, transcriptional regulation of PIF4 involves gating by means of the evening complex (EC) of the circadian clock. In the light, transcriptional repression by HY5 is relieved by the COP1-SPA E3 ubiquitin ligase and the COP10–DDB1–DET1 (CDD) complex. **b**, PIF4 post-translational regulation contributing to temperature signaling involves phosphorylation by an as-yet unidentified kinase and sequestering of free PIF4. It remains to be established whether other PIF4-interactors/modifiers known from the light signaling context contribute to temperature signaling. **c**, PIF4 mediates transcriptional regulation of its target genes through binding to G-box promoter elements. This regulation

is counteracted by HY5, which competes for the same binding sites. In addition, FCA can attenuate PIF4–G-box binding by removing H3K4Me2 chromatin marks. Further chromatin modifications such as eviction of H2A.Z-containing nucleosomes have been shown to contribute to thermomorphogenesis. However, whether this process directly affects PIF4-target genes remains to be established. Elongation growth is subsequently triggered by PIF4-mediated induction of auxin biosynthesis and auxin signaling, resulting in SAUR-mediated elongation growth, and by a cascade involving PAR1, PRE1, IBH1 and HBI1, ultimately resulting in the induction of EXPANSIN genes. Both downstream pathways involve feedback regulations and, at least partially, the transcription factors BZR1 and ARF6 (BAP module). Other phytohormones are involved in thermomorphogenesis, with brassinosteroids (BR) and gibberellic acid (GA) having an essential or permissive signaling function, respectively, involving the DELLA repressor proteins. a–c, Mechanisms with demonstrated relevance in temperature signaling are depicted by solid black lines; connections known from other biological processes that may potentially contribute to temperature signaling are shown as dashed grey lines (Quint *et al.*, 2016).

1.2.1 Negative regulation of PIF4 at low temperatures

Transcriptional regulation of PIF4 is influenced by competition for binding sites on target gene promoters. This competition involves 'evening complex' (EC) component EARLY FLOWERING 3 (ELF3), as well as the bZIP transcription factor LONG HYPOCOTYL 5 (HY5). For example, the EC/ELF3 complex, which exhibits peak expression during the night (cold regime), modulates the circadian clock by synchronizing light signals. During this peak expression, EC/ELF3 competes with PIF4 for binding to the promoters of targets genes, including *PIF4* itself (Covington *et al.*, 2001; Nieto *et al.*, 2015). In the presence of light, HY5 suppresses the activity of PIF4. Interestingly, under low ambient temperature conditions (20°C), *hy5* mutants show an increased expression level of *PIF4* at midday, indicating a negative regulatory role of HY5 in controlling *PIF4*'s expression (Delker *et al.*, 2014).

One of the major breakthroughs in thermomorphogenesis signaling was the discovery of the first plant thermosensor. Surprisingly, the well-known photoreceptor phytochrome B (phyB) possesses a dual function and can also perceive temperature changes (Jung *et al.*, 2016; Legris *et al.*, 2016). Phytochromes have two photo-

7

convertible forms: the red light absorbing inactive Pr conformation and the far-red light absorbing and active Pfr conformation, acting as switches in response to different light spectra (Klose *et al.*, 2015). The inactive Pr form is converted into the active Pfr form by red light absorption while far-red light reverts Pfr back to Pr (Rockwell *et al.*, 2006). Interestingly, the dimerization properties of phytochromes are crucial for their action and only Pfr–Pfr homodimers are functional and able to inhibit hypocotyl growth (Klose *et al.*, 2015). The localization of phyB plays an important role, phyB localizes to the nucleus only in its active Pfr conformation, while Pr remains cytoplasmic. Pfr in the nucleus then phosphorylates PIFs which destines them for proteasomal degradation, preventing transcriptional induction of growth-promoting genes (Chen *et al.*, 2005; Franklin *et al.*, 2011). Hence, in cold temperatures Pfr suppresses PIF4 action in the nucleus, while PIF4 is derepressed upon conversion to Pr when temperature increases (reviewed in Delker *et al.*, 2017).

There are a number of additional players that negatively control PIF4 activity, sequestration, or protein levels like BRASSINOSTEROID-INSENSITIVE 2 (BIN2) or LONG HYPOCOTYL IN FAR-RED (HFR1) (Hong *et al.*, 2013; Bernardo-García *et al.*, 2014). However, since they are not in the focus of this thesis, a detailed explanation of the underlying molecular mechanism is omitted here.

1.2.2 Derepression (positive regulation) of PIF4 at high temperature

Similar to light, warm temperatures trigger Pfr to Pr transformation, referring to the exit of phyB from the nucleus. This transition allows PIF4 to access target promoters in the nucleus, leading to thermomorphogenic responses (Jung *et al.*, 2016; Legris *et al.*, 2016). Recently, two new thermosensory events have been reported (Chung *et al.*, 2020; Jung *et al.*, 2020). Jung et al. (2020) proposed that a prion-like domain (PrD) at the C-terminus of ELF3 enables plant thermo-sensing ability via liquid-liquid phase separation. At elevated temperatures, ELF3 forms liquid droplets in a PrD-dependent

manner, possibly displacing active ELF3 from the EC (evening complex) and thereby also relieving its occupation of PIF4 target gene promoters (Jung *et al.*, 2020). Another thermo-sensing mechanism involves temperature modification of RNA secondary structures. Chung et al. (2020) discovered that diurnal translation of PIF7, which is equally important for thermomorphogenesis signaling as PIF4 (Fiorucci *et al.*, 2020), responds to warmer daytime temperature by mediating conformational changes of an RNA hairpin structure within its 5 prime untranslated region, causing rapid accumulation of PIF7 protein at elevated temperature. Additionally, temperature regulation of CONSTITUTIVE PHOTOMORPHOGENESIS 1-SUPPRESSOR of *phyA-105* (COP1-SPA) module targets HY5 for proteasomal degradation, representing a positive regulation of PIF4 (Delker *et al.*, 2014).

1.2.3 Thermosignaling downstream of PIF4

PIF4-targeted phytohormone regulation is prominent in temperature-induced hypocotyl growth (Stavang *et al.*, 2009). Additionally, the involvement of auxin in mediating hypocotyl elongation in response to elevated temperatures has been well-established (Gray *et al.*, 1998). There is an increase in the levels of free indole-3-acetic acid (IAA) in shoot tissues under elevated temperatures (Franklin *et al.*, 2011; Sun *et al.*, 2012). This increase is attributed to the temperature-dependent binding of PIF4 to the promoters of specific target genes, including *YUCCA 8* (*YUC8), CYTOCHROME P450 FAMILY 79B* (*CYP79B*) and *TRYPTOPHAN AMINOTRANSFERASE OF ARABIDOPSIS 1* (*TAA1*) (Sun *et al.*, 2012). These genes are primary targets of PIF4. Supporting evidence comes from the observation of unchanged IAA levels in *pif4* mutants at higher temperatures (Franklin *et al.*, 2011; Sun *et al.*, 2012). The fluctuation of auxin levels influences transcriptional responses by perceiving auxin via TRANSPORT INHIBITOR 1/AUXIN SIGNALING F-BOX proteins (TIR1/AFBs) and AUXIN/INDOLE-3-ACETIC ACID (Aux/IAA) proteins. As a result of auxin perception, Aux/IAA proteins undergo proteasomal degradation and AUXIN RESPONSE FACTOR

(ARF) transcription factors differentially regulate genes involved in, e.g., cell elongation (Quint & Gray, 2006; see also Fig. 1-4B for detailed overview about the auxin signaling pathway). Supporting the essential role of auxin in thermomorphogenesis, Delker *et al*. (2014) demonstrated that both auxin biosynthesis and signaling mutants exhibit defects in thermomorphogenic responses. Furthermore, several auxin target genes like SMALL AUXIN UP RNA 19–24 (SAUR19–24) and SAUR61–68 subfamilies have been reported to regulate hypocotyl elongation via cell expansion (Chae *et al*., 2012; Spartz *et al*., 2014). It is important to note that unless auxin is directly synthesized in the elongating tissues, the auxin produced in response to elevated temperatures must be transported to the sites of action. Auxin transport is achieved primarily via the so called polar auxin transport machinery, which generates directed auxin maxima through PIN-FORMED (PINs) auxin efflux transporters that polarly localize to the plasma membrane side facing the auxin maximum (Fig. 1-4C). Specifically, in petioles, PIN3 has been identified as the key transporter responsible for directing auxin towards the lower side of these organs, resulting in upward leaf movement known as hyponasty (Park *et al*., 2019).

In addition to auxin, brassinosteroids (BR) and gibberellins (GA) also play fundamental roles in high-temperature-induced hypocotyl elongation (Bai *et al*., 2012). For example, BR-activated transcription factor BRASSINAZOLE RESISTANT 1 (BZR1) interacts with PIF4 to regulate hypocotyl elongation in response to high temperature (Oh *et al*., 2012). Moreover, mutants deficient in BR biosynthesis exhibit severe impairments in temperature-induced hypocotyl elongation (Gray *et al*., 1998; Ibañez *et al*., 2018), and the exogenous addition of BR inhibitor blocks temperature-responsive growth, highlighting the necessity of BR in thermomorphogenic growth (Stavang *et al*., 2009; Ibañez *et al*., 2018). In accordance with the synergistic role between auxin and BR, a recent study has demonstrated that BRs act downstream of PIF4 and auxin to regulate hypocotyl elongation, and BZR1 binds to the promoter of PIF4, enhancing its

transcription at elevated temperature (Ibañez *et al.*, 2018). GA negatively regulates DELLA proteins by inducing degradation via ubiquitin/proteasome pathway, whereas DELLA proteins block PIFs action of light signaling via to reducing GA levels (Achard *et al.*, 2007; Feng *et al.*, 2008). Detailed mutagenesis showed that GA signaling and biosynthesis are required for high temperature induced hypocotyl elongation (Stavang *et al.*, 2009). Interestingly, the DELLA–BZR1–PIF4 transcription module provides a mechanism where GA promotes hypocotyl cell elongation by involving both BZR1 and PIFs to orchestrate downstream target genes (Bai *et al.*, 2012).
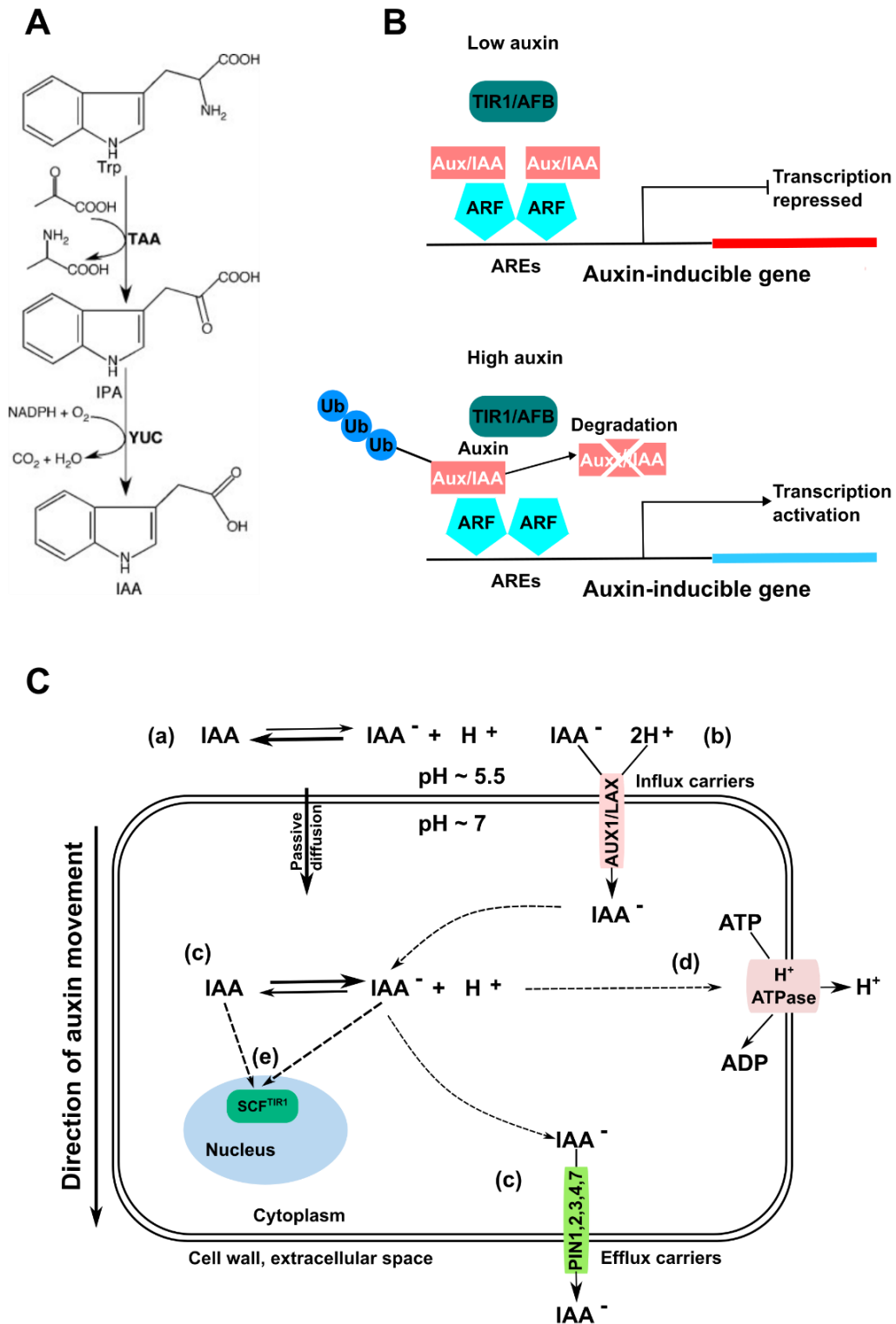
Fig. 1-4 Canonical auxin pathways

A Tryptophan-dependent auxin biosynthesis. In the initial stage, TRYPTOPHAN AMINOTRANSFERASEs (TAAs) facilitate the transfer of the amino group from

Tryptophan (Trp) to an alpha keto acid, like pyruvate, resulting in the production of IPA (indole-3-pyruvic acid) along with another amino acid. Subsequently, the second phase involves a reaction that relies on oxygen and NADPH, catalyzed by the YUC flavin-containing monooxygenases (Zhao, 2012). **B** The canonical auxin signaling pathway. In the presence of low levels of auxin, auxin-inducible genes possess specific sequences called auxin responsive elements (AREs) in their promoters. These AREs are bound by dimers of the auxin responsive factor (ARF) protein family. To prevent gene expression, Aux/IAA transcriptional repressors are recruited to these promoters through their interaction with the ARFs. This interaction leads to the recruitment of chromatin modifying enzymes (not depicted), which stabilize the repressed state of the genes. Conversely, when auxin levels are high, auxin acts as a molecular glue, facilitating the association between Aux/IAAs and F-box proteins belonging to the TIR1/AFB family. These F-box proteins are components of an SCF-type E3 ubiquitin protein ligase complex that transfers activated ubiquitin (Ub) from an E1/E2 enzyme system. The polyubiquitination of the Aux/IAAs triggers their degradation, thereby releasing the repression at promoters containing ARE sequences. **C** Auxin transport directs the auxin movement. The transport process involves both passive diffusion and the participation of specific auxin influx and efflux carriers across the plasma membrane. Undissociated molecules of auxin (IAA) are able to enter cells through passive diffusion **(a)**, while the less lipophilic and less permeable dissociated auxin anions (IAA-) are transported inside the cells through auxin influx 2H+ co-transporters belonging to the AUX1/LAX family **(b)**. In the more basic intracellular environment **(c)**, IAA dissociates and requires active transport through the PIN or ABCB efflux transporter proteins (not depicted) to exit the cell. In addition, PIN transporters are believed to rely on a maintained H+ gradient generated by the plasma membrane H+-ATPase **(d)**. Intracellular auxin binds to its nuclear receptor derived from the family of F-box proteins known as TRANSPORT INHIBITOR RESPONSE 1/AUXIN SIGNALING F-BOX (TIR1/AFB), which are subunits of the SCF E3-ligase protein complex **(e)**.

1.3 Tissue-and organ-specific responses of thermomorphogenesis

While shoot thermomorphogenesis is reasonably well understood, the mechanistic understanding of temperature-responsive root growth is less explored (Delker *et al.*, 2022) (Fig. 1-5). It is less likely that PIFs and phytochromes also regulate root thermomorphogenesis, but this remains to be tested experimentally. Since roots grow underground and are largely shielded from light, it is logical to assume that shoots and roots may exhibit different regulatory mechanisms in response to temperature stimuli. Lee et al. (2021) showed that neither expression nor the protein levels of PIF4 respond to temperature in root tissues, suggesting a PIF-independent regulation of root

13

thermomorphogenesis. Interestingly, in contrast to PIF4, HY5 seems to regulate both shoot and root thermomorphogenesis, but in in opposing ways: as a negative regulator in the shoot and a positive regulator in the root (Lee *et al.*, 2021). Furthermore, Gaillochet et al. (2020) have suggested that HY5 modulates shoot-root growth coordination during thermomorphogenesis together with PIF4 and phyB, which somewhat contradicts the above mentioned lack of function at least of PIF4. One important aspect of this study was the dependency of the root on shoot signals to respond to temperature stimuli. However, Bellstaedt et al. (2019) have shown that dissected roots can respond to temperature in the absence of any shoot tissue, indicating that the mobility of HY5 (or any other factor) in coordinating shoot and root growth may play, at most, a secondary role in root thermomorphogensis (Bellstaedt *et al.*, 2019). These spatial regulation differences between PIF4 and HY5 provide new insights into organ-specific thermo-responses, suggesting that shoots and roots may act differently in response to thermal stimuli. PILS6 (PIN-LIKES 6), a putative intracellular auxin carrier, has been proposed as a negative regulator of root growth in response to high temperature, as elevated ambient temperature destabilizes the PILS6 protein, leading to increased auxin signaling and promoting root elongation (Feraru *et al.*, 2019). In addition to auxin, other phytohormones also play important role in regulating root thermomorphogenesis (Fonseca de Lima *et al.*, 2021).
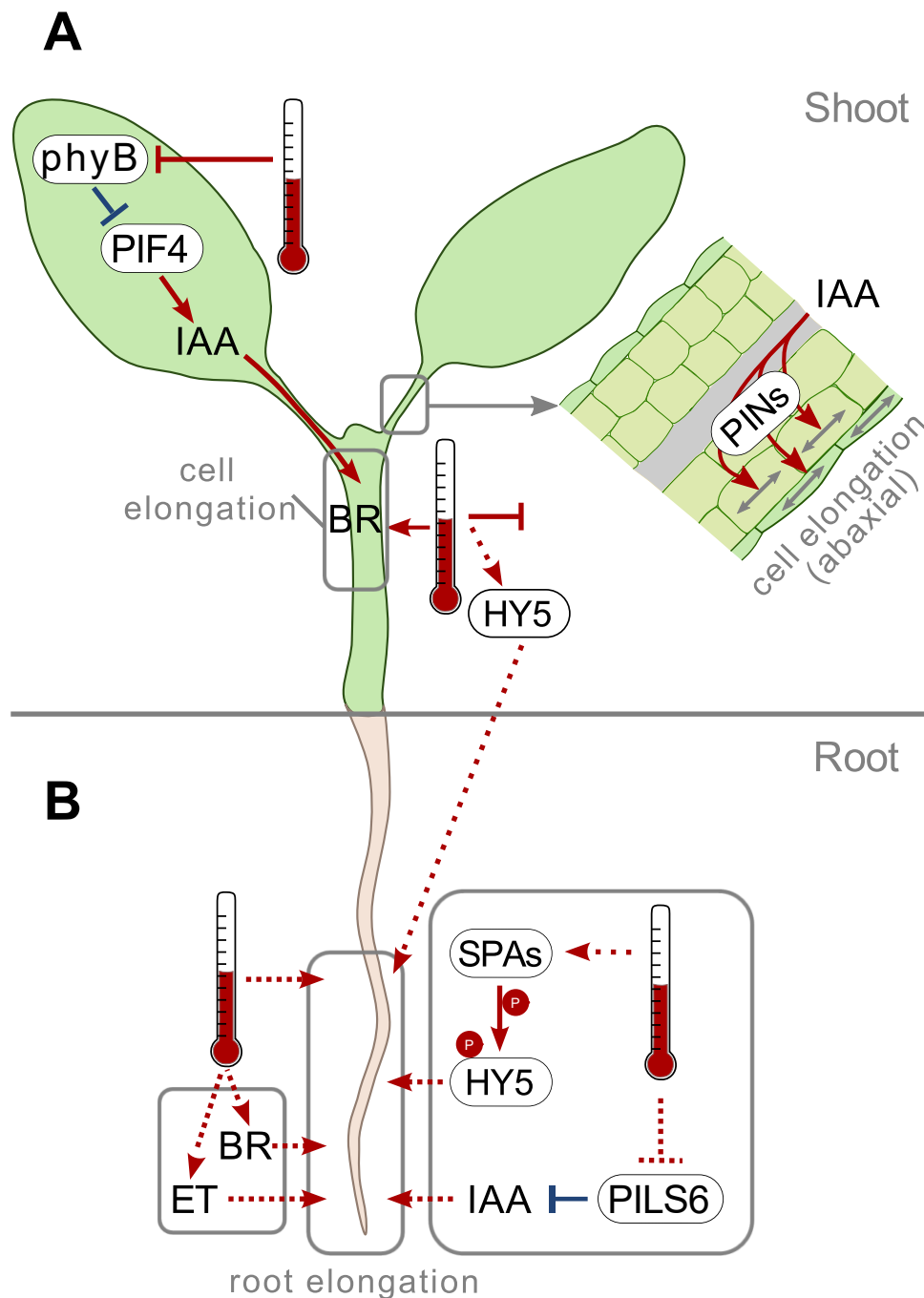
Fig. 1-5 Tissue- and organ-specific aspects of thermomorphogenesis.

A Simplified model of shoot thermo-signaling pathway as introduced in chapter 1.1. **B** In general, mechanisms involved in root thermomorphogenesis are far less understood. Apart from IAA which is induced by temperature-induced repression of PIN-LIKES 6 (PILS6), brassinosteroids (BR) and ethylene (ET) seem to contribute to temperature-induced root elongation. In contrast to its role in the shoot, ELONGATED HYPOCOTYL 5 (HY5) acts as a positive regulator of root thermomorphogenesis. HY5 is phosphorylated by

SUPPRESSOR OF PHYA (SPA) which promotes HY5 stability under warm temperatures. Red and blue colors indicate the function of components at higher or lower ambient temperature, respectively. Solid lines show experimentally verified connections, whereas dotted lines indicate that the exact mechanism or connection is not yet elucidated. (Delker *et al.*, 2022).

1.4 The basic cell cycle machinery in plants

In plants, the cell cycle machinery orchestrates the precise coordination of cell division, expansion, and differentiation, enabling the formation of intricate multicellular structures. While the effect of temperature on cell elongation seems to be the primary cellular target of shoot thermomorphogenesis, regulation of cell division may be another mechanism for growth control in response to environmental stimuli. The fundamental cell cycle machinery in plants shares similarities with other eukaryotic organisms, while also exhibiting unique features specific to plant growth and development. The plant cell cycle can be divided into distinct phases, including the G1 (Gap 1), S (Synthesis), G2 (Gap 2), and M (Mitosis) phases. Each phase is tightly controlled by a complex network of regulatory proteins and checkpoints, ensuring the accurate progression and completion of cell division (De Veylder *et al.*, 2007).

The plant cell cycle machinery comprises essential components such as cyclin-dependent kinases (CDKs), cyclins, and cyclin-dependent kinase inhibitors (CKIs: e.g., KIP-RELATED PROTEIN, ICK/KRP; SIAMESE, SIM) (Inzé & De Veylder, 2006) (Fig. 1-6). CDKs are serine/threonine protein kinases that act as central regulators of cell cycle progression. They form active complexes with specific cyclin proteins, which activate their kinase activity and facilitate the transition between cell cycle phases. CKIs, on the other hand, negatively regulate CDK activity, providing a mechanism for cell cycle control and coordination. In Arabidopsis, at least 12 CDKs and more than 49 cyclins have been reported (Vandepoele *et al.*, 2002; Wang *et al.*, 2004), reflecting their functional complexity. CDKs and cyclins are classified into various groups based on their distinctive sequence features. The major CDKs in plants are A and B-type,

which drive the cell cycle progression. A-type CDKs (CDKA) are functionally conserved and regulate the G1-S and G2-M transitions (Inzé & De Veylder, 2006). B-type CDKs (CDKB), unique to plants, play a pivotal role in determining the phase dependency of the cell cycle, with peak levels during the G2-M transition (Boudolf *et al.*, 2006). Cyclins cooperate with CDKs to regulate cell cycle progression. A-type cyclins (CYCA) are predominantly active during the S-G2-M phase. D-type cyclins (CYCD) drive the G1-S transition, while B-type cyclins (CYCB) are rate-limiting factors for the G2-M transition (Inzé & De Veylder, 2006). In response to stimuli or environmental signals, CDKA-CYCD complexes can be inactivated by CDK inhibitory proteins (ICK/KRP and SIM) (Churchman *et al.*, 2006; Verkest *et al.*, 2005).
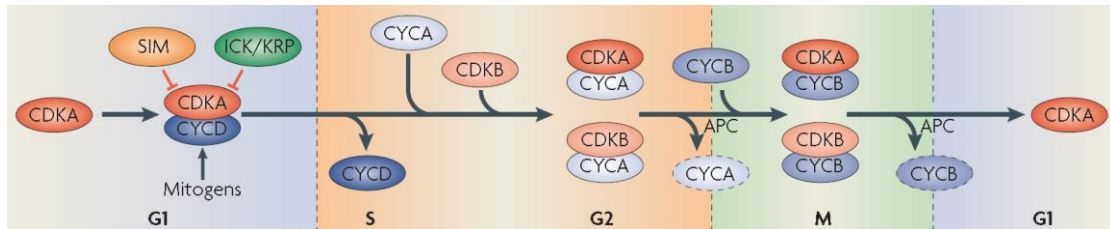
Fig. 1-6 The basic cell-cycle machinery in plants (Inzé & De Veylder, 2006).

The plant cell cycle is primarily regulated by two types of CDKs, namely A-type and B-type CDKs. CDKA controls the transition points from G1 to S phase and from G2 to M phase. CDKB, on the other hand, accumulates in a manner dependent on the cell cycle phase, reaching its peak during the G2-M transition when its activity becomes crucial. To progress through the cell cycle, the CDKs need to associate sequentially with different cyclin types. While D-type cyclins (CYCD) mainly regulate the G1-S transition, emerging evidence suggests they may also play a role in the G2-M transition. A-type cyclins (CYCA) are predominantly present from S phase to M phase, while B-type cyclins (CYCB) exhibit maximum levels during the G2-M transition and M phase. The activity of CDKA-CYCD complexes can be inhibited by associating with CDK inhibitory proteins (ICK/KRP and SIM). Additionally, the anaphase-promoting complex (APC) selectively degrades CYCA and CYCB, marking the exit from mitosis (Inzé & De Veylder, 2006).

The cell cycle in plants is tightly regulated at the transcriptional level to ensure accurate progression and regulation of cell division. Transcriptional control involves the activation or repression of specific genes encoding proteins that are essential for

17

different phases of the cell cycle.

One key group of transcription factors involved in cell cycle regulation is the E2F/DP family. E2F transcription factors, along with their dimerization partners DP proteins, control the expression of genes required for cell cycle progression and DNA replication. During the G1 phase, E2F/DP complexes are inactive due to their association with RETINOBLASTOMA-RELATED (RBR) proteins, which prevent their transcriptional activity. As cells transition into the S phase, RBR proteins are phosphorylated by cyclin-dependent kinases (CDKs), resulting in the release of E2F/DP complexes and activation of target gene expression (reviewed in Gutierrez, 2016, Fig. 1-7). In Arabidopsis, E2Fa and E2Fb are transcriptional activators, whereas E2Fc has the opposite function in repressing cell division (Sozzani *et al.*, 2006; del Pozo *et al.*, 2002). Apart from the E2F-DP family, MYB3R proteins serve as transcriptional regulators that govern the M-phase process of the cell cycle. By binding to the M-specific activator (MSA) box present in their target genes, MYB3R proteins control the expression of G2-M specific genes, ultimately influencing the determination of distinct cell fates (Ito *et al.*, 1998, 2001).

Interestingly, auxin plays a regulatory role in several cell cycle regulators. For example, auxin has been shown to transcriptionally upregulate CDKA and multiple cyclins, while it downregulates CDK inhibitory proteins from the KRP family (reviewed in Perrot-Rechenmann, 2010). Although the precise mechanisms underlying auxin-cell cycle link is still rather fragmentary, it may provide a new perspective for understanding temperature-mediated organ growth.
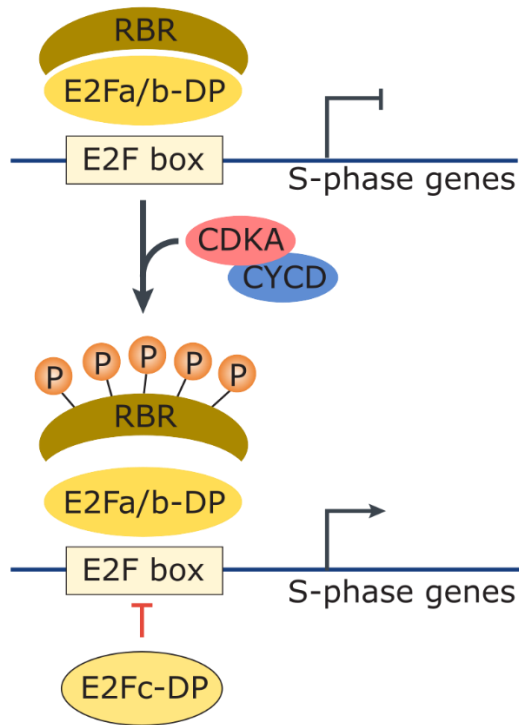
Fig. 1-7 The transcriptional control of cell cycle S-phase (De Veylder *et al*, 2007).

Plant E2Fs become activated through the phosphorylation of the RETINOBLASTOMA-RELATED (RBR) protein by CYCLIN-DEPENDENT KINASE (CDK)-D-type cyclin (CYCD) complexes. In Arabidopsis thaliana, E2Fa and E2Fb serve as transcriptional activators and positive regulators of the cell cycle, while E2Fc functions as a transcriptional repressor and suppressor of cell division. E2F target genes possess an E2F cis-acting element known as the E2F box in their promoter regions. Consequently, E2Fa, E2Fb, and E2Fc play essential roles in the G1-S transition by influencing the expression of genes involved in DNA replication, cell-cycle progression, and chromatin dynamics (De Veylder *et al*, 2007).

1.5 Objectives

As outlined in the previous introductory chapters, thermomorphogenesis sensing and signaling in shoot tissues is meanwhile reasonably well understood. The molecular mechanisms governing temperature-induced root growth are, in contrast, only poorly understood. The overall aim of my thesis is therefore to provide a general mechanistic understanding of the molecular regulation of root thermomorphogenesis. This includes the following objectives and questions to address:

1. I first ask whether roots are autonomously able to sense and respond to elevated temperatures or whether they require shoot-root long distance communication as proposed previously (Gaillochet *et al.*, 2020). On this basis, I seek to understand the following questions that will help to unravel the yet unknown above described molecular mechanism(s) and deliver a model for root thermomorphogenesis:

2. Which cellular process(es) is/are responsible for temperature-induced root elongation; is it cell elongation or cell division or a combination thereof?

3. How is temperature information tranduced from a yet unknown thermosensor to the cellular process that is target of objective 2.?

4. What is the mechanistic role of auxin in root thermomorphogenesis?

5. Lastly, I was interested to establish a methodological system to be able to study thermotropism, root growth towards or away from a temperature source, for future studies.

Together, answering these questions would help us to build a model which can serve as the basis for understanding the details of root thermomorphogenesis signaling in future studies.

Chapter 2: Material and methods

2.1 Root thermotropism: an underexplored thermo-directional root growth

2.1.1 Experimental setup of thermotropism

Arabidopsis thaliana wild type strain Col-0 and *Zea mays L.* 'Mikado' caryopses were used for experiments. Seeds were surface-sterilized, rinsed with sterile water, and then imbibed and stratified in sterile water before sowing.

For Arabidopsis, seedlings were grown on petri dishes with Arabidopsis thaliana solution (ATS) (Lincoln *et al.*, 1990) including 1 % (w/v) sucrose. Plates were then placed perpendicularly to an aluminum heating plate connected with a compact temperature-controller HT60 (Hillesheim GmbH) in a growth chamber set at 20°C for 7 days (Fig. 2-1, bottom), under long-day photoperiods (16h light/8h dark), 90 µmol m^{-2} s^{-1} photosynthetically active radiation. The heating plate was set to 35°C, which established a temperature gradient from one side of the Petri dish to the other (temperatures are indicated). After 7 days of growth, the thermo-image was captured using forward-looking infrared (FLIR) and bright field imaging. Next, the vertical growth index (VGI, defined as a ratio between root tip ordinate and root length, Grabov *et al.*, 2005) was introduced to assess the effect of thermotropism. Specifically, 5 individual roots of each picture on either hot side or cold side (Fig. 2-1, top left) were used for analysis.

Maize seeds were pre-germinated on petri dishes with ATS medium including 1% (w/v) sucrose at 28°C, 16h light/8h dark, 90 µmol m^{-2} s^{-1} photosynthetically active radiation. Plates with 1-2 cm long straight vertical radicles were selected and placed perpendicularly to an aluminum heating plate connected with a compact temperature-

controller HT60 (Hillesheim GmbH) in a growth chamber set at 20°C for 24h, under complete darkness. The heating plate was set to 45°C. Control plates (20°C) were kept in the same condition but in the absence of a heat source. At the end of each experiment, the thermo-image was captured using (FLIR) and bright field imaging. Next, the root bending angle was measured between the original root tip position (marked before heat treatment) and its final direction, relative to the gravitropic vector.
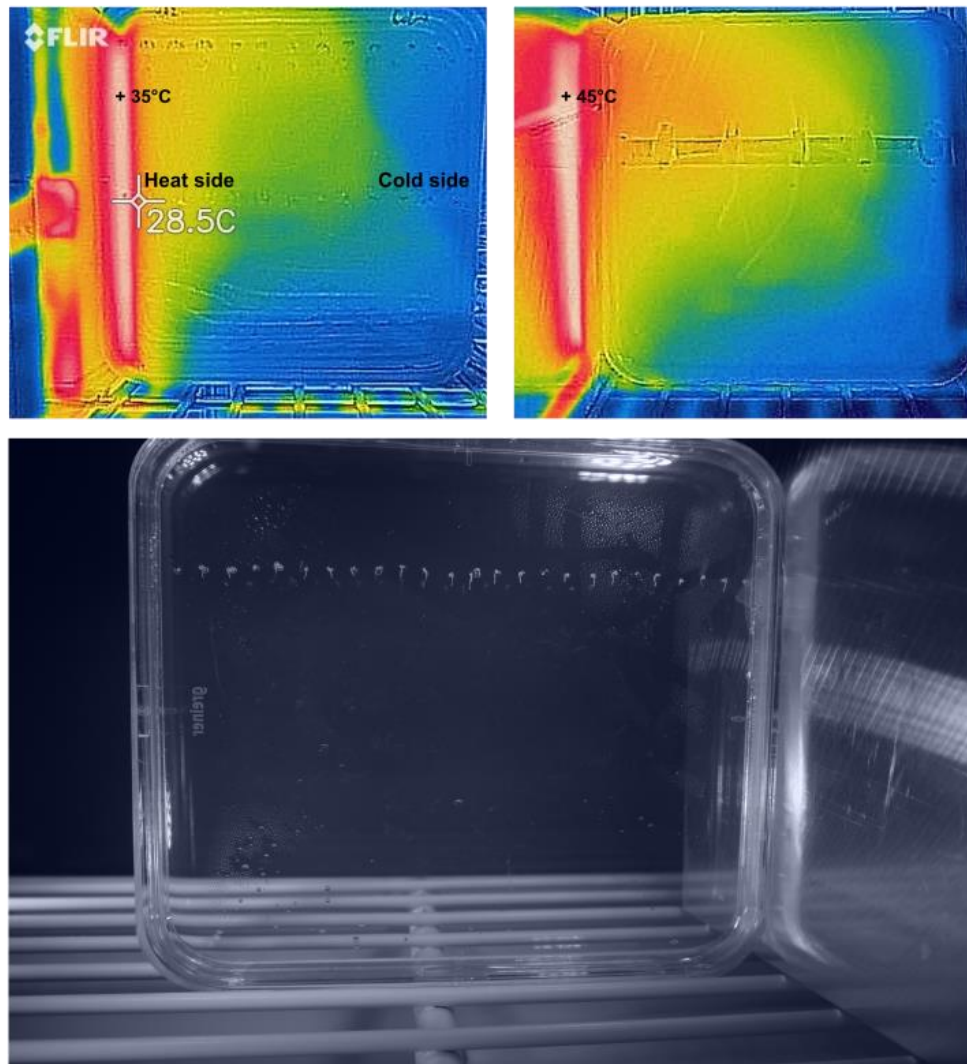
Fig. 2-1 Thermotropism experimental setup.

Top left: Representative thermo-image of Arabidopsis.
Top right: Representative thermo-image of maize.
Bottom: Image of thermotropism assay setting.

2.2 Auxin-dependent cell cycle acceleration regulates root thermomorphogenesis

2.2.1 Plant material and growth conditions

Seeds of *Arabidopsis thaliana* and all other species were surface sterilized, rinsed with sterile water, and then imbibed and stratified for 3 days at 4°C in sterile water before sowing. Wild type strains were Col-0 (N19992), and Ler-0 (NW20). Seeds from other species are designated as follows: Solanum lycopersicum (cv West Virginia 106) and Brassica oleracea (cv collard, NASC ID N29002). Unless stated otherwise, seedlings were grown on solid ATS nutrient medium (Lincoln *et al.*, 1990) including 1 % (w/v) sucrose on vertically oriented plates under long-day photoperiod (16h of light/8h of dark) with 90 µmol m^{-2} s^{-1} photosynthetically active radiation (PAR) from white fluorescent lamps (T5 4000K). *Arabidopsis thaliana* genotypes used in this study have been described previously or were obtained from the Nottingham Arabidopsis Stock Centre (NASC; http://arabidopsis.info):

Table 1 *Arabidopsis thaliana* genotypes used in this study.

Mutant abbreviation	Gene name	NASC/Salk /GK ID	Pathway	Reference
axr5-1	AUXIN RESISTANT 5	/	Auxin signaling	Yang *et al.*, 2004
cop1-6	CONSTITUTIVE PHOTOMORPHOGENIC LOCUS 1	/	Light signaling	McNellis *et al.*, 1994
cycd3;1-3	CYCLIN D3	/	Cell cycle	Collins *et al.*, 2012
cycd3;2	CYCLIN D3	/	Cell cycle	Collins *et al.*, 2012

cycd4;2-1	CYCLIN D4	Salk_0857 20c	Cell cycle	/
cycd4;2-3	CYCLIN D4	Salk_1270 16c	Cell cycle	/
cycd7;1-2	CYCLIN D7	FLAG_498 H08	Cell cycle	Weimer *et al.*, 2018
Cytrap [pHTR2::CDT1a (C3)-RFP; pAtCYCB1::AtCY CB1-GFP]	/	/	Cell cycle marker	Yin *et al.*, 2014
DR5revp:GFP	/	/	Auxin reporter	Friml *et al.*, 2003
DR5revp:SV40:3 ×GFP	/	/	Auxin reporter	Weijers *et al.*, 2006
e2fa-2	E2Fa	GABI_348 E09	Cell cycle	Berckmans *et al.*, 2011b
e2fb	E2Fb	SALK_103 138	Cell cycle	Berckmans *et al.*, 2011a
e2fc	E2Fc	GK- 718E12	Cell cycle	/
e2fab	/	/	Cell cycle	Yao *et al.*, 2018
e2fabc	/	/	Cell cycle	Yao *et al.*, 2018
eir1-1	ETHYLENE INSENSITIVE ROOT 1	/	Auxin transport	Luschnig *et al.*, 1998
elf3-1	EARLY FLOWERING 3	N3787	Circadian clock	Hicks *et al.*,

24

				1996
hy5-51	ELONGATED HYPOCOTYL 5	N596651	Light signaling	Alonso *et al.*, 2003
krp2 krp7	KIP-RELATED PROTEIN 2, 7	/	Cell cycle	genetic cross from *krp7* (Salk_1235 48) and *krp2* (Salk_0698 17)
KRP2OE (35S:HA-GFP-KRP2)	KIP-RELATED PROTEIN 2	/	Cell cycle	Noir *et al.*, 2015
KRP7OE	KIP-RELATED PROTEIN 7	/	Cell cycle	Anzola *et al.*, 2010
phyB-1	PHYTOCHROME B	/	Light/temperature signaling	Reed *et al.*, 1994
phyABCDE	PHYTOCHROME A, B, C, D, E	/	Light/temperature signaling	Hu *et al.*, 2013
pif4-2	PHYTOCHROME INTERACTING FACTOR 4	N66043	Light/temperature signaling	Leivar *et al.*, 2008
pifQ	PHYTOCHROME INTERACTING FACTOR 1, 3, 4, 5	N66049	Light/temperature signaling	Leivar *et al.*, 2008
35S::PIF4-HA	PHYTOCHROME INTERACTING FACTOR	/	Light/temperature signaling	Nozue *et al.*, 2007

	4			
pin1-1	PIN-FORMED 1	/	Auxin transport	Okada *et al.*, 1991
pin3-4	PIN-FORMED 3	/	Auxin transport	Friml *et al.*, 2003
pin4-2	PIN-FORMED 4	/	Auxin transport	Friml *et al.*, 2002a
PIN1::PIN1-GFP	PIN-FORMED 1	/	Auxin transport reporter	Benková *et al.*, 2003
PIN2::PIN2-GFP	PIN-FORMED 2	/	Auxin transport reporter	Luschnig *et al.*, 1998; Müller *et al.*, 1998
PIN3::PIN3-GFP	PIN-FORMED 3	/	Auxin transport reporter	Žádníková *et al.*, 2010
PIN4::PIN4-GFP	PIN-FORMED 4	/	Auxin transport reporter	Blilou *et al.*, 2005
tir1-1 afb2-3	TRANSPORT INHIBITOR RESPONSE 1; AUXIN SIGNALING F-BOX 2	/	Auxin signaling	Parry *et al.*, 2009
wei8-1 tar1-1	WEAK ETHYLENE INSENSITIVE 8; TRYPTOPHAN AMINOTRANSFERASE RELATED 1	/	Auxin biosynthesis	Stepanova *et al.*, 2008
YHB (P35S:AtPHYB-Y276H in phyA-	PHYTOCHROME B	/	Light/temperature signaling	Su & Lagarias, 2007

201 phyB-5)				
yucQ	YUCCA 3, 5, 7, 8, 9	/	Auxin biosynthesis	Chen *et al.*, 2014

2.2.2 Root growth assays

Seedlings were placed on ATS medium, grown at 20°C or 28°C and root length was determined 7 days after sowing (unless stated otherwise). Where indicated, plates were supplemented with various concentrations of auxin inhibitors kynurenine (He *et al.*, 2011) and yucasin (Nishimura *et al.*, 2014) or 2-(1H-Indol-3-yl)-4-oxo-4-phenyl-butyric acid (PEO-IAA, Hayashi *et al.*, 2012), N-1-naphthylphthalamic acid (NPA, Scanlon, 2003). All measurements were analyzed based on digital photographs of plates using RootDetection (www.labutils.de) and depict the total length of the root.

For detached root assays, four days-old Col-0 and *B. oleracea* seedlings, as well as 5 days-old *S. lycopersicum* seedlings grown at 20°C were dissected at the root-shoot junction to obtain roots only. The detached roots were then grown on vertically oriented ATS plates at either 20°C or 28°C for another 4 days.

2.2.3 Infrared imaging of root growth

Vertically oriented ATS plates (with two days-old seedlings grown at 20°C or 28°C) were put perpendicular to the camera, the imaging platform with infrared illumination was previously described (Anwer *et al.*, 2020) (Fig. 2-2, Panasonic G5 with hotmirror filter replaced by an IR filter, enabling only IR light to reach the sensor; www.irrecams.de). To monitor root growth dynamics, pictures were automatically taken every hour. Derived root lengths were used to calculate root growth rates.
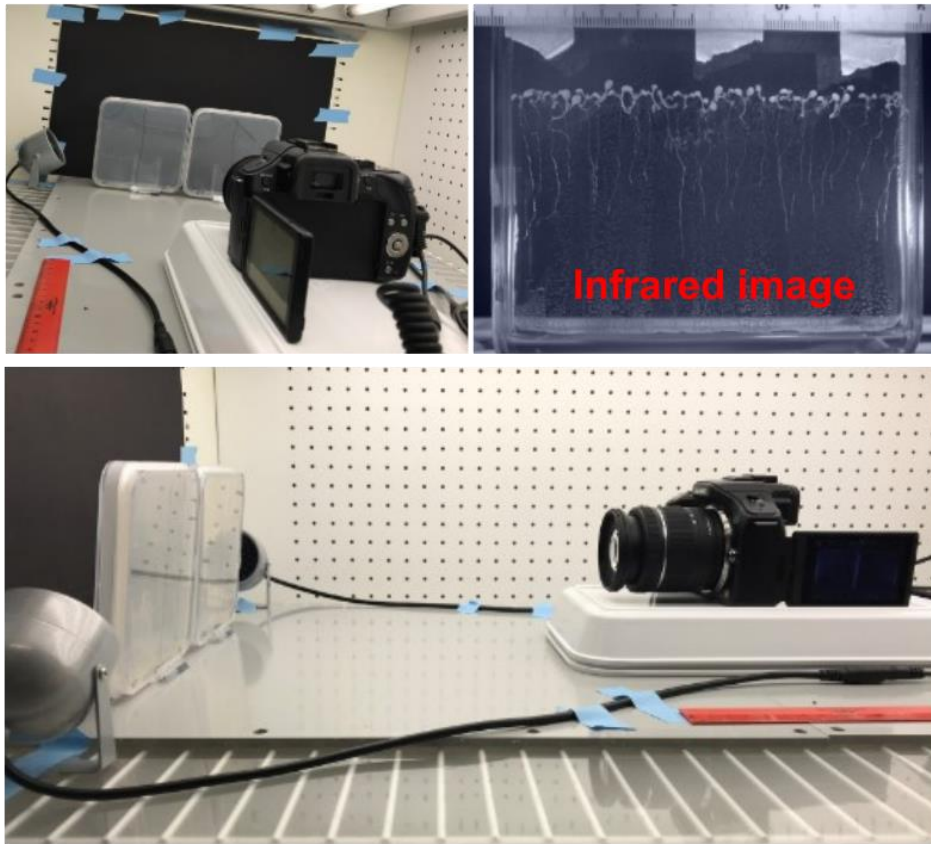
Fig. 2-2 Infrared imaging platform for root growth analysis.

Top left and bottom: Front and side view of imaging settings, respectively.
Top right: Representative picture showing root growth captured by the camera.

2.2.4 NPA treatment assays

2 mm strips of filter paper were soaked in lukewarm ATS medium (around 40°C) with or without the addition of 0.5 mM NPA (Duchefa) and carefully placed across petioles, root-shoot junction or around the root transition zone above the root apical meristem. For petiole treatments, seedlings were pre-grown at 20°C for 5 days and then for an 6additional 3 days applying NPA strips at either 20°C or 28°C, respectively. For root treatments, seedlings were grown at constant 20°C or 28°C for 5 days. Subsequently, NPA strips were applied for additional 3 days. Hypocotyl length and/or root length were

then determined using RootDetection.

2.2.5 Hypocotyl micrografting

Micrograftings have been performed by our former lab member Kai Steffen Bartusch from the Institute of Molecular Plant Biology, Department of Biology, ETH Zürich, Switzerland.

Arabidopsis grafting was performed on 7 days-old seedlings and carried out according to previously published protocols (Melnyk, 2017) and as described in (Serivichyaswat *et al.*, 2022). In brief, seeds were sown on ATS medium at 4°C darkness, stratified for two days at 4°C and then shifted to 20°C in a growth cabinet for another seven days under long-day photoperiods (16 h of light/8 h of dark) with 90 µmol m^{-2} s^{-1} white light (T5 4000K). Next, seedlings were grafted and recovered for 7 days on a water mounted filter paper/membrane. Successfully recovered grafted plants were selected, transferred to new ATS medium and cultivated at 20°C or 28°C, respectively, under the same conditions described above for another 7 days. Root growth differences were then determined by measuring root growth between day 16 and day 23. The micrografting procedure is detailed in (Fig. 2-3).
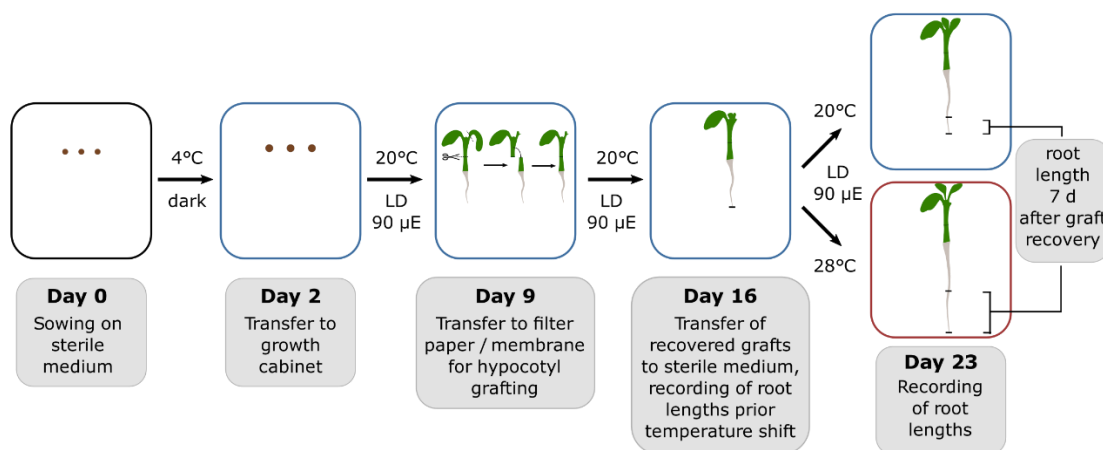
Fig. 2-3 Schematic representation of the micrografting assays (Bartusch *et al.*, 2020).

2.2.6 Measurement of cell length and cell number

Root cell measurements were conducted either by staining seedlings with Calcofluor White (Merck, 18909-100ML-F) or propidium iodide (Merck, P4170). Briefly, seedlings were fixed in pure ethanol for 2 hrs to overnight, washed twice with 1x PBS, followed by a permeabilization step using 3 % Triton X-100 + 10 % DMSO in 1x PBS for 30 min to 1 h. Next, 0.1 % Calcofluor White or 0.1 mg ml^{-1} propidium iodide in 1x PBS was freshly prepared and the seedlings were stained for 30 min or 3 min, respectively. Subsequently, seedlings were washed twice in 1x PBS with gentle shaking. To image Calcofluor White, we used 405 nm excitation and detected signals at 425 - 475 nm; for image propidium iodide, we used 488 nm excitation and detected signals at 600 - 637 nm. All measurements were performed on all individual cells of a consecutive cortex cell file using the ZEN 3.1 software (Zeiss) for 8 - 12 independent seedlings per experiment. The meristematic zone was defined as the zone between the quiescent centre and the last cell that did not yet double its size in comparison with the previous cell. The elongation zone followed the meristematic zone and was defined as the zone from the first cell with double the size of the previous cell to the last cell before root hair bulges became visible. The following differentiation/maturation zone was defined as the zone from first cell below the first trichoblast bulge to the root-shoot junction.

2.2.7 EdU staining

5-Ethynyl-2'-deoxyuridine (EdU) staining was performed with the EdU Click-488 Imaging Kit (Carl-Roth) according to the manufacturer's protocols. Briefly, 5 days-old Col-0 seedlings (at Zeitgeber time 1, ZT1, 1 h after lights on) were immersed for 1 h in liquid ATS medium containing 10 µM EdU, and fixed in 4 % (w/v) paraformaldehyde and 0.5 % Triton X-100 for 20 min. After washing twice with 1x PBS, samples were incubated in the reaction cocktail for 30 min in the dark. The reaction cocktail was then

removed, and samples were washed with 1x PBS, followed by confocal microscopy with a Zeiss LSM 780 AxioObserver (excitation wavelength: 488 nm; emission wavelength: 491-585 nm). The region of interest (root meristem) was determined with the same fixed area in all measurements, and positively stained cells were counted in this area to calculate cells per 1000 μm^2.

When stated, seedlings were co-incubated with the auxin antagonist PEO-IAA or the synthetic auxin NAA (Duchefa). Here, seedlings were stained with EdU (10 µM) + PEO-IAA (50 µM) or EdU (10 µM) + NAA (100 nM) in liquid ATS for 2-3 hrs (DSMO as mock) prior to fixation as described above.

2.2.8 DAPI staining

At ZT2 - ZT3 (2-3 hrs after lights on), 5 days-old Col-0 seedlings were fixed with pure ethanol for 2 hrs, rinsed twice with 1x PBS, followed by a permeabilization step using 3 % Triton X-100 + 10 % DMSO in 1x PBS for 30 min. Seedlings were subsequently washed three times with 1x PBS, and then stained with 100 µg mL^{-1} 4',6-diamidino-2-phenylindole (DAPI) in the dark for 15 min at room temperature, and processed under a Zeiss LSM 780 AxioObserver (excitation wavelength: 405 nm; emission wavelength: 425-508 nm). The region of interest (root meristem) was determined, and all stained nuclei in this area were counted by using the ImageJ software. The mitosis ratio was determined by counting cells in mitosis (condensed chromosomes visible) divided by all nuclei in this area.

2.2.9 Auxin reporter assay

5 days-old Col-0, *pin1-1*, *pin4-2* and/or *wei8-1 tar1-1* seedlings carrying DR5revp:SV40:3×GFP (DR5NLS::GFP) (Weijers *et al.*, 2006) reporters were fixed directly with 4 % (w/v) paraformaldehyde at room temperature, washed with 1x PBS, and kept in the dark until imaging (excitation wavelength: 561nm; emission wavelength:

31

571-615 nm). Columella cells including the quiescent center were determined as the fixed area through all measurements. Mean grey values were measured by using ImageJ.

2.2.10 IAA analytics

IAA measurements have been performed in collaboration with Gerd Balcke from the Leibniz Institute of Plant Biochemistry, Halle. Col-0 seedlings were grown for five days as described above at 20°C or 28°C. On day 5, root tips were harvested and immediately homogenized in liquid nitrogen. Extraction of indole 3-acetic acid (IAA) was done using 50 mg homogenized material and three rounds of extraction with 400 µL, 200 µL or 100 µL of 80 % methanol, which was acidified to pH 2.4 with hydrochloric acid. In order to enhance cell rupture and extraction one steel bead of 3 mm, three steel beads of 1 mm diameter, and glass beads of 0.75 to 1 mm diameter (Carl Roth GmbH) were added to each sample and bead milling was performed for 3 x 1 min in a homogenizer (FastPrep24, MP Biomedicals). The combined extracts were centrifuged and stored on ice until measurement on the same day.

IAA was separated on a Nucleoshell RP Biphenyl column (100 mm x 2 mm, 2.1 µm, Macherey und Nagel, Düren, Germany) with the following gradient: 0-2 min: 95 % A, 5 % B, 13 min: 5 % A, 95 % B, 13-15 min: 5 % A, 95 % B, 15-18 min: 95 % A, 5 % B. The column temperature was 40°C, solvent A was 0.3 mM ammonium formate, acidified with formic acid to pH 3.0, solvent B was acetonitrile. The autosampler temperature was maintained at 4°C. Per sample 600 µL of plant extract was injected to a divinylbenzene stationary phase micro-SPE cartridge (SparkHolland B.V., Emmen, The Netherlands) at a rate of 200 µL min^{-1} where IAA is trapped by simultaneous addition of excess water (3800 µL min^{-1}). Transfer from the SPE cartridge to the UPLC column was accomplished by 120 µL 20 % acetonitrile under continuous dilution with water, which gave with a final share of 2.5% acetinitrile on-column. The entire

procedure was conducted on a prototype device consisting of a CTC Combi-PAL autosampler equipped with a 1 mL injection loop, an ACE 96-well plate SPE unit, a high-pressure dispenser, a SPH1299 UPLC gradient pump, an EPH30 UPLC dilution pump and a Mistral column oven (all AxelSemrau GmbH, Sprockhövel, Germany).

Mass-spectrometric detection of IAA on a QTrap 6500 (Sciex) was accomplished by electrospray ionization in positive mode and multiple reaction monitoring (MRM). IAA quantification was made based on transition 176/130 and was confirmed by transition 176/103 using these parameters: declustering potential: 81 V, collision energy: 27 and 46 V, cell exit potential: 8 and 11 V, respectively. For this, the ion source was heated to 450°C. Curtain gas 35 psi, ion source GS1 was set to 60 psi, GS2: 70 psi, the electrospray ion spray voltage was 5500V. IAA quantification was performed based on authentic IAA (Olchemin, Olomouc, Czech Republic).

2.2.11 Confocal microscopy of PIN-GFP reporters

These experiments have been performed in collaboration with Tonni Grube Andersen from the Max Planck Institute for Plant Breeding Research, Cologne.

Plants were stratified at 4°C for two days, grown on standard ½ MS media (Murashige & Skoog, 1962) containing 1 % sucrose in a 16/8 hrs light/dark cycle at 20°C or 28°C for five days. For short term 20°C → 28°C shift experiments, plants grown at 20°C were incubated for an additional 4 hours at 28°C. All plants were fixed and cleared using a previously established Clearsee-based protocol (Kurihara *et al.*, 2015) modified to include Calcofluor White for staining of cell walls (Ursache *et al.*, 2018). Briefly, plants were fixed in 4 % paraformaldehyde in 1x PBS for 1 h followed by three brief washes in 1x PBS and incubated overnight in Clearsee solution containing Calcofluor White. Images were acquired on a Zeiss LSM-980 confocal system equipped with an Airyscan 2 detector using either a 40x (1.0 NA) water immersion

objective or a 63x (1.4 NA) oil immersion for Airyscan images. Calcofluor White signal was detected using a 405 nm laser for excitation and an emission window from 420 - 430 nm. For GFP, excitation was achieved using a 488 nm laser and the emission window was 500 - 525nm. All images were acquired as non-saturated 16-bit sequential scans for further quantification. The basal-to-lateral GFP signal in the cortical cell file was determined where indicated. GFP signal intensity was measured by using ImageJ software, and at least ten meristems cortical cells per seedling were measured.

2.2.12 RT-qPCR expression analyses

Col-0 seedlings were cultivated at either 20°C or 28°C for 5 days in long-day photoperiods (16/8 h) in 90 µmol $m^{-2}s^{-1}$ PAR. Seedlings were harvested at ZT1 and dissected by cutting off whole roots or root tips to perform expression analyses. Total RNA was extracted from three biological replicates using the NucleoSpin RNA Plant Kit (Macherey-Nagel). First-strand cDNA was synthesized using the PrimeScript RT Reagent Kit (Perfect Real Time) from Takara Bio. qPCR analyses were performed on an AriaMx Real-Time PCR System (Agilent) using Absolute Blue Low Rox Mix (Thermo Fisher Scientific). *At1g13320* was used as a reference gene (Czechowski *et al.*, 2005) to calculate relative expression values (2^{DCt} values). Oligonucleotide primers used in the analysis are listed as follow: At1g13320_F ACACAAGGTTCACAATCCGTG; At1g13320_R CATTCAGGACCAAACTCTTCAGC; PIN1-RT-F GGAGACTTAAGTAGGAGCTCAGCA; PIN1-RT-R CCAAAAGAGGAAACACGAATG; PIN2-RT-F:GGTTGAAGCTTGAAGGTAGTCGC; PIN2-RT-R TGAAATGTTTCTTTCTCCACGCA; PIN3-RT-F CGGCTCCGAATCCAGAGTT; PIN3-RT-R ATGGCTGTTTGACTTGCCGC; PIN4-RT-F CAACCCAAAATCATTGCTTGTG; PIN4-RT-R CGGACCGGTTATAAATCTGACC

Chapter 3: Results

As it was rather a side project, I would like to start the *Results* section of my thesis with a classic physiological response that is, however, difficult to approach experimentally, and therefore largely lacks mechanistic understanding. Thereafter, I will turn to the focus of my thesis project, the understanding of the molecular regulation of root thermomorphogenesis.

3.1 Root thermotropism: an underexplored thermo-directional root growth[1]

Plants constantly encounter fluctuations in ambient temperatures, and since they cannot internally regulate their temperature, they have evolved acclimation mechanisms to adapt to a wide range of temperature conditions, from freezing to heat stress. One scenario of growth response that plants utilize when exposed to varying environmental temperatures is called thermotropism, where directional growth occurs in response to directional temperature cues. The objective of this chapter is to propose an experimental approach that can facilitate mechanistic research on thermotropic responses in plants. It is important to note that while both thermotropism and thermomorphogenesis involve thermosensing and signaling events, they may be regulated through different mechanisms.

To investigate thermotropism, I established an experimental setup with a device that can introduce a temperature gradient perpendicular to the petri dish (Fig. 2-1). This configuration allowed me to quantify the positive (thermo-engaging) or negative (thermo-avoiding) tropism effects exhibited by plants growing on agar-based petri dishes at specific temperatures. The main objective was to determine whether temperature could induce a deviation from the gravitropic growth angle, either towards or away from the heat source, thus demonstrating a thermotropic response in

---

[1] The data in this chapter have been published in van Zanten et al., 2021

Arabidopsis. I therefore tested seedlings grown in constant 20°C for 7 days, while exposing them to a temperature gradient perpendicular to their root elongation axis. I observed minimal impact on the gravitropic deviation of the roots, as indicated by the vertical growth index, regardless of the distance between the plants and the heat source (Fig. 3-1A-B, E). Hence, I concluded that under our conditions, Arabidopsis roots do not display directional growth patterns in response to different temperatures. Building upon the findings of Fortin and Poff (1990), who reported positive thermotropism in maize, I proceeded to adapt our experimental setup for studying maize. Following the methodology outlined in their study (Fortin & Poff, 1990), with slight modifications to our heating setup, I conducted experiments. Consistent with their observations, I likewise observed positive thermotropism in maize roots (Fig. 3-1C-D, F).

In summary, despite several notable early studies that have demonstrated the directional responses of plants to temperature (both positive and negative thermotropism), the molecular mechanisms underlying these processes remain largely unexplored. This knowledge gap presents an exciting opportunity for future research to delve into the distinct characteristics and underlying mechanisms of thermotropism compared to thermomorphogenic growth. Notably, investigating the mechanisms driving positive thermotropism in maize holds particular interest, given the availability of diverse genetic tools such as mutants and reporter lines (e.g., auxin-responsive lines) that can be employed in maize research. Addressing these questions could significantly advance our understanding of thermotropism and its unique features.
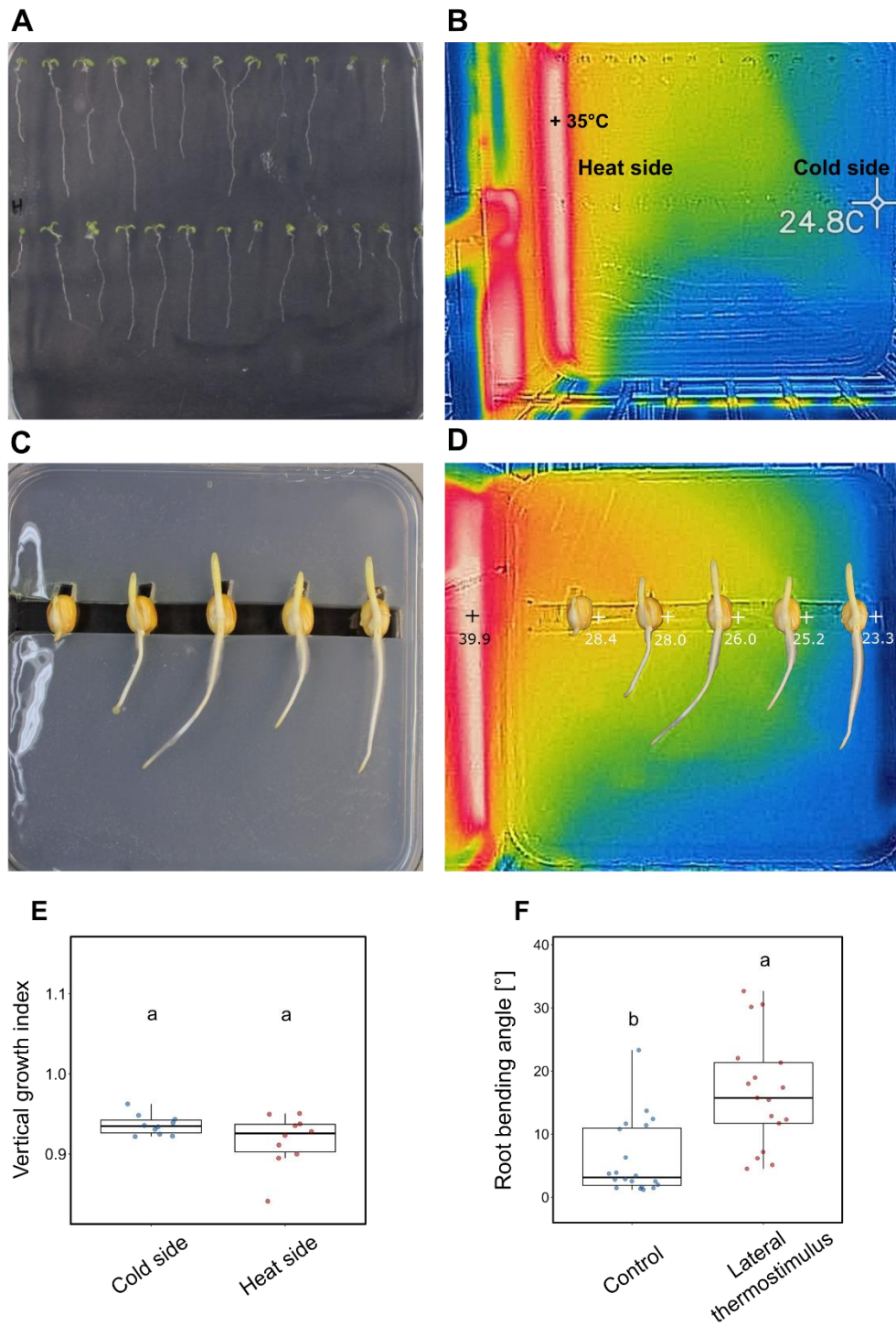
Fig. 3-1 Thermotropism effect in Arabidopsis and Maize.

A, C Represetative bright field image of Arabidopsis seedlings grown for 7 days in LD (A) and maize seedling grown for 24h in darkness (C) with a decreasing temperature gradient

from left to right perpendicular to the root axis. **B, D** Thermo-image of A and C. **E** Quantification of A as assessed by VGI (vertical growth index). For each picture, the mean VGI of 5 individual roots at either the cold or the heat side was calculated, n = 10. **F** Quantification of C, control plants were put in the 20°C chamber without lateral heating treatment, each individual root bending angle was measured, n > 17. Boxplots show medians, interquartile ranges and min -max values. Individual data points are superimposed as colored dots. Different letters denote statistical differences at P < 0.05 as assessed by two-way ANOVA and Tukey's HSD *posthoc* test.

3.2 Auxin-dependent cell cycle acceleration regulates root thermomorphogenesis[2]

In this study, I aimed to elucidate the molecular mechanism that is responsible for TIRE. Together with my collaborators, I show that although the messenger auxin delivering temperature information from a thermosensor to the cells appears to be the same, the cellular process enabling thermo-responsive root growth differs fundamentally from the one regulating thermomorphogenesis in above-ground tissues.

3.2.1 Root growth dynamics in response to different temperatures

Based on recently published work from other laboratories (e.g., Martins *et al.*, 2017; Feraru *et al.*, 2019; Gaillochet *et al.*, 2020; Lee *et al.*, 2021) and our own previous comprehensive phenotypic analysis (including root growth) of various Arabidopsis accessions grown at different ambient temperatures (Ibañez *et al.*, 2017), I sought to better understand how temperature specifically affects root growth. In the temperature range investigated (20°C *vs.* 28°C), elevated ambient temperature obviously promoted primary root elongation in the *Arabidopsis thaliana* accession Col-0 (Fig. 3-2 A-C), but also across species (Fig. 3-2 D-E), demonstrating that temperature-induced root elongation is a universal response. Daily measurements of root length in *Arabidopsis thaliana* suggested that growth differences were absent during the first four days of cultivation (Fig. 3-2B). To substantiate this observation, I conducted continuous and real-time monitoring of seedlings between days 2 and 7 after germination. Using infra-red imaging, I was able to document the growth behaviour on an hourly basis, even in darkness. Consistent with the endpoint analysis illustrated in Fig. 3-2B, I observed significant variations in growth rates only after day 4 (Fig. 3-2C). Regardless of temperature, the root growth rates exhibited significant diurnal fluctuations (Fig. 3-2C). Within the context of the long day photoperiods implemented, the root growth rates demonstrated an increase during the late afternoon, reaching their peak at the end of

---

[2] The data presented in this chapter have been published in Ai et al., 2023. Data that have been generated by collaborators are indicated in the corresponding figure captions.

the night. Notably, this pattern corresponded to the high temperature-driven hypocotyl growth observed in the same plants (Fig. 3-2F). These findings indicate that (under our conditions) root growth rates experience an early acceleration during seedling development, while temperature sensitivity of growth rates appears to be gated in the initial few days of seedling growth.
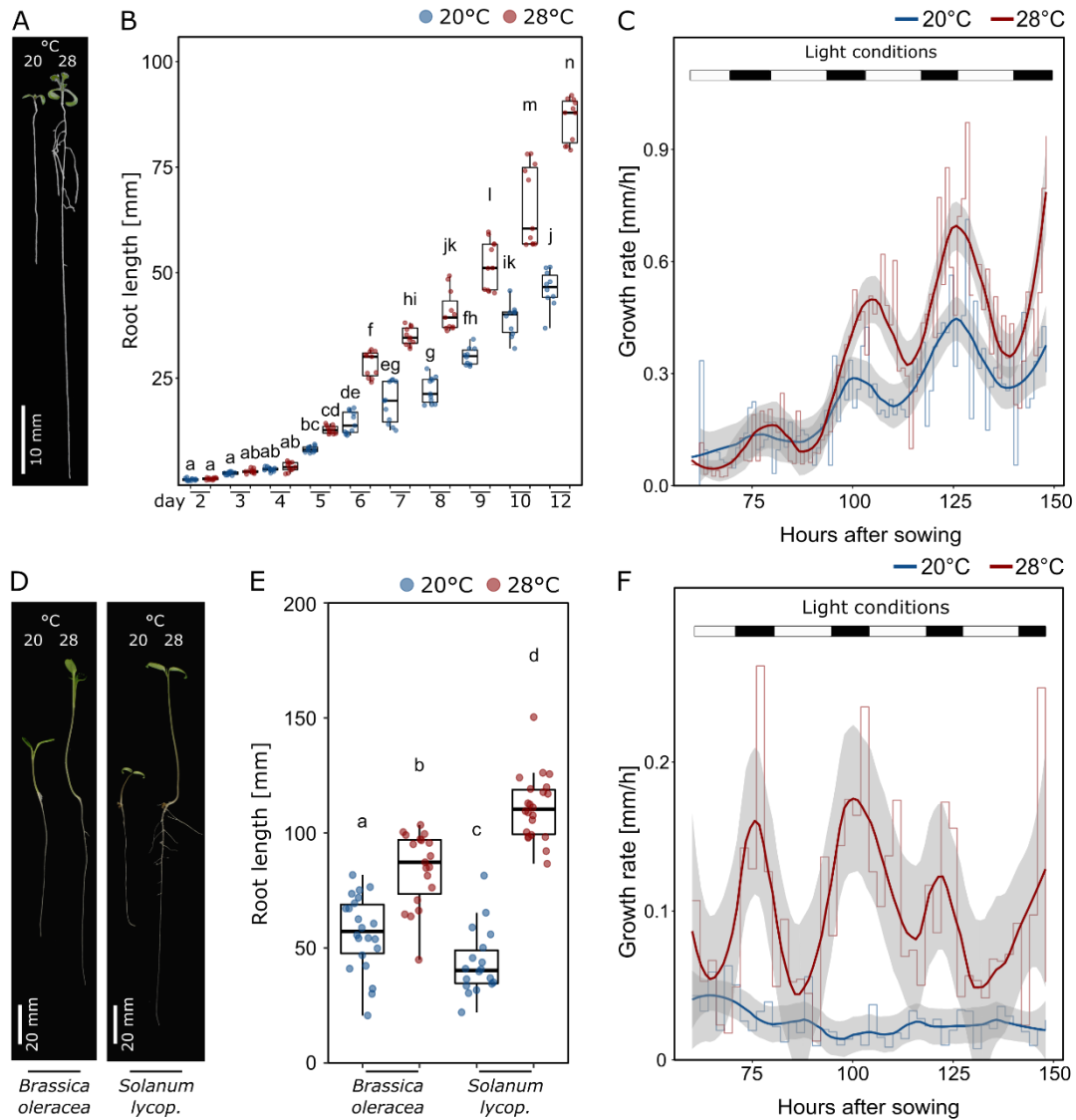
Fig. 3-2 Root growth dynamics in response to different temperatures.

A Arabidopsis seedlings grown for 7 days in LD at 20°C or 28°C. **B** Root lengths of seedlings from day 2 to day 12 after sowing (grown as in A). **C** Root **F** hypocotyl growth

40

rates of seedlings between days 2-7 were assessed by hourly infra-red real-time imaging. Mean growth rates are shown as step-wise lines (n = 8) that were fitted with a smoothing function ("loess") shown as solid lines and the respective 95% confidence intervalls shown as grey ribbons. **D** Seedlings of *Brassica oleracea*, *Solanum lycopersicum* (lycop.) grown for 7 days at 20°C or 28°C. **E** Root lengths of 7 days old seedlings grown at 20 or 28 °C (n = 18-22). B+E Boxplots show medians, interquartile ranges and min-max values with individual data points superimposed as colored dots. Different letters denote statistical differences assessed by 2-way ANOVA and Tukey's HSD, P< 0.05.

3.2.2 Autonomous root temperature sensing and response

We had previously suggested that roots are able to autonomously sense and respond to temperature without the need for shoot-derived signals (Bellstaedt *et al.*, 2019). However, Gaillochet *et al.* (2020) proposed the necessity of shoot-to-root communication for root thermomorphogenesis. To revisit this question and to assess whether or not the root response requires such long-distance signals from a temperature-sensing shoot, I first tested temperature-induced root elongation assays with excised roots (only the root, no shoot attached) in Col-0. Confirming previously published data from our lab (Bellstaedt *et al.*, 2019), I found that detached roots were not only able to continue growing in the absence of shoot tissue, but actually elongated more at 28°C than at 20°C (Fig. 3-3A), suggesting that roots can be regarded as autonomous in terms of sensing and responding to temperature signals. This behaviour was similar in *Brassica oleracea* and *Solanum lycopersicum* (Fig. 3-3A), indicating its conservation across species.

As this assay is rather rude, I next performed an also invasive but certainly less rude hypocotyl micrografting assay to substantiate these results, also in different genetic backgrounds. Here, a shoot mutant that is unable to transduce temperature cues would be informative, as in such a genetic background the relay of temperature-induced signals from the shoot to the root is unlikely. For these experiments, we first used the essentially temperature-blind quadruple *pifQ* (*pifQ = pif1-1 pif3-7 pif4-2 pif5-3*) mutant. Fig. 3-3B shows that all possible *pifQ*/wt scion > rootstock combinations showed a wild-

type-like root elongation in response to elevated temperature. This behaviour was, not surprisingly, reflected by a *pif4-2* single mutant (Fig. 3-3C). Likewise, *hy5-51* mutant shoots on wild-type rootstocks behaved like wild type, arguing against a role for shoot-localized or shoot-derived HY5 in root thermomorphogenesis (Fig. 3-3D). Only *hy5-51* self-grafts showed slightly shorter roots at both temperatures, which might be consistent with the decreased temperature response of intact *hy5-51* seedlings (Fig. 3-3D and Lee *et al.*, 2021; Gaillochet *et al.*, 2020). The only line with a potential shoot-to-root effect in these experiments was the shoot thermosensory mutant *phyB-9*. While wild-type shoots on *phyB-9* rootstocks did not differ from the wild type, graft combinations including *phyB-9* shoots displayed significantly shorter roots at high temperature when compared to graft combinations with wild-type shoots (Fig. 3-3E). However, these graft combinations were still able to respond to the temperature stimulus, suggesting only a minor role in this process. It should be noted that the growth conditions and times required for grafting assays (Fig. 2-3) differ from the experimental setup for intact seedlings. This, together with the still invasive nature of micrografting and some hypocotyl tissue remaining with the rootstock, should be taken into account when interpreting these data. Furthermore, I am aware that at this point there is no true negative control available showing a severe root elongation defect in response to temperature. In conclusion, although a shoot-derived function of phyB cannot be ruled out, the thermoresponsive behaviour of micrografted seedlings with thermosensing/-signaling defective scions on wild type rootstocks largely supports an autonomous character of roots in terms of their capability to sense and respond to elevated ambient temperature.
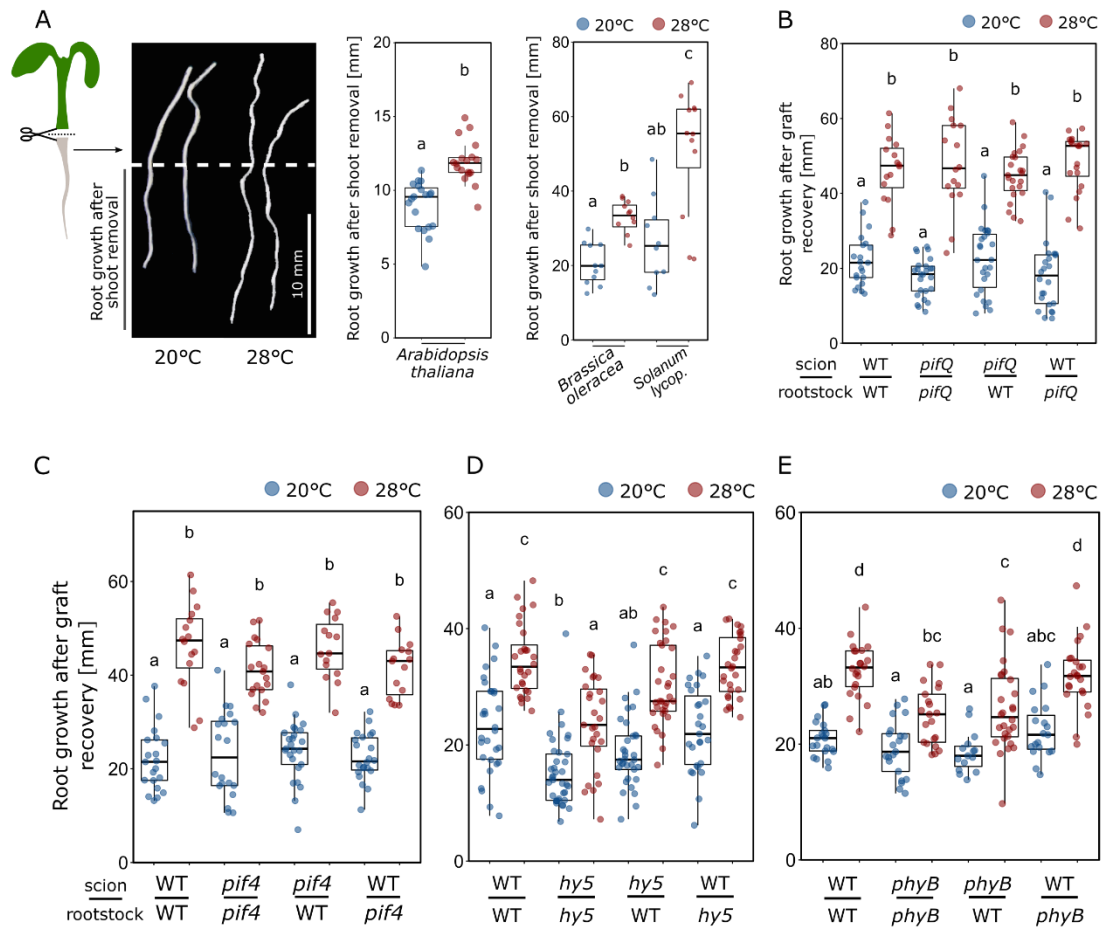
Fig. 3-3 The root is able to autonomously sense temperature and respond to it.

A Elongation responses of detached roots. Shoots were removed from 4 days-old *Arabidopsis thaliana* (n = 18-19), 4 days-old *Brassica oleracea* (n = 11) and 5 days-old *Solanum lycopersicum* (lycop., n = 10-12) seedlings grown at 20°C. Detached roots were grown for additional 4 days at 20°C or 28°C , scale bar = 10 mm. **B-E** 9 days-old seedlings were hypocotyl-grafted, recovered for 7 days and then cultivated at 20°C or 28°C for additional 7 days (n = 16-26). Grafting data in B-E have been generated by Kai Steffen Bartusch, ETH Zürich. **A-E** Boxplots show medians, interquartile ranges and min-max values with individual data points superimposed as colored dots. Different letters denote statistical differences at P < 0.05 as assessed by one-way (A, Arabidopsis) or two-way (A-E) ANOVA and Tukey's HSD *posthoc* test.

In intact seedlings I found that none of the shoot thermomorphogenesis mutants tested (*phy* loss- and gain-of-function lines, *cop1-6*, *elf3-1*, *pif* loss-of-function and overexpression lines) showed a root response defect that was remotely reminiscent of

their severe shoot phenotypes (Fig. 3-4A, B; Delker *et al.*, 2014; Jung *et al.*, 2016; Legris *et al.*, 2016). Although there were statistically significant differences for selected mutant lines in comparison to the wild type (see also Gaillochet *et al.*, 2020), these differences were mostly subtle. All lines tested were obviously still able to sense elevated temperatures and respond by promoting root growth. Again, the lack of a temperature-unresponsive root mutant complicates the interpretation of these data, as such a negative control is not available. However, It has to be noted that others have provided solid evidence, suggesting that at least HY5 seems to play a role in root thermomorphogenesis (Gaillochet *et al.*, 2020; Lee *et al.*, 2021). Taken together, with the expectation of severe phenotypes in loss-of-function backgrounds of key signaling components, I conclude so far that roots are able to sense and respond to temperature autonomously, most likely via a signaling pathway different from that regulating the shoot temperature response. While a role for phytochrome-dependent thermosignaling, which dominates shoot thermomorphogenesis, cannot be generally ruled out, this role is likely to be secondary or indirect in thermoresponsive root growth.
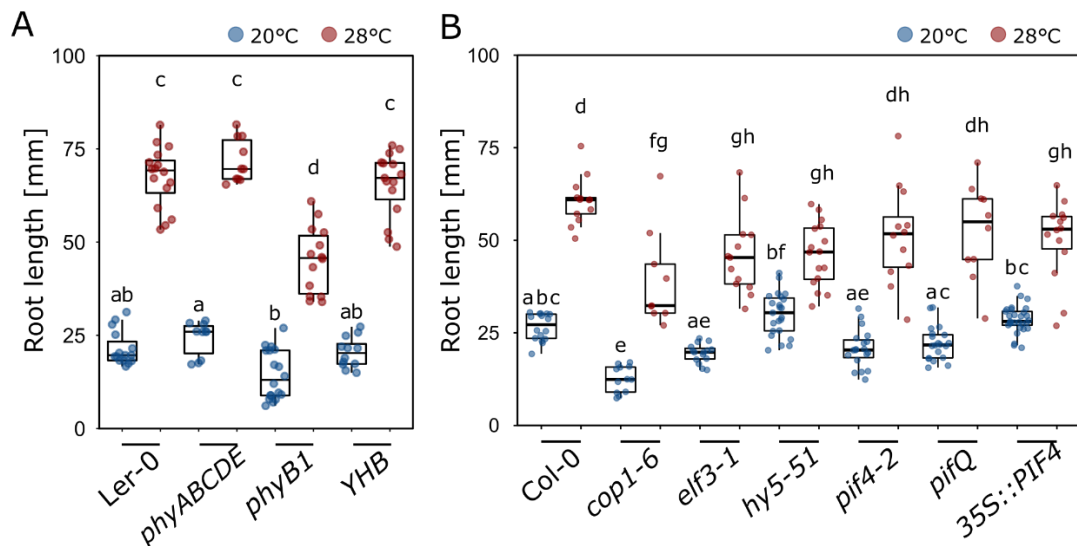
Fig. 3-4 Shoot temperature signaling genes play non-essential role in root thermomorphogenesis.

A-B Temperature-induced root growth assay of seedlings grown for 7 days (A, n = 10-18,

B, n = 9-29). Boxplots show medians, interquartile ranges and min-max values with individual data points superimposed as colored dots. Different letters denote statistical differences at $P < 0.05$ as assessed by two-way ANOVA and Tukey's HSD *posthoc* test.

3.2.3 Cell cycle characteristics during temperature-induced root elongation

Theoretically, temperature-induced primary root elongation could be a consequence of temperature-promoted cell elongation (as in the shoot), temperature-promoted cell division, or a combination thereof. To assess the potential of both processes, we first compared the number of hypocotyl or radicle/root cells in mature embryos *vs.* 7 days-old seedlings (Col-0). We observed that the number of cortical hypocotyl cells along a longitudinal cell file from the root-shoot junction to the shoot apical meristem was only marginally greater in seedlings compared to mature embryos, with a significant but minor temperature effect (Fig. 3-5A). This incremental production of hypocotyl cells during early seedling development practically leaves only cell elongation as the primary mechanism of vertical organ growth in response to warmth, while cell division can likely be neglected. In roots, the picture changed dramatically. The embryonic radicle consists of only a few cells, whereas cell division generates hundreds of new root cells post germination along a longitudinal cell file (Fig. 3-5B), and therefore thousands in the whole 3-dimensional root. Furthermore, the number of root cells continued to increase at 28°C. This suggests that cell division contributes substantially to thermo-responsive root growth. I therefore next investigated cellular growth patterns by counting and measuring root cells along a longitudinal cell file from the quiescent center to the root-shoot junction in wild-type (Col-0) seedlings grown at different temperatures. Fig. 3-5D shows temperature dependency of cell proliferation and its consequences for root elongation.
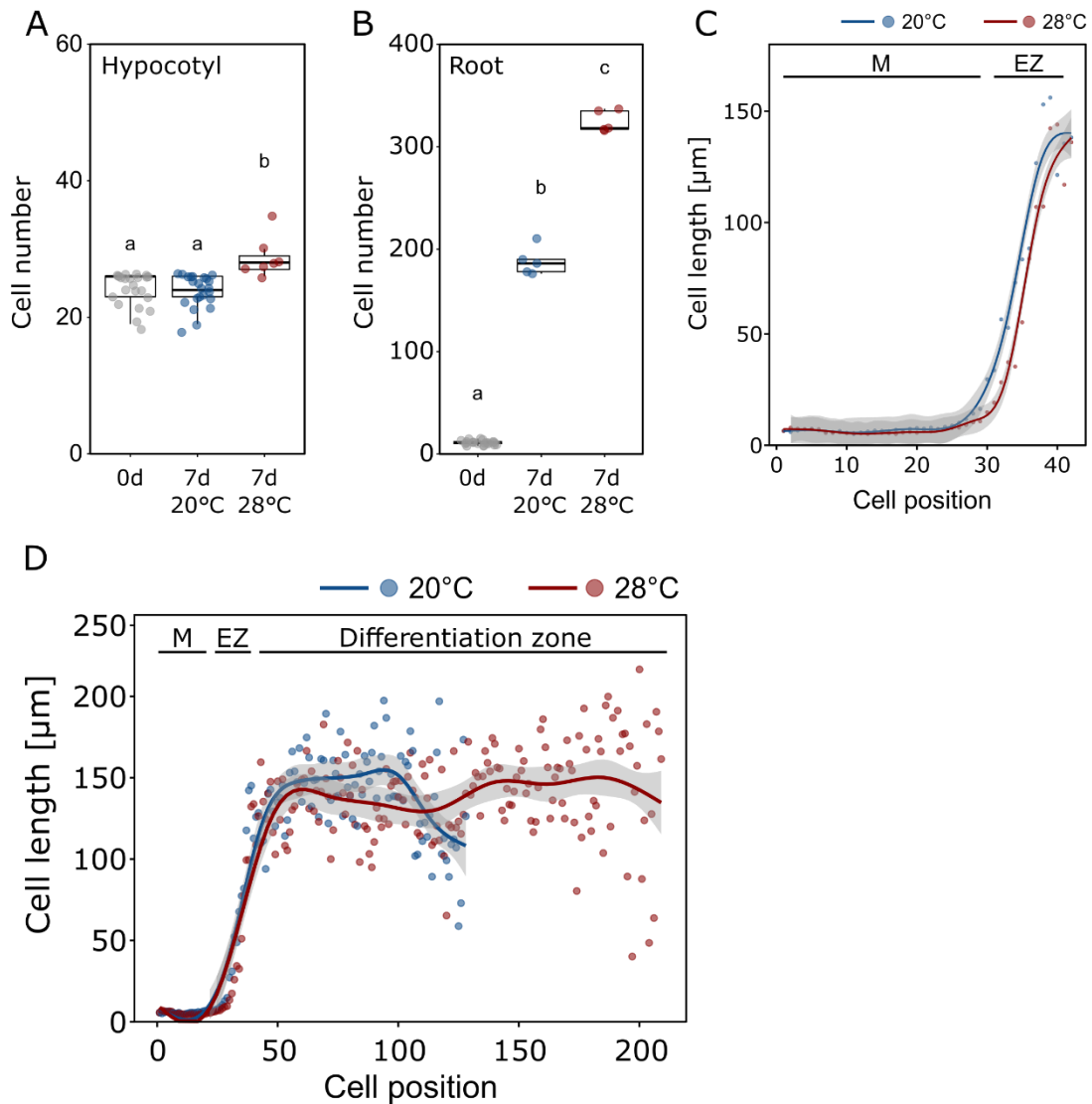
Fig. 3-5 Temperature effects on cell length and cell numbers.

Number of cells in a consecutive cell file of **A** hypocotyls and **B** roots of mature embryos prior to germination (0d) and in 7 days-old seedlings grown at 20°C or 28°C. Data in A and B have been generated by Julia Bellstaedt, MLU Halle-Wittenberg. **C** Close-up view on the first 43 cells comprising M and EZ of the data shown in D. **D** Cell lengths in consecutive cortex cell files of 5 days-old seedlings starting from the root tip (quiescent center = position 1) spanning the meristem (M), elongation zone (EZ), and differentiation zone up to the root-shoot junction. Individual dots represent mean cell lengths (n = 8), lines show a fitted smoothing function (generalized additive models) with the 95 % confidence intervals shown in light grey ribbons. Boxplots show medians, interquartile ranges and min-max values with individual data points superimposed as colored dots. Different letters denote statistical differences at P < 0.05 as assessed by one-way ANOVA and Tukey's HSD *posthoc* test.

Previous studies (Yang *et al.*, 2017; Feraru *et al.*, 2019) had reported a slight decrease in the size of the meristematic zone under high temperatures. However, in my experiments with 5 days-old seedlings, I did not observe any significant temperature-related effects on the number and length of cells in either the meristematic or elongation zones of the roots (Fig. 3-5C). Daily inspection of the meristematic zone revealed that seedlings grown at 28°C displayed a slightly longer meristematic zone until day 5, after which the length seemed to stabilize (Fig. 3-6A). Conversely, only the meristems of seedlings grown at 20°C continued to elongate after day 5, resulting in a slightly longer meristematic zone at day 7 (Fig. 3-6A). Although I consider these differences to be subtle and minor, I acknowledge that they may contribute to the discrepancies observed in the literature regarding the effect of temperature on the size of the root apical meristem. The elongation zone showed a similar behavior with only minor differences between temperatures (Fig. 3-6B). However, the differentiation zone showed a substantial extension in roots of seedlings grown at 28°C at all time points analyzed, with the differences increasing over time (Fig. 3-6C).

While the variances in cell length across the different root zones appeared to be negligible (Fig. 3-5D), it became obvious that the differentiation zone between the end of the elongation zone and the root-shoot junction, consisted of a significantly higher number of cells in seedlings grown at high temperatures (Fig. 3-5D, Fig. 3-6D). After a further two days of growth, moderate yet significant differences in average cell length across the differentiation zone started to emerge (Fig. 3-6E).

Collectively, these findings suggest that in the absence of notable differences in (i) cell length throughout the root, and (ii) cell number in the meristematic and elongation zones, the most reasonable explanation for temperature-induced root elongation is a higher rate of cell division in the root apical meristem, resulting in more cells being released into the elongation zone in a defined time period.
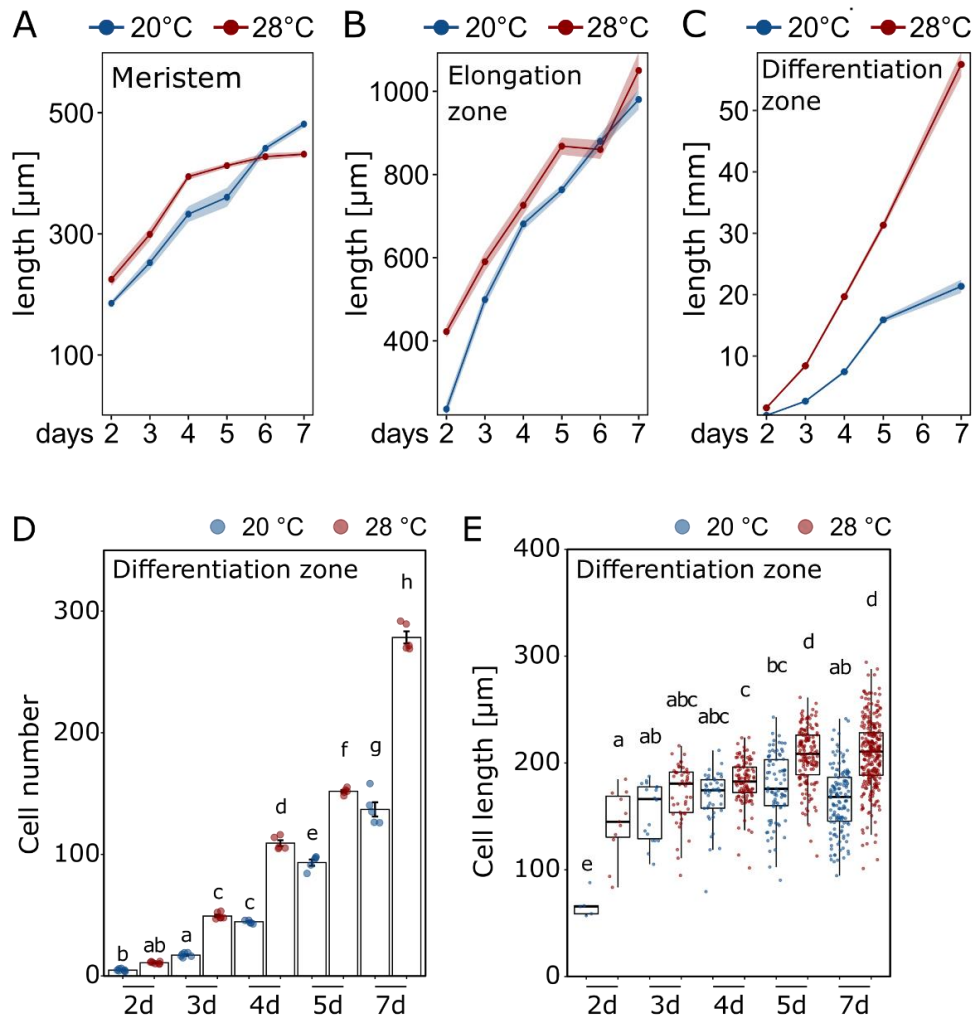
Fig. 3-6 Temperature effects on root zone sizes and differentiation zone specifics

Total length of root zones between day 2 and 7 after sowing of Arabidopsis seedlings grown for 7 days in LD at 20°C or 28°C. **A** Meristem, **B** elongation zone, **C** differentiation zone. **A-C** Solid lines and points show mean root zone length with half-transparent ribbons denoting SEM (n= 5-7 individual roots) **D** Total number of cells in differentiation zone. Barplots show mean values, error bars indicate SEM. Individual data points are plotted as colored dots (n= 5-7). **E** Mean lengths of all cells in a consecutive cell file in differentiation zone measured in 5-7 individual roots. Number of cells ranges from 5 (2d, 20°C) to 272 (7d, 28°C). Boxplots show medians, interquartile ranges and min-max values with individual data points superimposed as colored dots. D+E Different letters denote statistical differences at P <0.05 as assessed by two-way ANOVA and Tukey's HSD *posthoc* test.

Hence, while shoot thermomorphogenesis is driven by cell elongation, root

thermomorphogenesis seems to be dominated by temperature effects on cell division, representing a fundamental mechanistic difference between these two organs. This observation implies that temperature sensing and signaling are governed by distinct pathways in roots and shoots, which is supported by largely different transcriptome responses to elevated temperature in root *vs*. shoot tissues as we observed previously (Bellstaedt *et al.*, 2019).

To test whether cell division rates increase at elevated ambient temperatures, I quantified the number of meristematic cells that are either entering the cell cycle (S-phase) or are actively dividing (M-phase). 5-ethynyl-2'-deoxyuridine (EdU), a thymidine analog, is widely used in DNA proliferation assays. EdU is incorporated into newly synthesized DNA and stains meristematic cells in the S-phase. When EdU labeled cells divide, each daughter cell also contains EdU-labeled nuclei. Consequently, an increased number of labeled cells indicates a higher cell division rate. 4',6-diamidino-2-phenylindole (DAPI) is a fluorescent stain that binds strongly to adenine-/thymine-rich regions in DNA and enables identification of cells in mitosis (M-phase). In addition, I also quantified the pCYCB1::CYCB1-GFP reporter expressed in cytrap lines (Yin *et al.*, 2014) to monitor G2/M phase transition. The experiments were conducted with 5 days-old seedlings, which is after the temperature-response gates opened as shown above (Figs 3-2B, C). Wild-type Col-0 seedlings were grown at either constant 20°C or constant 28°C. Fig. 3-7A shows that high temperature significantly increased the number of cells entering the cell cycle. Likewise, cells in G2/M transition (Fig. 3-7B) and those actively dividing (Fig. 3-7C) increased significantly in high temperature. This strongly supports that elevated temperature promotes cell division rates in the root apical meristem.
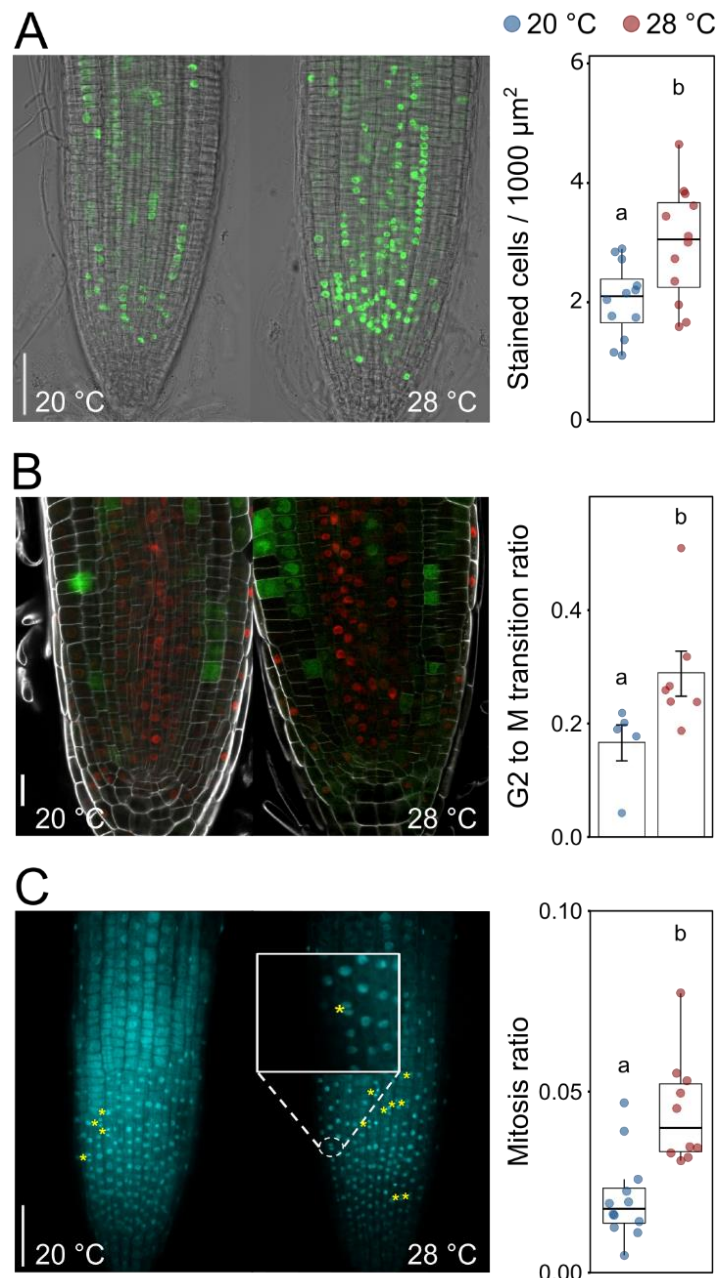
Fig. 3-7. Warm temperature induces cell cycle acceleration.

Different stages of the cell cycle were assayed in 7 days-old Arabidopsis seedlings grown in LD at 20°C or 28°C. **A** EdU staining marks cells that were in S-phase. Scale bar = 50 μm, n= 12. **B** Cytrap lines highlight cells in G2 to M phase transition (GFP signal represents cells in G2-M phase). Scale bar = 20 μm, n= 5-7. **C** DAPI staining was used to identify cells currently in cytokinesis stage (examples are highlighted by yellow asterisks. Scale bar = 50 μm. Boxplots show medians, interquartile ranges and min-max values with individual data points superimposed as colored dots. Different letters denote statistical differences at P < 0.05 as assessed by one-way ANOVA and Tukey's HSD *posthoc* test.

To seek genetic support for a substantial role of the cell cycle as a target of ambient

temperature, I screened a number of cell cycle regulator mutants in their ability to respond to elevated temperatures with root growth behaviour. The E2F genes encode transcription factors responsible for regulating the expression of genes involved in controlling the G1-S phase transition. While single mutants defective in E2F genes showed no (*e2fa, e2fc*) or rather weakly (*e2fb*) impaired temperature responses, higher order mutants exhibited a temperature-dependent phenotype, resulting in a significant reduction in root elongation at higher temperatures compared to that of the wild type (Fig. 3-8A). While the impaired temperature response observed in the *e2fab* double mutant showed a tendency towards partial restoration in the *e2fabc* mutant, the growth difference between both mutants remained unsignificant. This observation may explain the known role of E2Fc as a negative regulator on cell cycle entry, whereas E2Fa and E2Fb act as transcriptional activators (Fig. 1-7). Similarly, mutations in several D-type cyclin genes which are reported to be positive regulators of cell cycle entry as shown in (Fig. 1-7) displayed also a reduction in temperature-induced root elongation, with *cycd7;1_2* showing the strongest effect (Fig. 3-8B). Although lines overexpressing *KRP2* exhibited wild type-like temperature-induced root responses and overexpressing *KRP7* is slightly shorter at both temperatures, *krp2 krp7* double mutants showed the opposite effect, displaying hyperelongated roots under elevated temperature conditions (Fig. 3-8C). As KRP genes appear to exert a negative function on cell cycle initiation (Fig. 1-6), these findings might strengthen the significance of KRPs in controlling cell division and growth. Together, the cell cycle markers and genetic data support the hypothesis stated above that higher temperature targets the cell cycle, resulting increases of cell division rates in the root apical meristem.
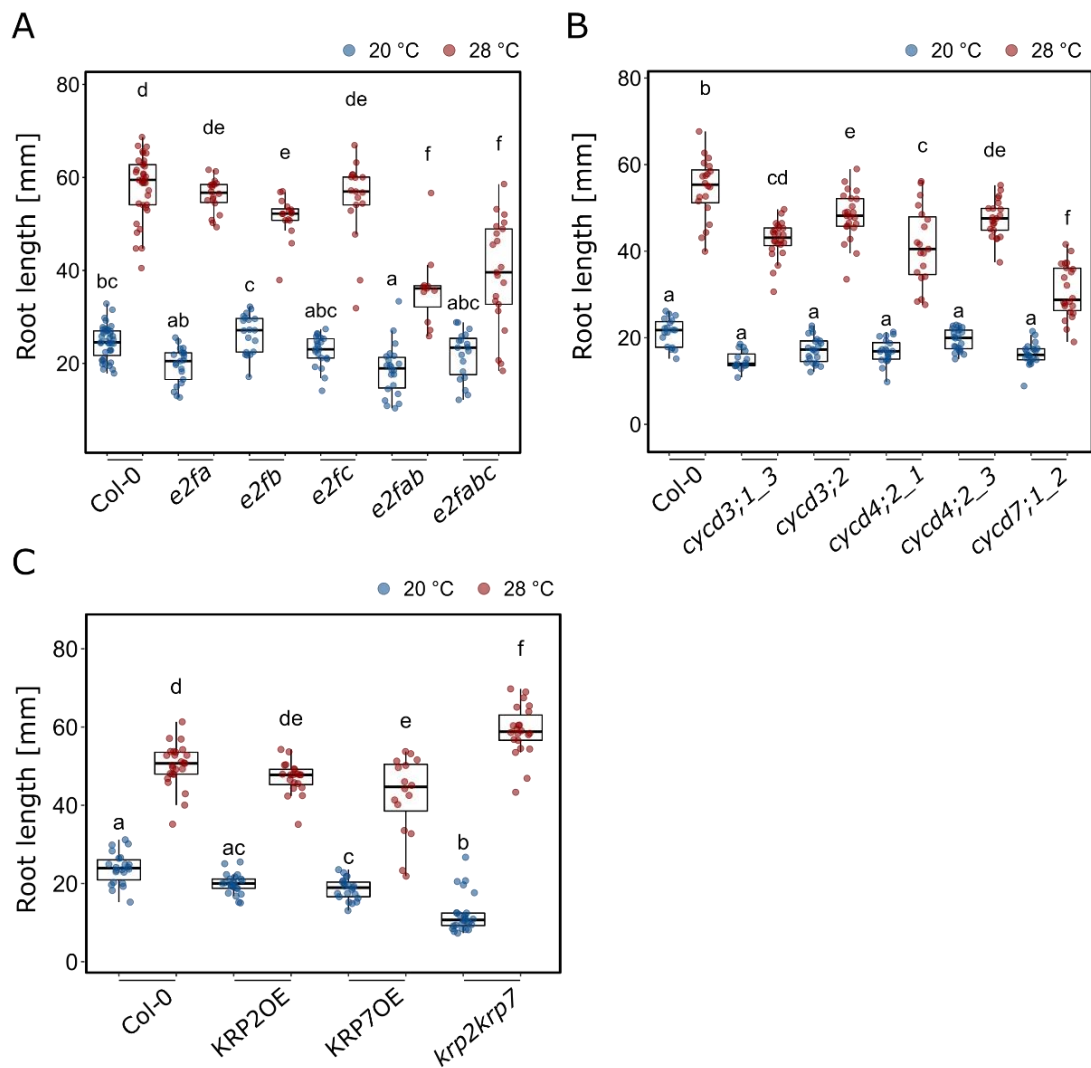
Fig. 3-8 Cell cycle regulations may be involved in root thermomorphogenesis.

A Temperature-induced root elongation in 7 days-old wild type, single, and higher order *e2f* mutants (n = 11-39). **B** Temperature induced root elongation in 7 days-old wild type and selected D type cyclin mutants (n = 15-24). **C** Temperature-induced root elongation in 7 days-old wild type, *KRP2* and *KRP7* overexpression lines, and *krp2 krp7* double mutant (n = 16-27). Boxplots show medians, interquartile ranges and min-max values with individual data points superimposed as colored dots. Different letters denote statistical differences at P < 0.05 as assessed by two-way ANOVA and Tukey's HSD *posthoc* test.

3.2.4 Auxin effects on temperature-induced root elongation

While these data indicated that the increase of cell division rates is an important driver of root growth at elevated temperatures, it remained unclear how temperature

52

information is perceived in the root and how it reaches the cell cycle. A likely intermediate signal between a yet unknown root thermosensor and the cell cycle, which has been shown to be involved in both root thermomorphogenesis (Hanzawa *et al.*, 2013; Wang *et al.*, 2016; Feraru *et al.*, 2019; Gaillochet *et al.*, 2020) and cell cycle regulation (reviewed in Perrot-Rechenmann, 2010; del Pozo & Manzano, 2014), is the phytohormone auxin.

The majority of auxin mutants tested with temperature-responsive root growth exhibited relatively mild phenotypes (e.g., Fig. 3-9A, Hanzawa *et al.*, 2013; Martins *et al.*, 2017; Feraru *et al.*, 2019; Gaillochet *et al.*, 2020). To overcome genetic redundancies and to assess the impact of several levels of auxin biology on temperature-induced root growth, I employed a pharmacological approach. To test the necessity of *de novo* auxin biosynthesis, I used a combined treatment of seedlings with the two IAA biosynthesis inhibitors kynurenine (He *et al.*, 2011) and yucasin (Nishimura *et al.*, 2014), which had previously been shown to effectively block temperature-induced hypocotyl elongation (Ibañez *et al.*, 2018). Fig. 3-9B shows that increasing concentrations of the two inhibitors gradually reduced the growth-promoting temperature effect also in the root. However, as the inhibition of IAA biosynthesis already affected root growth at 20°C control conditions, this should be regarded only as indirect evidence because it is not strictly conditional. Direct evidence for an association of auxin biosynthesis with root thermomorphogenesis is provided by measurements of free IAA levels in root tips of 5 days-old seedlings grown at 20°C or 28°C. Here, higher temperature increased auxin levels in the root tip (Fig. 3-9C). Severe temperature-sensitive and conditional root growth phenotype in *yucQ* mutants, which are defective in five root-expressed *YUCCA* genes (*yuc3,5,7,8,9*; (Chen *et al.*, 2014; Gaillochet *et al.*, 2020) and mild phenotypes in the same root growth assay but strict dependency of temperature-induced *DR5NLS::GFP* reporter gene expression on *TAA1/WEI8* and *TRYPTOPHAN AMINOTRANSFERASE RELATED 1* (*TAR1*) (Fig. 3-

9A; Fig. 3-9D) suggests that high temperature induces *de novo* auxin biosynthesis via the indole-3-pyruvic acid pathway.

Noteworthy, quantitative RT-PCR analysis of auxin biosynthesis genes (*TRYPTOPHAN AMINOTRANSFERASE OF ARABIDOPSIS 1*, *TAA1*; *YUCCA 8*, *YUC8*) and signaling genes (*TRANSPORT INHIBITOR RESPONSE 1*, *TIR1*; *AUXIN SIGNALING F-BOX 2*, *AFB2*) did not reveal any distinct temperature-responsive expression patterns in either whole root or root tip samples (Fig. 3-9E, F). This suggests that the regulation of auxin biosynthesis and signaling during root thermomorphogenesis is unlikely to occur at the transcriptional level.
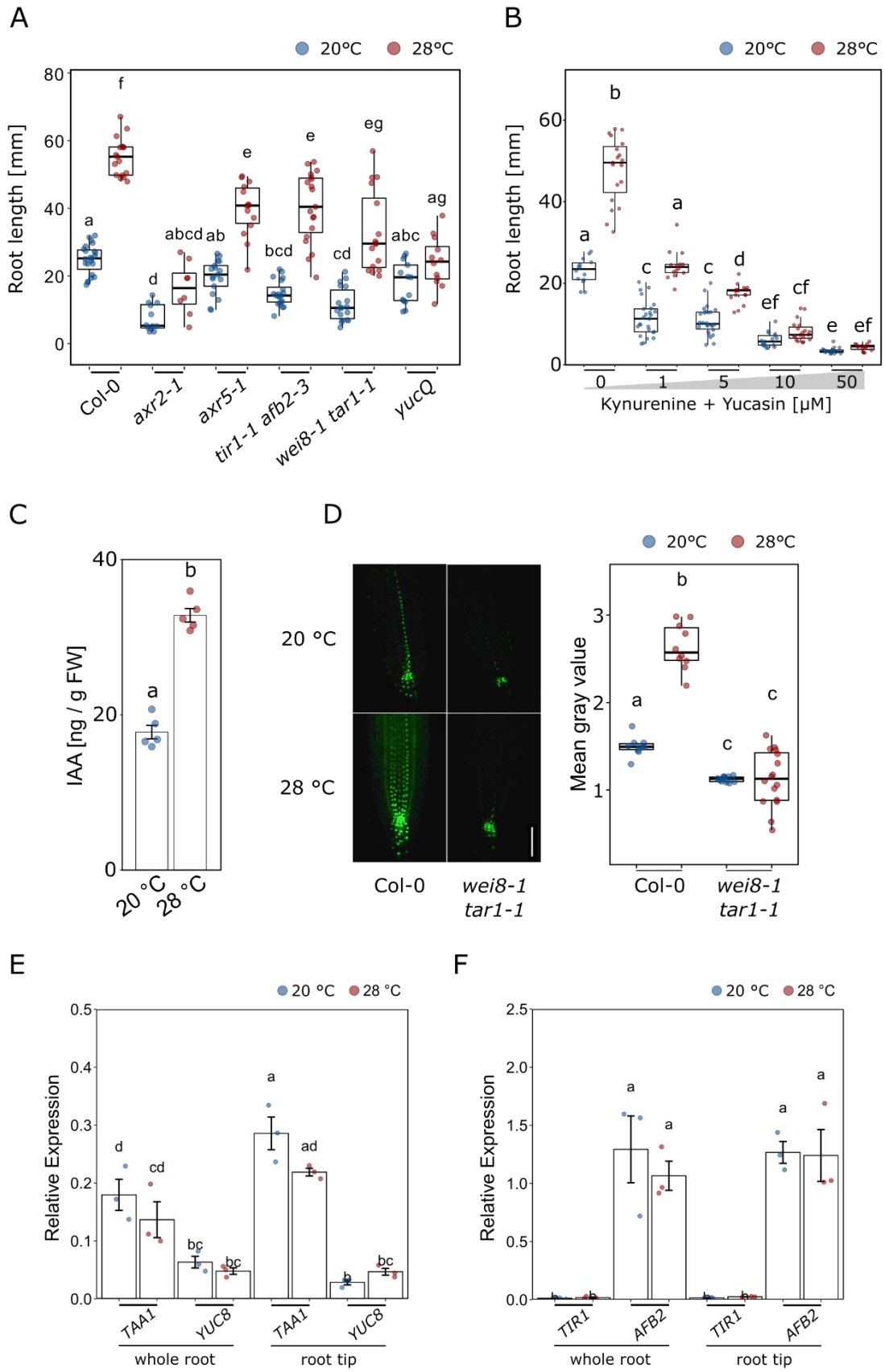
Fig. 3-9 *De novo* auxin biosynthesis is required for temperature induced root elongation.

A Root length of 7 days-old Arabidopsis seedlings grown in LD at 20 or 28 °C (n = 8-23). **B** Root growth assay of seedlings grown for 7 days in the presence of increasing concentrations of auxin biosynthesis inhibitors kynurenine and yucasin (n = 14-26, both inhibitors in equal concentrations) at the indicated temperatures. **C** Free IAA levels of root tip samples of 5 days-old Col-0 (n = 5). Data in C has been generated in collaboration with Gerd U. Balcke, IPB Halle. **D** Imaging and quantification of *DR5NLS::GFP* reporter activity in root tips of 5 days-old seedlings (scale bar = 50 μM, n = 10-16). Quantitative RT-PCR expression analyses of **E** auxin biosynthesis and **F** signaling genes from whole root and root tip of 5 days-old Arabidopsis seedlings, respectively (n = 3). Boxplots show medians, interquartile ranges and min-max values (A, B, D). Barplot shows mean values and error bars show SEM (C, E, F). Individual data points superimposed as colored dots. Different letters denote statistical differences at P < 0.05 as assessed by one-way (C) or two-way (A, B, D, E, F) ANOVA and Tukey's HSD *posthoc* test.

To address the spatial origin of temperature-induced auxin biosynthesis, I next applied strips of filter paper soaked with the polar auxin transport inhibitor N-1-naphthylphthalamic acid (NPA) specifically to the root-shoot junction of seedlings grown at 20°C or 28°C, respectively, to block auxin flow from the shoot to the root. At concentrations that I have previously found to inhibit auxin flow from the cotyledon to the hypocotyl, thereby inhibiting temperature-induced hypocotyl elongation when applied to the petioles (Fig. 3-10B; Bellstaedt *et al.*, 2019), I find that application of NPA directly to the root-shoot junction has no effect on temperature-induced root elongation (Fig. 3-10A). This provides further evidence for temperature-sensitive and shoot-independent local auxin biosynthesis in the root.

To assess the general impact of polar auxin transport, I conducted the same dose-response assay as described above for auxin biosynthesis inhibitors, using NPA applied to the whole media. Here, I observed a similar picture as for yucasin and kynurenine with a gradually decreasing temperature responsiveness on increasing concentrations of NPA (Fig. 3-10C). Also here, low concentrations of the inhibitor already affected root growth at both temperatures. Since PIN-FORMED (PIN) auxin

efflux transporters regulate large parts of the auxin flow through the root, I tested several *pin* mutants for their behaviour in root elongation assays. I found that while *pin1-1* and *eir1-1* (a *pin2* allele) mutant roots were similar to wild type at 20°C control conditions, *pin1-1* did not respond at all to high temperatures, and *eir1-1* showed a significantly reduced temperature response (Fig. 3-10D), the latter confirming a previous report (Hanzawa *et al*., 2013). A mutant allele of *PIN3* (*pin3-4*) behaved like wild type in both temperatures, suggesting that it is not required. In contrast, *pin4-2* mutants, which were likewise not significantly different from the wild type at 20°C, hyperelongated at 28°C (Fig. 3-10D). As such, *PIN1* and *PIN2* seem to act as positive regulators of temperature-induced root growth, while *PIN4* inhibits excessive root growth at elevated temperatures. Importantly, these phenotypes were conditional, suggesting that these are genuine temperature effects.
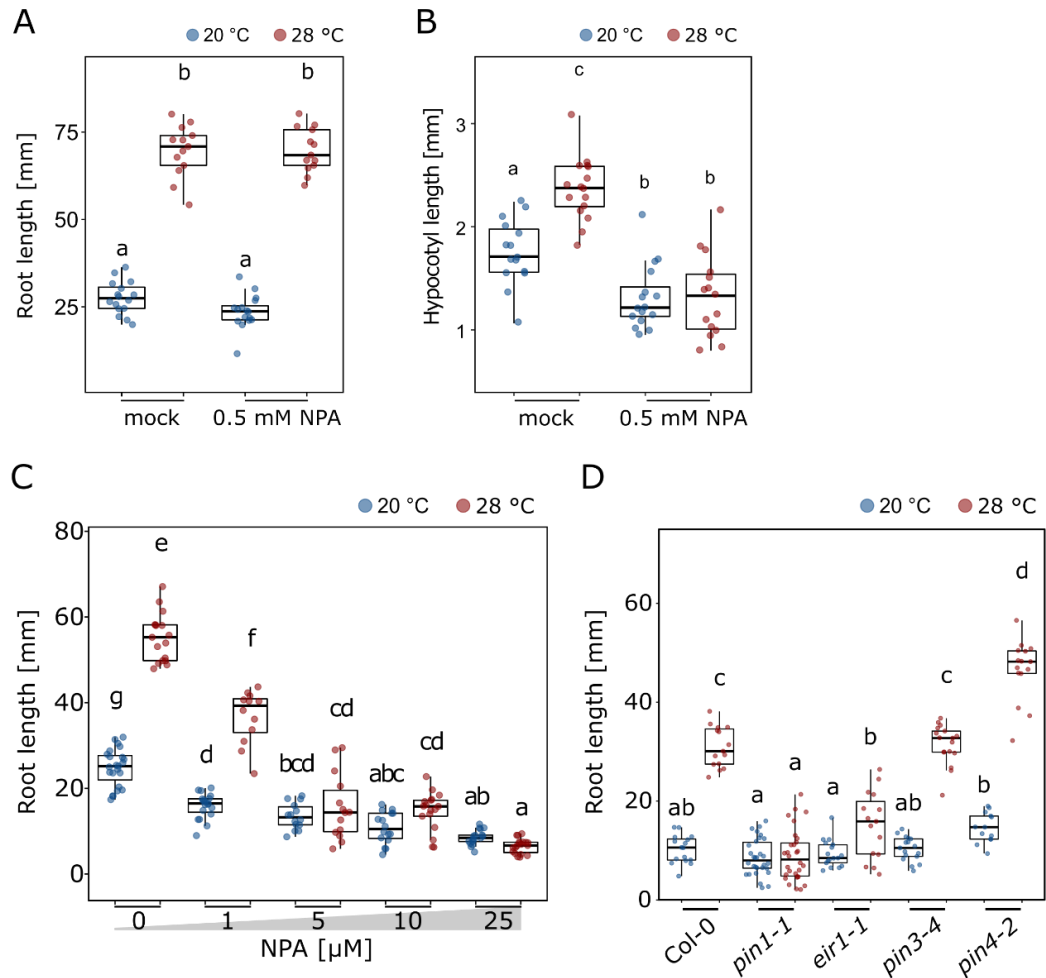
Fig. 3-10 Polar auxin transport governs temperature-induced root elongation driven by root-derived auxin.

A Temperature-induced root growth is unaffected in 8 days-old seedlings if 0.5 mM NPA is applied to the root shoot junction on day 5 (n = 13-16) at the indicated temperatures. **B** Temperature-induced hypocotyl elongation in 8 days-old seedlings with mock or 0.5 mM NPA applied to the cotyledons (n = 15-16). **C** Root growth assay of seedlings grown for 7 days in the presence of increasing concentrations of NPA (n= 12-23) at the indicated temperatures. **D** Root growth assay of seedlings grown for 7 days at the indicated temperatures (n = 13-30). Boxplots show medians, interquartile ranges and min-max values. Individual data points superimposed as colored dots. Different letters denote statistical differences at $P < 0.05$ as assessed by two-way ANOVA and Tukey's HSD *posthoc* test.

Lastly, I blocked auxin signaling by applying the auxin antagonist α-(Phenylethyl-2-one)-IAA (PEO-IAA), which competes with native free IAA for auxin co-receptor binding

(Nishimura *et al.*, 2009). While root elongation was not affected by PEO-IAA concentrations up to 10 µM at 20°C, increasing concentrations of the inhibitor within the same range gradually and significantly decreased root growth at 28°C (Fig. 3-11A), providing a strictly conditional phenotype. Above 10 µM PEO-IAA, seedlings grown in both temperatures were affected, albeit root lengths of seedlings grown at 28°C decreased more severely. I also checked the activity of an auxin-inducible reporter as assessed by *DR5::GFP* which is highly temperature-responsive (Fig. 3-11B), confirming the previous auxin reporter assays from (Hanzawa *et al.*, 2013; Feraru *et al.*, 2019; Gaillochet *et al.*, 2020). Together, these results support the essential role of auxin in temperature-induced root elongation as proposed previously.

Auxin controls the G1/S phase transition of cells entering the cell cycle (Perrot-Rechenmann, 2010; del Pozo & Manzano, 2014). To assess a direct link between temperature, auxin and cell division rates, I next asked whether exogenous addition or inhibition of auxin would influence the number of meristematic cells entering the cell cycle. I therefore performed an EdU staining assay in the presence of the synthetic auxin naphthalene-1-acetic acid (NAA) or the auxin antagonist PEO-IAA. I found that the S-phase promoting effect of temperature alone (28°C, see also Fig. 3-7A) could be mimicked by adding NAA (100 nM) to the 20°C samples (Fig. 3-11C). Vice versa, the temperature-mediated increase in the number of cells entering the S-phase could be counteracted by adding PEO-IAA (50 µM) to the 28°C samples (Fig. 3-11C).
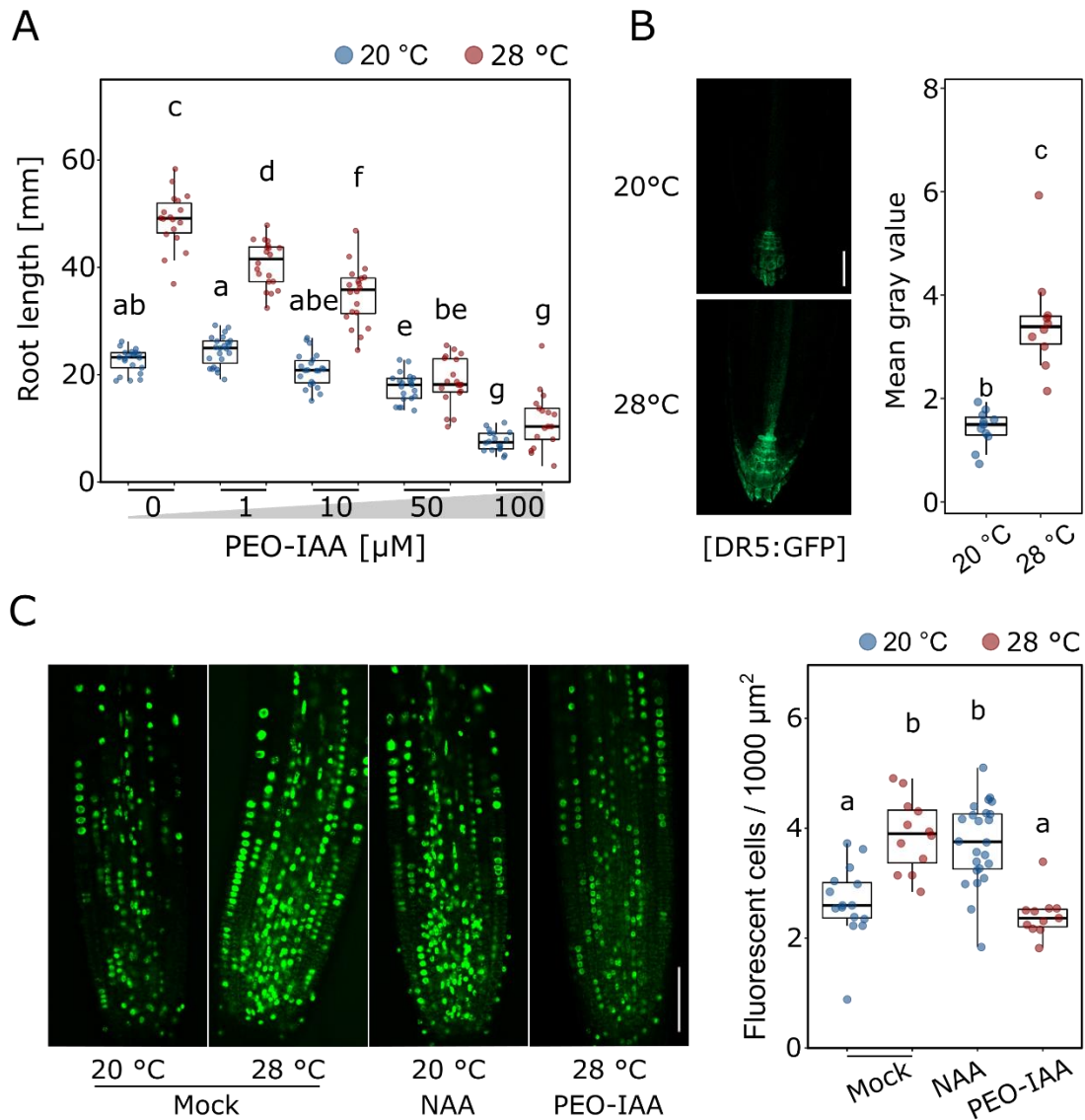
Fig. 3-11 Auxin is able to reversibly affect cell cycle entry at different temperatures.

A Root growth assay of seedlings grown for 7 days in the presence of increasing concentrations of the auxin antagonist PEO-IAA (n = 17-23) at the indicated temperatures. **B** Imaging and quantification of DR5::GFP reporter activity in root tips of 5 days-old seedlings (scale bar = 50 μM, n = 10). **C** (Co-)incubation of 5 days-old seedlings for 3h with 10 μM EdU only or in combination with 100 nM NAA or 50 μM PEO-IAA (n = 11-24), scale bar = 50 μm. Boxplots show medians, interquartile ranges and min -max values. Individual data points superimposed as colored dots. Different letters denote statistical differences at P < 0.05 as assessed by one-way (B) or two-way (A,C) ANOVA and Tukey's HSD *posthoc* test.

Collectively, these data suggest that auxin relays temperature information from a yet unknown thermosensor to the root apical meristem where it promotes cell proliferation at elevated ambient temperatures.

3.2.5 Temperature regulates PIN protein expression patterns in the root tip

To investigate how the temperature-induced increase of auxin levels is maintained in root apical meristems, I next investigated the role of polar auxin transport in more detail. To further analyze *pin* mutant phenotypes, I used propidium iodide staining and confocal microscopy to count the number of meristematic cells in those mutants with defects in temperature-induced root elongation growth, namely *pin1-1*, *eir1-1*, and *pin4-2*. Along a longitudinal cell file, *pin1-1* showed a tendency for fewer meristematic cells, but these differences were not statistically significant (Fig. 3-12A, B). Likewise, the *eir1-1* mutant did not differ from the wild type. In contrast, I observed an increased meristem cell number in *pin4-2* at 28°C compared to the wild type (Fig. 3-12A, B), which may explain its long root phenotype at 28°C. Although NPA application to the root-shoot junction already suggested independence of shoot-derived auxin (Fig. 3-10A), I selected one short root *pin* mutant (*pin1-1*) and one long root *pin* mutant (*pin4-2*) and asked whether the temperature-induced root growth phenotypes (Fig. 3-10D) originate in the root or may possibly be caused by long-distance transport of shoot-derived auxin requiring PIN function. Hypocotyl micrografting showed that the observed phenotypes did only occur when *pin* mutants were used as rootstocks (Fig. 3-12C, D), further strengthening that the elevated auxin levels at high temperatures in the root tip are root-derived.

To better understand how temperature potentially affects PIN functions, I first asked whether *PIN*s might be transcriptionally regulated by temperature. Quantitative RT-PCR of *PIN1-4* in whole roots or root tips of 5 days-old seedlings grown at 20°C *vs.*

28°C displayed little temperature responsiveness (Fig. 3-12E). Although I did observe a slight decrease of *PIN1* expression levels in root tips at high temperature (Fig. 3-12E), overall transcriptional regulation of *PIN*s seems to be hardly affected by temperature changes. Interestingly, when I assessed the activity of fluorescent DR5 reporter constructs in *pin* loss-of-function backgrounds in response to temperature, I found no response in *pin1-1* and increased DR5 signal in *pin4-2* (*eir1-1* lines with DR5 reporters were not available; Fig. 3-12F), which aligns with the root growth defects of the same mutants shown in Fig. 3-10D.
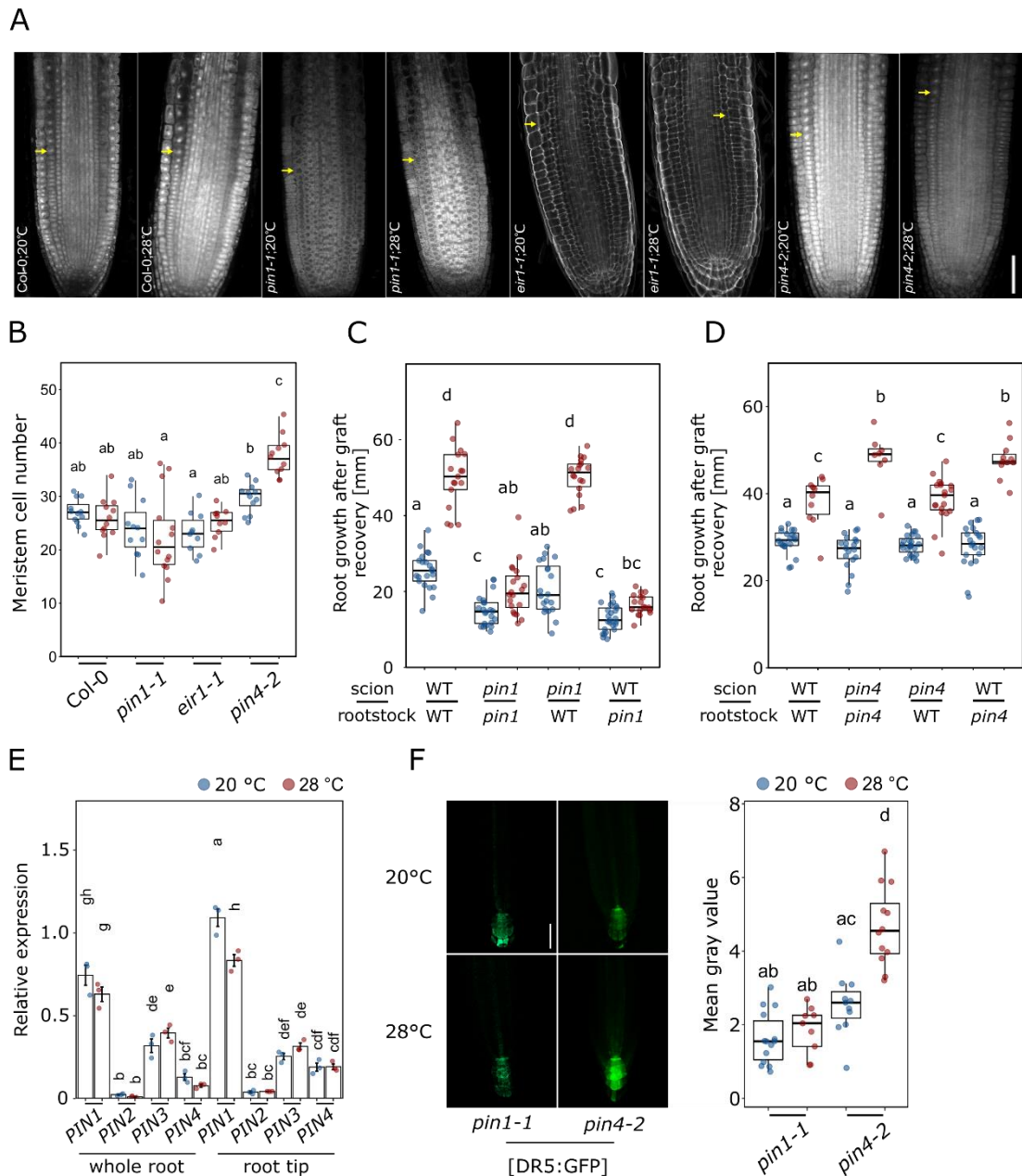
Fig. 3-12 Non-transcriptional regulation of polar auxin transport in root thermomorphogenesis.

A Microscopic photographs of root tips of 5 days-old seedlings grown in LD at 20°C or 28°C. Yellow arrows mark the end of the meristem. Scale bar = 50 µm. **B** Quantification of meristem cell numbers in consecutive cortex cell files in (A). **C-D** 9 days-old seedlings grown at 20°C were hypocotyl-grafted, recovered for 7 days and then cultivated at 20°C or 28°C for another 7 days (C: n = 17-25, D: n = 8-23). Data in C and D have been generated by Kai Steffen Bartusch, ETH Zürich. **E** qRT-PCR expression analyses of *PIN1-4* from whole root and root tip samples, respectively, Col-0 RNA was extracted with respective

organs and first-strand cDNA was then synthesized (n = 3). **F** Imaging and quantification of DR5::GFP reporter activity in root tips of 5 days-old seedlings (scale bar = 50 μM, n = 9-14). B-F Boxplots show medians, interquartile ranges and min-max values (B-D, F). Barplots shows mean values and error bars show SEM (E). Individual data points superimposed as colored dots. Different letters denote statistical differences at P < 0.05 as assessed by twoway ANOVA and Tukey's HSD *posthoc* test.

Since temperature-mediated PIN functions are not regulated on the transcriptional level, I assessed the behavior of GFP fusion proteins of PIN1, PIN2, and PIN4 in response to temperature in root tips. PIN-GFP fusion proteins responded in parts strongly to temperature changes. When 5 days-old seedlings were shifted from 20°C to 28°C for 4 h, GFP fusion protein signals of PIN1 and PIN2 in the root tip virtually disappeared, while PIN4 reporter levels remained unaffected (Fig. 3-13A-C). However, these PIN1 and PIN2 effects were transient, as indicated by unchanged GFP signal intensities in seedlings constantly grown at the respective temperatures (Fig. 3-13A, B). It is therefore unclear whether this transient disappearance affects root growth at all. PIN4-GFP levels in the columella showed a tendency to decrease at constant 28°C (Fig. 3-13C), but the differences were not statistically significant. Furthermore, I found that both *PIN1* and *PIN2* are essential for temperature-induced increase of cell division rates as shown by reduced EdU staining of root apical meristems in *pin1-1* and *eir1-1* seedlings (Fig. 3-13D, E), further substantiating the proposed function of auxin in the thermo-responsive regulation of the cell cycle.

As the polar localization of PINs controls the direction of auxin flow, I also quantified the ratio of basal (lower)/apical (upper)-to-lateral PIN-GFP ratios in response to temperature. For PIN2-GFP I observed an increased basal-to-lateral ratio in cortical cells of seedling roots grown at constant 28°C compared to constant 20°C (Fig. 3-13F). A shift of cortical PIN2 to the basal membrane would cause auxin to be preferably transported downwards to the root tip, consistent with the increase of IAA levels (Fig. 3-9C). A parallel shift of epidermal PIN2 to the apical membrane as also shown by

Hanzawa *et al*. (2013) would promote the auxin flow back upwards, consistent with the reverse fountain model.
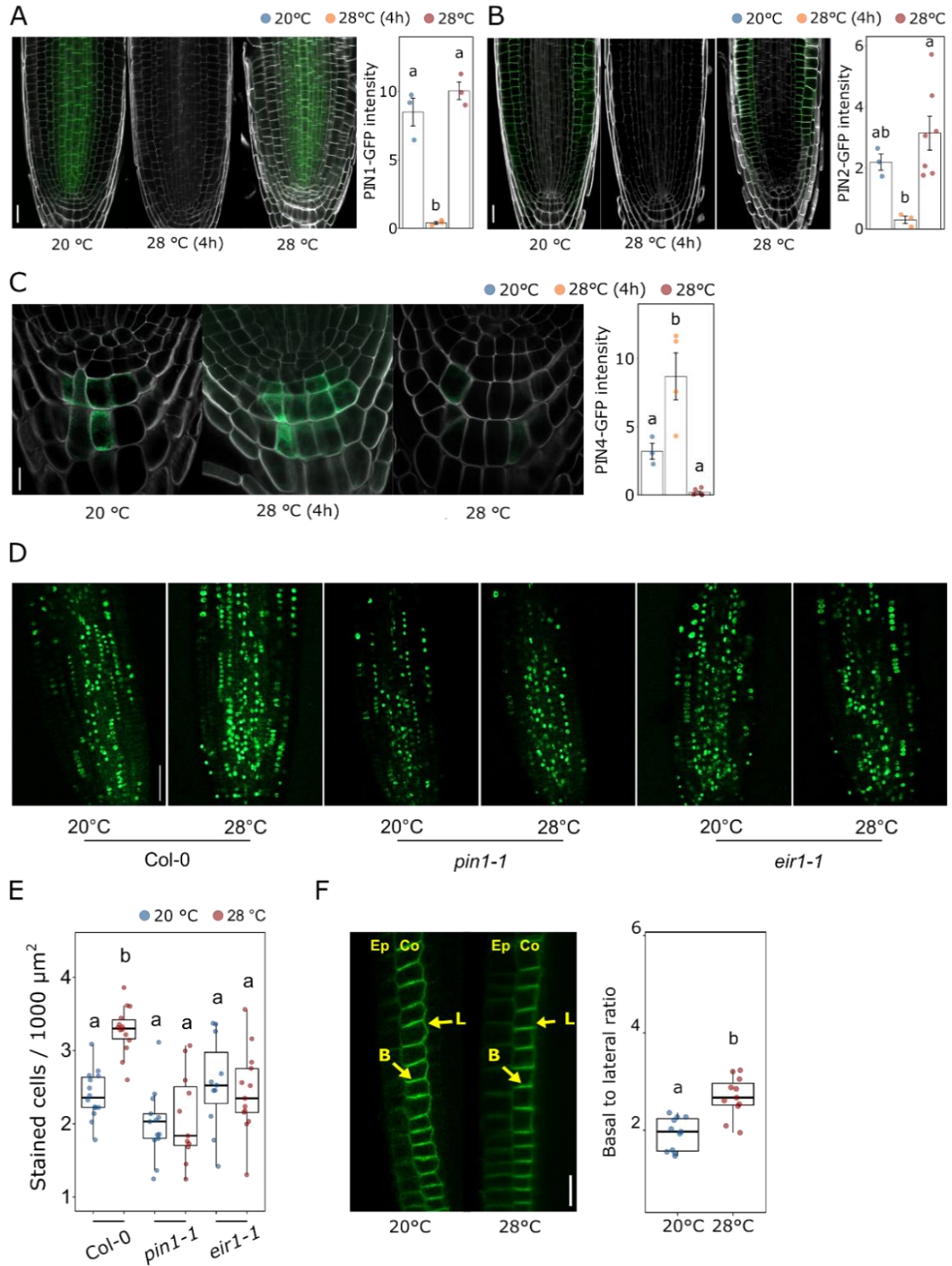
Fig. 3-13 Elevated temperature affects PIN protein behaviors.

A-C Temperature effects on PIN1-GFP (E, scale bar = 20 μm), PIN2-GFP (F, scale bar = 20 μm), and PIN4-GFP (G, scale bar = 10 μm) levels. Seedlings were grown for 5 days at constant temperatures (20°C or 28°C) or grown at 20°C for 5 days and shifted to 28°C for 4 h (n = 3-7). Data in A-C have been generated by Tonni Grube Andersen, MPI Köln. **D** EdU staining of 5 days-old seedlings at indicated temperatures (n = 11-14) and quantification in **E**. **F** PIN2-GFP relocalization patterns of root meristem of 5 days-old seedlings grown at the indicated temperatures. Ep = epidermis, Co = cortex, yellow arrows mark the localizations of lateral or basal membranes in a cell (n = 12-13), scale bar = 20μm (n = 10-11). Boxplots show medians, interquartile ranges and min-max values (E-F). Barplots shows mean values and error bars show SEM (A-C). Individual data points superimposed as colored dots. Different letters denote statistical differences at P < 0.05 as assessed by one way (A-C, F) or two-way ANOVA (E) and Tukey's HSD *posthoc* test.

Collectively, the reported results indicate that elevated temperature is perceived by a yet unknown root thermosensor, which either directly or indirectly activates local *de novo* auxin biosynthesis via the indole-3-pyruvic acid pathway and a PIN-dependent increased auxin flux through the root tip, resulting in an auxin maximum. This causes an acceleration of cell division rates in the root apical meristem, potentially *via* auxin regulated E2F transcription factors, ultimately resulting in increased primary root elongation at elevated temperatures.

Chapter 4: Discussion

Research efforts over the last 15 years have provided a reasonable understanding of moderate high-temperature responsive shoot growth and sensing (reviewed in Quint *et al.*, 2016; Delker *et al.*, 2017; Casal & Balasubramanian, 2019). Experimental insights into ecophysiological benefits of thermomorphogenesis favors the scenario in that moderate high temperatures promote transpirational cooling of shoot organs, thereby enhancing photosynthesis efficiency in *Arabidopsis thaliana* (Crawford *et al.*, 2012; Park *et al.*, 2019). However, knowledge of root thermomorphogenesis remains literally fragmentary and less explored. Naturally, unlike shoot organs, root systems are below-ground within a range of different soil temperatures that could affect water and nutrients circulation, root plasticity and development (Fonseca de Lima *et al.*, 2021). Therefore, the goal of my thesis was to integrate known aspects of thermo-responsive root growth and connect the current fragmentary knowledge with substantial experimental data to deliver a comprehensive model of root thermomorphogenesis signaling.

4.1 High temperature triggers a shoot-independent root elongation

While it is widely known that shoot organs can sense and respond to temperature stimuli, it still remains to be seen whether roots have the same capabilities. This question is of great importance because its answers may affect the direction of searching for root thermosensors and signaling networks. Several possibilities stand: (i) root thermosensing may depend on shoot-mediated long-distance signals in relaying temperature information; in contrast, (ii) roots may possess an autonomous system to sense and respond to temperature cues independent of the shoot; or (iii) to some extent roots may acquire temperature information that originates in the shoot to support temperature-induced below-ground growth responses. In favor of the essential role of shoot derived signals on root thermomorphogenesis, Gaillochet *et al.* (2020)

have implicated that HY5 combined with PIFs and phytochromes functions as a central module in integrating shoot-root communication, which coordinates above-ground with below-ground growth under elevated temperatures. The authors proposed that a PHY-PIF-HY5 module may acquire auxin to regulate root growth. However, temperature responsiveness of detached wild type roots (Bellstaedt *et al*., 2019; Fig. 3-3A) in combination with an equally wild type-like response of temperature-blind shoot mutants grafted onto wild type rootstocks (Fig. 3-3B-D) supports a scenario in which roots are to be regarded as an autonomous system which can sense and respond to temperature independent of shoots. This does not exclude potential temperature-sensitive shoot-root communication, possibly including phyB (Fig. 3-3E), but suggests a rather indirect or secondary role for temperature-induced root elongation. Furthermore, recent advances from (Borniego *et al*., 2022) provided evidence that none of the shoot thermosensors PHYB, ELF3 and PIF7, possess thermosensory function in the root. Although intact seedlings of selected shoot thermomorphogenesis mutants displayed weak growth defects in temperature-induced root growth assays, all investigated lines were still able to respond to some degree to elevated high temperatures (Fig. 3-4A, B; Yang *et al*., 2017; Gaillochet *et al*., 2020). Hence, I draw the conclusion that while the primary regulators of shoot thermomorphogenesis most likely fulfill only a secondary function in root thermomorphogenesis, the key regulators governing root thermomorphogenesis remain unknown.

In addition, transcriptome analysis in different tissues including cotyledons, hypocotyls and roots revealed minimum overlap in temperature-responsive genes, supporting the argument of distinct regulatory mechanisms operating across different tissues (Bellstaedt *et al*, 2019). Taken together, these findings strongly suggested that shoot and root thermomorphogenesis follow distinct signaling pathways.

4.2 Growth kinetics of primary roots at elevated ambient temperature

From the 1950s to the 1970s, early attempts were made to analyze the spatial growth rates of plants using intricate equations and the concept of fluid compression, which could be applied to calculate plant development (Erickson & Sax, 1956; Silk & Erickson, 1979). These analyses were based on the fundamental hypothesis that fluid flow could be viewed as a continuum analogous to plant growth (Silk & Erickson, 1979). Based on these pioneer insights, the effects of temperature on growth dynamics can be determined. For instance, studies have shown that leaf cell division and elongation rates increase with rising temperature across various species, including maize, sunflower, and Arabidopsis, indicating a conserved pattern of temperature response over time (Ben-Haj-Salah & Tardieu, 1995, Granier & Tardieu, 1998, Granier *et al.*, 2002). Furthermore, temperature response curves across 18 species, encompassing temperate to tropical varieties, exhibit similar patterns in various developmental processes such as organ expansion rates (pollen tube, roots, leaves and embryo), cell division rates and germination rates. This suggests that the impact of crop domestication and breeding on temperature response in developmental processes may be limited (Parent & Tardieu, 2012).

Compared to the shoot, the root as below-ground organ tends to be more easily affected by surrounding environments. Detailed root growth experiments in response to a range of temperatures have been performed by (Yang *et al.*, 2017), and a gradual increase of total root length, root elongation rate, velocity, cell division rates, and transit of cells through the different root zones, have been reported for a temperature range from 15°C to 25°C, while elongation zone length remained unchanged. Based on these observations Yang *et al.* (2017) concluded that root growth promotion at high temperatures depends on increased cell elongation as the overall cell flux remains invariant. This is contradictory to the results of maize roots from (Silk, 1992) and also to our data shown in Fig. 3-5D, both of which suggest that high temperature does not

significantly change cell length but increases overall cell production, leaving cell division being the major factor in this process. Similarly, Ban-Haj-Salah and Tardieu (1995) observed the same feature in maize leaves that cell length is spatially uniform across a temperature range. Obviously, these partially controversial observations can result to some extent in different conclusions favoring either cell division or cell elongation as the primary driver of temperature-promoted root growth. Nevertheless, a final conclusion is at this point difficult because of differences in the applied methods, cultivation and technical handlings, as also suggested by (Nagel *et al.*, 2009; Yang *et al.*, 2017).

Pahlavanian & Silk (1988) conducted a study on the growth patterns of maize primary roots. They monitored the displacement of cells from the root apex over time (root growth trajectory), under different temperature conditions. The key findings of their study are as follows:

Firstly, they discovered that root growth velocity increased as the temperature rose from 16°C to 29°C, regardless of the monitored positions. The higher the temperature, the faster the cells moved away from the root apex. Secondly, they observed a rapid expansion in element length (cell length) under higher temperatures within a specific time frame. This means that, at a given time point, cells in the monitored zones were longer at higher temperatures. However, temperature effects (19°C *vs*. 29°C) are negligible when the position of the cells was analyzed as x-axis (cell length as y-axis). This finding implies that whether a cell moves quickly away from the apical meristem at high temperatures or slowly at low temperatures, the final cell size remains the same.

Noteworthy, they did observe that the length of mature (final) cells remained stable over a temperature range between 16°C to 29°C (Pahlavanian & Silk 1988), which was also found in studies of wheat (Burström, 1953) and onion (Carmona & Cuadrado,

1986). While all these observations pointed towards cell length being a rather invariable growth feature regarding temperature changes, they also identified parameters like cell production and growth velocity that were strongly temperature responsive (Silk *et al.*, 1989; Silk, 1992). Thus, increased cell production is synchronized with accelerated cell division, resulting in spatially uniform root anatomy in response to fluctuated surrounding temperatures.

4.3 High temperature alters cell cycle features

Considering that high temperatures do not alter cell and zone lengths, the increased cell production can be attributed to enhanced rate of cell division, leading to a more rapid transition of cells from the meristem to the elongation/maturation zones. To accurately assess temperature impacts on cell division rates, the concept of 'cellochron' is introduced, which defines the time required for cell displacement from the meristem. It has been shown that the cellochron at 29°C is half of that at 19°C, which means high temperature accelerates cell flux (Silk *et al.*, 1989, Silk, 1992). The changes of cellochron between high and low temperatures may indicate that the cell cycle duration or the number of divisions per origin is temperature-dependent as proposed early on (Erickson, 1959). Since temperature does not change root anatomy, the most reasonable explanation of increased cell flux is that cell cycle duration shortens with rising temperatures (Silk, 1992). Grif *et al.* (2002) analyzed meta-data on cell cycle duration and phases of 170 species, further supporting a general effect of elevated temperatures on the promotion of cell cycle speed. Of note, root growth retardation at cold temperature aligns with the prolongation of the cell cycle duration (Grif & Valovich, 1973). Collectively, these observations strongly support the notion that high temperatures trigger the shortening of the cell cycle lifetime, or conversely, longer cell cycle durations are associated with lower temperatures.

To investigate a process like temperature-sensitive root growth, it makes sense to

explore which cellular features are associated with it. In juvenile shoots, cell elongation has been shown to be the primary process causing temperature-induced hypocotyl and petiole growth. In roots, I found that temperature dependent increase of cell numbers can be observed mainly in differentiating and mature cells, whereas changes in meristematic and elongating cells were negligible (Fig. 3-5C, D). For Arabidopsis, temperature effects on meristem size have been reported, being observed from shorter (Yang *et al*., 2017; Feraru *et al*., 2019) to even larger (Hanzawa *et al*., 2013) in response to moderately increased ambient temperatures. In our case, I observed meristem size to be rather invariant with only minor differences between cold and warm temperatures over time (Fig. 3-6A). Differences between studies may be explained by the general sensitivity of meristem size as a trait, different ages of seedlings used for measurements, or the way of defining a meristem, which varied from monitoring mitotic cells (Yang *et al*., 2017) via cell cycle phase reporters (Hanzawa *et al*., 2013) to morphological cell size characteristics (Feraru *et al*., 2019; this study). The same inconsistencies exist between studies when it comes to temperature effects on cell length. In order to precisely investigate the spatial and temporal dynamics of cellular temperature responses, the utilization of advanced live imaging and 3D confocal microscopy setups would provide superior resolution, enabling a more detailed analysis of cellular morphological variations (von Wangenheim *et al*, 2017; Christian Wenzl & Jan U. Lohmann, 2023).

Taken together, my data suggest that (i) cell division responses precede and predominate cell elongation responses; (ii) moderately elevated temperatures tend to facilitate both cell division and cell elongation with the former having greater impact on ultimate root length during early seedling stages investigated in this study. Furthermore, as temperature-responsive cell division precedes the observed differences in whole root length, a gating period (as suggested above based on Figs 3-2C, 3-6A-C) is unlikely to exist on the cellular level. Therefore, it is tempting to speculate that a

molecular gating signal exists between cell division and cell elongation. Obviously, a temperature dependent increase of cell division rates in the root apical meristem is the primary trigger for exaggerated root elongation, suggesting a fundamental mechanistic difference between root and shoot tissues in translating temperature information into growth responses.

Using cell cycle stage markers on root tissues can strengthen this conclusion. I found that at 28°C there were more cells in the DNA synthesis phase which indicates that more cells entered the cell cycle (Fig. 3-7A). Similarly, more cells were actively dividing (= in mitosis) (Fig. 3-7B, C) compared to plants grown at 20°C. These results further complement research spanning the last 60+ years, describing cell cycle and cell division acceleration is triggered by elevated temperatures across species (e.g., Erickson, 1959; Murín, 1981; Silk *et al*., 1989; Silk, 1992; Murín, 1966; Grif *et al*., 2002; Hanzawa *et al*., 2013; Yang *et al*., 2017). While cell division may consume more energy and cell material compared to cell elongation, a larger number of cells also means more cell walls are integrated, supporting the rigidity of root structure in the long term. In contrast, such an investment for shoot tissues may not make sense as they are confronted with less physical resistance in their aerial environment. In this regard, building more cell walls means increased durability towards soil pressure, which is a valuable investment when roots explore deeper soil layers.

4.4 Auxin is essential for temperature-induced primary root elongation

To better understand how root growth behavior differs in response to elevated temperatures, we need to find out how temperature information is integrated into diverse growth responses. One such link is supposed to be auxin which associates with wide aspects of root growth, for example, primary root growth, lateral root branching, adventitious root and root hair development. Besides, auxin is known as a messenger in integrating shoot thermomorphogenesis sensing and signaling

(Bellstaedt *et al*., 2019). It has also been found to promote the initiation of the mitotic cycle by interacting with genes involved in the G1-S phase (Perrot-Rechenmann, 2010; del Pozo & Manzano, 2014). Although previous studies have demonstrated the essential role of auxin in regulating root thermomorphogenesis (Hanzawa *et al*., 2013; Wang *et al*., 2016; Feraru *et al*., 2019; Gaillochet *et al*., 2020), the underlying molecular mechanism(s) remained to be explored.

My data propose a model that highlights the role of auxin in linking temperature signals to the cell cycle in the root apical meristem. I observed that high temperature results in an increase of free IAA levels in the root tip (Fig. 3-9C). In contrast, Gaillochet *et al.* (2020) detected no changes of free IAA levels between 21°C and 27°C in seedling roots and concluded that an increase of auxin levels is not necessary for root thermomorphogenesis. However, as Gaillochet *et al*. (2020) sampled whole roots, which most likely diluted the spatial temperature effects in root tips. Therefore, these differing conclusions may not be contradictory at all.

Micrografting experiments (Fig. 3-3B-C), blocking shoot-root auxin flow (Fig. 3-10A), the necessity of enzymes acting in the indole-3-pyruvic acid pathway of auxin biosynthesis to activate auxin-responsive *DR5NLS::GFP* reporters (Fig. 3-9D), strongly suggest that high temperature facilitates local *de novo* auxin biosynthesis via the YUC/TAA pathway. This newly generated IAA is unlikely to be derived from the shoot since local blocking of auxin flow from the shoot to the root by NPA does not influence temperature-induced root elongation (Fig. 3-10A). Instead, it is more likely that the auxin originates from the root apical meristem itself or elsewhere in the root where it transported to the meristem via the polar auxin transport machinery.

Interestingly, auxin has the ability to induce reversible temperature-dependent changes of cell division rates (Fig. 3-11C), demonstrating a direct connection between

temperature, auxin, and the cell cycle. Temperature conditional root growth phenotypes of *pin* loss-of-function mutants (Fig. 3-10D) and the dependency of enhanced DR5 signal on *PIN* genes in higher temperature (Fig. 3-12F) demonstrate the requirement of polar auxin transport for generating or maintaining the auxin maximum in the root tip. This is further supported by a quantitative signal shift of PIN2-GFP at 28°C from the lateral to the basal (lower) membrane in cortex cells (Fig. 3-13F), promoting auxin transport towards the root apical meristem at high temperatures. While this result contradicts Sauer *et al.* (2006) who discovered that exogenous addition of synthetic auxin NAA in the root leads to lateralization (basal to lateral shift) of PIN2 in cortex cells towards epidermal cells in a non-temperature context, it complements Hanzawa *et al*. (2013) who reported a lateral-to-apical (upper) shift of PIN2-GFP in epidermal root cells at elevated temperature. Together, the observations reported in this thesis and those by Hanzawa *et al*. (2013) indicate an enhanced auxin flow throughout the root apical meristem at higher temperatures.

Under the reverse fountain model (Benkova *et al*., 2003; Grieneisen *et al*., 2007), PIN4 is required to redistribute auxin in the columella, where an auxin sink is located, maintaining an auxin gradient in the root tip (Friml *et al*., 2002a). I observed a trend of decreasing PIN4-GFP levels in columella cells at 28°C (not significant; Fig. 3-13C), possibly turning off the break of auxin flow, leading to an increased auxin maximum as detected in Fig. 3-9C. However, the *pin4-2* mutant showed a hyper-elongating root phenotype at 28°C (Fig. 3-10D), which means PIN4 has a negative effect on this response, implicating that at higher temperature PIN4's role in establishing a new auxin maximum in the root apical meristem is likely secondary to the role of restricting meristem size (Fig. 3-12A-B). While PIN1 is essential for temperature-promoted root elongation as its loss-of-function *pin1-1* mutant roots were completely temperature blind (Fig. 3-10D), its localization patterns seemed temperature unresponsive and were only transiently affected by high temperature (Fig. 3-13A).

As a consequence of increased auxin levels in the root tip, cell division rates accelerate in the root apical meristem. This process is possibly reversible because exogenous addition of the synthetic auxin NAA or the auxin antagonist PEO-IAA mimicked the observed temperature effects on the number of S-phase cells in the root apical meristem (Fig. 3-11C). Intriguingly, Zhu *et al.* (2015) reported that low temperature impaired cell division rates which additionally correlated with reduced auxin levels, a shorter meristem and a decreased number of cells therein. This indicates that temperature may have general effects on targeting the same cellular process, cell division, via the same messenger, auxin, in either an inhibiting (low temperature) or promoting (high temperature) manner.

4.5 Temperature affects root system architecture across species

Root system architecture (RSA) defines the below-ground organization of root tissues which is essential for water and nutrient uptake efficiency (Rogers & Benfey, 2015). In nature, soil temperatures drop as soil depth increases, leading to high plasticity of root growth. Due to difficulties of evaluating RSA in the field, many setups have been established on the laboratory level, for example, observable medium-based growth systems (Fang *et al.*, 2009) and devices generating temperature gradients along root zones which is adaptable to agar-based petri dishes or soil-based pots (González-García *et al.*, 2022). Especially the latter enables growing of plants under conditions that are closer to natural systems than the sterile petri dish setup employed by myself throughout this thesis. Recent studies have demonstrated that soil (medium) temperature differences between the top layer (higher temperature) and deeper layers (lower temperature) may result in different root traits across species (Luo *et al.*, 2020; González-García *et al.*, 2022; Boter *et al.*, 2023). RSA responses to elevated ambient temperatures are generally genotype- and species-specific, as the optimal growth temperatures can vary among different genotypes and species. Furthermore,

temperature effects on root growth are highly variable, with some studies reporting promotion (Domisch *et al.*, 2001), while others observe repression (Forbes *et al.*, 1997), or a combination of both, depending on the temperature range from optimal to suboptimal (Seiler, 1998). As such, the conclusions drawn in this thesis, which are based on a specific experimental setup in a single species (with exceptions, see Figs 3-2D, E; 3-3A), should not be generalized at this point.

A recent study showed that in *Brassica napus* a large number of root traits responds to elevated temperatures, especially an increased root biomass and an extended root system (Boter *et al.*, 2023). The changed RSA caused by temperature likely equips *Brassica napus* with enhanced soil exploration and nutrient uptake ability. Interestingly, different *Brassica napus* varieties tend to establish specific RSA traits in response to warmth, as the variety Drakkar displayed a wider but not deeper root system, while the variety Duplo showed the opposite with a combination of wider and longer roots (Boter *et al.*, 2023). Thus, *Brassica napus* roots seem to make use of adaptive RSA traits to cope with changing surroundings. The biological function of such root traits therefore seems to enable exploration of deeper and wider soil areas with access to potentially moist and/or fertile soil layers.

In addition, Boter *et al.* (2023) observed a reduction of meristem size and meristem cell numbers in both Drakkar and Duplo under higher temperature, whereas my data showed more subtle differences regarding meristematic parameters (Figs 3-5C-D, 3-6A). The authors examined the same parameters in elongation zone (EZ) and the first cell of the differentiation zone (DZ). For the variety Duplo, they observed promotion of root cell elongation at elevated temperature. Although the cellular profile of *Brassica napus* varies between varieties, this is obviously different from what I found in Arabidopsis roots (Fig. 3-5D). To test cell division rates, Boter *et al.* (2023) conducted EdU staining in *Brassica napus* roots, and they found that EdU incorporation rates

were similar at both tested temperatures in each of the two varieties. They concluded that warm temperatures do not strongly affect DNA replication in *Brassica napus* roots, whereas I observed the opposite in Arabidopsis (Fig. 3-7A). By scoring the ratio of DAPI-stained nuclei, the authors found a significant increase mitotic ratios in Duplo roots but not in Drakkar roots at 29°C, At least the behavior of Duplo seems therefore consistent with what I observed for (Fig. 3-7C). However, taken together, this strongly suggests that temperature-dependent changes of root system architecture are highly variable between species and even varieties/accessions on both morphological and anatomical levels.

Lateral roots occupy a certain volume ratio of RSA, which facilitates soil resource uptake capability (Rogers & Benfey, 2015). Soil temperature fluctuations have varying impact on lateral root growth and development across species. One example from sunflower demonstrated that lateral root length and branching positively correlate with increased soil temperature within an optimum range between 25°C to 30°C. In contrast, in a suboptimal range (below 25°C or above 30°C) both features decreased with temperature approaching suboptimum (Seiler, 1998). Nagel *et al*. (2009) found that in *Brassica napus* lateral root length was hardly affected by increased temperature, but they did observe temperature-promoted lateral root branching. In potato (Solanum tuberosum), root system development as generally indicated by lateral root numbers and length was largely inhibited at supra-optimum temperature, which coincided with reduced cell division of apical root as shown by mitotic index (Sattelmacher *et al*., 1990). Luo *et al*. (2020) reported that three common subtropical plant species with different forms of above-ground organs (herb, shrub and tree) displayed highly varying RSA at the seedling stage in a temperature range from 18°C to 34°C. They observed that the optimum growth temperature of *Corchorus capsularis L.* (a herb that often grows in humid environment in tropical Asia) roots is around 22°C with where lateral branching and length maximized. On the contrary, *Mimosa sepiaria* (a shrub favoring sunny

78

habitats native to tropical America) seems to be more temperature-tolerant as root traits (total root length, root depth, root width) were continuingly promoted by increased temperature up to 34°C (Luo *et al*., 2020). Interestingly, *Ormosia glaberrima* (an evergreen tree species preferring sunny habitats) seems to be temperature-insensitive as the overall RSA traits were hardly affected across the temperature range (Luo *et al*., 2020). Gladish & Rost (1993) showed that in garden pea seedlings (*Pisum sativum L.*) primary root growth is biphasic, either being promotive with decreasing temperature from 32°C to 25°C, or inhibitive with increasing temperature from 25°C to 32°C. This reversible growth pattern seems to associate with lateral root distribution along 10-12 cm of the primary root proximal to the above-ground organ. Here, the density of lateral roots is inversely dependent on respective temperature ranges shown above. A recent study in canola (*Brassica napus L.*) showed that temperature-sensitive RSA traits depend on developmental stages, with temperature responses of lateral roots contributing final changes of total root surface area and root volume in early and late flowering stages (Wu *et al.*, 2021). So far, the underlying molecular mechanisms controlling RSA modification (including lateral root branching and elongation) in a temperature context remain to be understood.

Based on this wealth of studies and observations from diverse species, it becomes evident that different species in different habitats may respond very differently to elevated temperatures in terms of root system architecture. Accordingly, the findings from Arabidopsis presented in this thesis ought not to be generalized. However, it is likely that the underlying molecular mechanism proposed in this thesis (temperature – auxin – cell cycle) is adopted across species.

4.6 Temperature regulation of adventitious roots and root hair development

Adventitious roots originate from shoot tissues, initiating at either normal or stress

conditions (Steffens & Rasmussen, 2016). Similar to the previous section, adventitious root formation also varies under different temperatures across different species, such as in *Eucalyptus, Bouteloua gracilis,* and Arabidopsis (Wilson, 1981; Garrido *et al.*, 1996; Kumar *et al.*, 1999; Corrêa & Fett-Neto, 2004; Konishi & Sugiyama, 2003). Regarding temperature-dependent cellular changes of adventitious roots, their anatomical adjustments have also been noticed: while adventitious root cell elongation rates seem to be accelerated at higher temperature as indicated by the earlier maturation of protophloem elements (closer location to root apex), the elongation period of cells is reduced. This suggests that cell division may precede cell elongation at higher temperatures or, vice versa, cell elongation takes precedence over cell division at lower temperatures (Beauchamp & Lathwell, 1966).

From an anatomical perspective, adventitious roots are classified as shoots tissues. Therefore, it is of great interest to determine whether they exhibit a similar response to moderately elevated temperatures as shoots do. This hypothesis can be investigated in Arabidopsis, as demonstrated by the presence of shoot temperature signaling mutants listed in Fig. 3-4A-B. Moreover, it is reasonable to anticipate that in Arabidopsis, adventitious roots will experience increased length at elevated temperatures due to cell elongation. However, further research is necessary to substantiate this claim. Additionally, it would be intriguing to explore whether shoot and root tissues demonstrate divergent responses across different species, potentially involving distinct cellular mechanisms such as cell elongation, cell division, or a combination thereof. Furthermore, auxin is also a driver of adventitious root formation, and it might also play a role in relaying temperature information here as well (Gutierrez *et al.*, 2012; Pop *et al.*, 2011; Fig. 3-11C)

Root hairs display small protuberance features along the root surface, aiding for nutrient and water uptake and anchorage of the root in the soil (Gilroy & Jones, 2000).

They are derived from specification and polarization of epidermal cells. Due to their unique stages of development, root hairs have emerged to be a useful model in understanding how plants specify cell fate and growth (Gilroy & Jones, 2000). Although research investigating root hair-related questions in a temperature context is still scarce, the temperature influence no doubt plays a crucial role on root hair growth and development in various species. For instance, Macduff *et al.* (1986) showed that temperature dependency of root hair density affected the total root surface area in oilseed and barley. They found that increased temperature (from 3°C to 25°C) had promoting effects on root hair density in both species, whereas oilseed and barley had the opposite temperature response patterns in terms of total root surface area, being either repressive or promotive respectively. In addition, (Dudeja & Khurana, 1989) showed that in pigeon pea (*Cajanus cajan*) above optimum temperature could lead to adverse impacts on root hair development and nodulation. More recently, temperature dependency of root hair development has been getting more attention, some even with detailed investigation on its molecular mechanisms (Fan *et al.*, 2022; Pacheco *et al.*, 2021; Pacheco *et al.*, 2022; Kim *et al.*, 2021). For example, Kim *et al.* (2021) identified a temperature-sensitive mutant *feronia-temperature sensitive* (*fer-ts*) which displayed cessation of root hair initiation and growth at 30°C. Based on fluorescent fusion protein carrying *fer-ts* mutation FER(G41S), they observed that at higher temperature FERONIA protein tends to be diffused or degraded within root hair cells, whereas apically polarized protein accumulation was observed at lower temperature. Furthermore, the authors used time-lapse imaging to monitor subcellular localization of FERONIA-eYFP reporters in either wild type or *fer-ts* backgrounds, and they found that the high temperature dependent cease of root hair growth in FER(G41S)-eYFP is perfectly correlated with decreased reporter signal intensity, whereas FER(WT)-eYFP signal was invariant with progressive root hair growth before and after high temperature treatment (Kim *et al.*, 2021). Taken together, this suggests that high temperature dependent FERONIA protein degradation is mediated by the point

mutation of FER(G41S), which is likely the reason contributing to root hair growth cessation.

In summary, the effects of temperature on root growth phenotypes extend beyond primary root elongation. Temperature also plays a significant role in adventitious root formation and root hair development, both of which are vital for plant development and growth.

4.7 Temperature association of below-ground interactions – plant fitness and microbiome behavior

In addition to its direct impact on root growth, temperature also influences the intricate interactions between roots and microorganisms within the soil, highlighting the root's role as an integral part of a complex ecosystem. Temperature variations in the soil environment can significantly affect the composition and activity of microorganisms that interact with roots. The diversity and abundance of beneficial microorganisms, such as endophytes and plant growth-promoting rhizobacteria (PGPR) are able to form symbiotic relationships with plant roots, facilitating nutrient uptake and enhancing the overall health and resilience of the plant under stress condition (Shaffique *et al.*, 2022). Temperature fluctuations also have a notable impact on the dynamics of nitrogen-fixing bacteria, including *Bradyrhizobium japonicum*, which form nodules on soybean roots. This, in turn, affects the efficiency of nitrogen fixation processes, and influences in conjunction with other rhizobacteria plant growth and the overall nitrogen cycling within the ecosystem (Zhang *et al*, 1997; Zhang *et al*, 1996)

Obviously, the impact of temperature extends beyond root growth and the interactions between roots and microorganisms. These interactions can significantly impact the physical and biological properties of the below-ground environment by giving rise to a diverse array of organic compounds derived from either plants or the microbiome.

Examples of such compounds include siderophores, 1-Aminocyclopropane-1-carboxylate (ACC) Deaminase, phytohormones, and volatile compounds (VOCs) (Shaffique *et al*., 2022). Notably, the interaction between plants and microorganisms can stimulate the production of VOCs, which have the potential to enhance RSA traits in Arabidopsis thaliana (García-Gómez *et al*., 2020). The improvement in RSA is correlated with increased activity of the DR5::GUS auxin reporter upon exposure to fungal VOCs. Interestingly, this response aligns with the root phenotypes and auxin reporter activity observed in seedlings exposed to moderately high temperatures (García-Gómez *et al*., 2020; Feraru *et al*., 2019; My data Fig. 3-2A, D, Fig. 3-11B). Hence, in natural soil conditions, elevated temperatures within the rhizosphere have the potential to enhance the interaction between the root system and microbiome. This can lead to an increased release of microbial VOCs with synergistic effects, resulting in improvement of root system with potentially better access to nutrient and water-rich soil layers.

By considering the influence of temperature on both root growth and the intricate web of microorganisms in the soil, we gain a deeper understanding of the root's pivotal role within the ecosystem. The root-microorganism interactions are highly sensitive to temperature variations, highlighting the complexity of below-ground processes and emphasizing the importance of holistic approaches in studying plant development, growth, and ecosystem dynamics. While research exploring temperature-mediated root-microbial interactions remains limited, their synergistic role in maintaining beneficial below-ground environment is evident. In this context, microorganisms are expected to produce distinct anti-stress or growth-promoting substances within the plant root system to ensure their proliferation in response to varying temperatures. Therefore, several key questions warrant further investigation: (i) What precise mechanisms drive temperature-induced alterations in plant-microbial interactions? (ii) What are the shared targets of their interaction? (iii) Do they evolve shared

temperature sensing and signaling pathways? Additionally, unraveling distinct temperature sensing mechanisms between plants and microorganisms represents an important avenue for future exploration.

4.8 Biological significance of temperature-induced growth phenotypes and their potential applications for crop production

Exploring the potential benefits of shoot thermomorphogenic and root thermomorphogenic phenotypes, as well as their likelihood of occurrence, sheds light on the adaptive responses of plants to temperature changes.

Shoot thermomorphogenic phenotypes refer to the alterations in shoot morphology and development driven by temperatures. These phenotypes encompass various responses in Arabidopsis seedlings, such as hyponasty, elongation of hypocotyls and petioles, as well as the development of opened rosette structures in mature stages (Fig. 1-2). A recent study by Saini *et al.* (2022) further identified leaf size as a temperature-responsive trait. It is noteworthy that shoot thermomorphogenesis, including hyponasty and petiole elongation, is commonly observed in field-cultivated crops, as these phenotypes are also associated with shade avoidance. And in the field, plants compete for access to light as soon as neighboring plants are detected. However, exaggerated elongation growth often leads to lodging, reducing stability and hindering higher yields during the reproductive stage. Therefore, there is a need for plants that do not exhibit shade avoidance or temperature-responsive traits, which would result in larger leaves with increased photosynthetic assimilation capacity, coupled with shorter stems for improved stability.

On the other hand, root thermomorphogenic phenotypes describe the temperature-induced changes in root architecture and growth. These phenotypes involve alterations in root length, branching, and distribution in the soil. Such adaptations can enhance

the plant's ability to access nutrients and water in response to varying temperature regimes. For instance, increased root branching can enhance nutrient acquisition and water uptake in cooler soils, whereas elongated primary roots may aid in reaching deeper soil layers during warmer conditions. Although an extended root system requires additional energy, which could otherwise be allocated to shoot growth, it can serve as a valuable acclimation for plants to withstand periods of drought.

Overall, the manifestation of shoot and root thermomorphogenic phenotypes in plants reflects their remarkable capacity to adjust and optimize their growth and development in response to temperature fluctuations. Understanding the benefits and likelihood of occurrence of these phenotypes contributes to our broader comprehension of plant resilience and their ability to thrive in diverse environmental conditions.

The repercussions of climate change have emerged as a significant global concern, with profound implications for wild species, including shifts in their distribution and seasonal behaviors on a large scale. Unexpected hot weather events, such as those in 2016 and 2020 (Data source: NASA's Goddard Institute for Space Studies, GISS), have raised alarms about crop productivity and global food security (Thuiller *et al.*, 2005; Battisti & Naylor, 2009; Bellard *et al.*, 2012). In contrast to thermomorphogenesis, the response of plants to actual episodes of heat stress is notably different and encompasses a wide range of physiological and biochemical changes. When subjected to heat stress, plants activate a complex set of responses aimed at mitigating detrimental effects of high temperatures. These responses include alterations in gene expression, changes in cellular metabolism, and adjustments in physiological processes (Guihur *et al.*, 2022; Lippmann *et al.*, 2019). Among these responses, the activation of heat shock proteins (HSPs) plays a critical role as molecular chaperones, preserving protein structure and cellular integrity under heat stress conditions (Guihur *et al.*, 2022). Thus, gaining a comprehensive understanding of these responses is

essential for developing strategies to enhance heat tolerance in crops and alleviate the adverse impacts of rising temperatures on agriculture and ecosystems.

During the process of domestication and modern plant breeding, it is possible that alleles conferring protection against extreme heat have been lost, leading to a reduction in genetic diversity. Consequently, exploring the wild progenitors becomes crucial to identify heat-protective alleles. Utilizing genome sequencing techniques with a wide range of genetic backgrounds is a viable approach in this endeavor. However, considering the massive amount of genetic data involved, this represents an indirect breeding method. An alternative and promising avenue in this context is the utilization of CRISPR/Cas9 technology, which enables precise engineering of targeted genome sequences. Moreover, as crop breeding is a complex process and target genes often exhibit minor effects on specific agronomic traits, it is common practice to combine multiple genes or even entire pathways to achieve the desired crop varieties.

Promising alleles that hold potential for enhancing stress tolerance include the receptor-like kinase ERECTA and the homeodomain (HD)-START transcription factor HDG11, both known for their crucial roles in drought stress tolerance (Shen *et al.*, 2015; Yu *et al*, 2008). Overexpression of ERECTA has been demonstrated to confer drought stress tolerance in Arabidopsis, tomato, and rice, without compromising crop yield. Similarly, overexpressing HDG11 has been shown to enhance thermotolerance in Arabidopsis and tobacco, resulting in expanded root systems and reduced stomatal density. Key regulators of thermomorphogenesis, such as PIF4 and components of the evening complex (EC), represent promising candidates as they contribute to early flowering time, which might associate with temperature fluctuations. In Arabidopsis, these genes have been shown to regulate thermomorphogenic responses in controlled laboratory conditions (Kumar *et al.,* 2012; Box *et al.*, 2015; Raschke *et al.*, 2015). However, it remains to be seen whether these temperature-dependent phenotypes are

still present under natural conditions, and whether these regulatory effects are conserved in major crop species. Additionally, allelic variations of ELF3 and ELF4, known for their influence on flowering time adaptation, have provided valuable insights for the introduction of crops into specific geographical and climatic regions (Nakamichi, 2015; Zhu *et al.*, 2022).

Despite significant advancements in understanding the mechanistic aspects of thermomorphogenesis over the past 15 years, the practical implementation of this knowledge in breeding programs is still in its early stages. Initial breeding efforts have primarily focused on integrating shoot traits such as flowering time and crop yield under specific temperature regimes. While investigating temperature-related root traits in natural conditions poses challenges, the importance of root temperature resilience in contributing to overall plant fitness has gained considerable attention. It is noteworthy that research on root thermomorphogenesis remains limited, and further advancements in this field are essential to meet the fundamental and advanced requirements for breeding thermo-resilient or thermotolerant crops, particularly in the context of global warming.

Chapter 5: Conclusion and outlook

In this thesis, I aimed to connect the missing dots between publications on specific perspectives of root thermomorphogenesis by carrying out experiments that cover the existing knowledge gaps. On this basis, I propose a comprehensive model suggesting that roots can autonomously sense and respond to elevated ambient temperatures (Fig. 5-1). In elevated temperatures, one or several yet unknown root thermosensor(s) activate(s) *de novo* local auxin biosynthesis via the indole-3-pyruvic acid pathway, most likely taking place within or close to the root apical meristem. The generated auxin maximum in the root tip is maintained in a PIN-dependent manner and promotes the cell cycle entry of root meristem cells, causing an acceleration of cell division rates. As such, auxin functions as a gas pedal. However, the role of PIN4 seems more complex than suggested in this simple model. I find that a likely reason for the hypersensitive root elongation response of *pin4-2* mutants in high temperature is an increase in meristem size. To use the same analogy as above, at elevated temperatures functional PIN4 might not only redistribute auxin in the columella, but also act as a brake pedal, restricting meristem size and thereby preventing hyperelongation of the root.
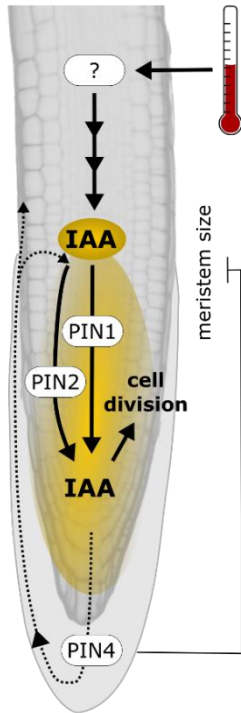
Fig. 5-1 Schematic model of the major regulatory processes in the root apical meristem during root thermomorphogenesis.

Elevated temperature sensed by a yet unknown thermosensor induces auxin biosynthesis, resulting in elevated auxin levels in the root tip. Polar auxin transporters PIN1, PIN2, and PIN4 help to maintain an auxin maximum in the root apical meristem which increases cell division rates, driving primary root elongation. In addition, functional PIN4 restricts meristem size at elevated temperature, possibly preventing excessive root growth.

Auxin action on the cell cycle seems to play an essential role in root thermomorphogenesis. Therefore, detailed mechanistic insights are needed to identify temperature-mediated cell cycle regulation, and to find out how hormonal crosstalk feeds into this regulatory network. In addition, transcriptional and translational analyses will be informative for specific temperature-responsive cell cycle components. For example, elucidation of temperature effects on (a) KRP interaction with CDKA/CYCD complexes; (b) RBR protein; (c) E2F transcriptional target gene activation; all of which are anticipated to expand new routes to explain the link between cell cycle progression and temperature-induced root growth (Fig. 1-7; Fig. 3-8A-C). Furthermore, application of single cell RNA-seq will provide exact information about how heterogeneity of cell types (root cells) integrates temperature information into different cell fates (cell cycle status) and then finally triggering of growth responses.

In any case, to understand root thermomorphogenesis on a mechanistic level, we might have to refrain from trying to find parallels to shoot thermo-signaling pathways, because thermosensing is likely differently regulated in root organs. Besides, we hardly know anything about the nature of root thermosensors. A hypothetical scene may be

thermosensing occurring in parallel with root growth events, which would allow 'short-distance' signal transduction from the site of sensing to the primary growth promoting cellular process, cell division, possibly both being located within or around the root apical meristem. Such a strategy would fit with the feature of root plasticity in response to changing soil temperatures, and the root can adjust its thermomorphogenic behavior based on the soil temperature it has been exposed to. While this seems rather one-dimensional, it certainly could be a highly versatile system. Provided that the same mechanism is incorporated in the whole root system, root plasticity in different soil temperatures may then be divided into separate root sensing modules. In this regard, multiple thermosensors may be active in different parts of root, integrating complex temperature information for optimizing growth. If this is the case, roots would require a carrier transporting temperature information from various regions in the root to the root apical meristem. Auxin would be an ideal candidate for this type of mobile signal.

References

GISTEMP Team. 2023. GISS Surface Temperature Analysis (GISTEMP), version 4. NASA Goddard Institute for Space Studies. Dataset accessed 2023-03-02 at https://data.giss.nasa.gov/gistemp/.

IPCC, 2018: Global warming of 1.5°C. An IPCC Special Report on the impacts of global warming of 1.5°C above pre-industrial levels and related global greenhouse gas emission pathways, in the context of strengthening the global response to the threat of climate change, sustainable development, and efforts to eradicate poverty [V. Masson-Delmotte, P. Zhai, H. O. Pörtner, D. Roberts, J. Skea, P.R. Shukla, A. Pirani, W. Moufouma-Okia, C. Péan, R. Pidcock, S. Connors, J. B. R. Matthews, Y. Chen, X. Zhou, M. I. Gomis, E. Lonnoy, T. Maycock, M. Tignor, T. Waterfield (eds.)]. In Press.

United Nations, Department of Economic and Social Affairs, Population Division (2019) World Population Prospects 2019: Highlights. ST/ESA/SER. A/423

Achard P, Liao L, Jiang C, Desnos T, Bartlett J, Fu X & Harberd NP (2007) DELLAs Contribute to Plant Photomorphogenesis. *Plant Physiology* 143: 1163–1172

Ali M. Pahlavanian & Silk WK (1988) Effect of Temperature on Spatial and Temporal Aspects of Growth in the Primary Maize Root. *Plant Physiology* 87: 529–532

Anwer MU, Davis A, Davis SJ & Quint M (2020) Photoperiod sensing of the circadian clock is controlled by EARLY FLOWERING 3 and GIGANTEA. *The Plant Journal* 101: 1397–1410

Bai M-Y, Shang J-X, Oh E, Fan M, Bai Y, Zentella R, Sun T & Wang Z-Y (2012) Brassinosteroid, gibberellin and phytochrome impinge on a common transcription module in Arabidopsis. *Nature Cell Biology* 14: 810–817

Bartusch K, Trenner J, Melnyk CW & Quint M (2020) Cut and paste: temperature-enhanced cotyledon micrografting for Arabidopsis thaliana seedlings. *Plant Methods* 16: 12

Battisti DavidS & Naylor RL (2009) Historical Warnings of Future Food Insecurity with Unprecedented Seasonal Heat. *Science* 323: 240–244

Beauchamp E & Lathwell DJ (1966) Root-zone temperature effects on the vascular development of adventitious roots in Zea mays. *Botanical Gazette* 127: 153–158

Bellard C, Bertelsmeier C, Leadley P, Thuiller W & Courchamp F (2012) Impacts of

climate change on the future of biodiversity. *Ecology Letters* 15: 365–377

Bellstaedt J, Trenner J, Lippmann R, Poeschl Y, Zhang X, Friml J, Quint M & Delker C (2019) A Mobile Auxin Signal Connects Temperature Sensing in Cotyledons with Growth Responses in Hypocotyls. *Plant Physiology* 180: 757–766

Ben-Haj-Salah H & Tardieu F (1995) Temperature Affects Expansion Rate of Maize Leaves without Change in Spatial Distribution of Cell Length (Analysis of the Coordination between Cell Division and Cell Expansion). *Plant Physiology* 109: 861–870

Berckmans B, Vassileva V, Schmid SPC, Maes S, Parizot B, Naramoto S, Magyar Z, Kamei CLA, Koncz C, Bögre L, *et al* (2011) Auxin-Dependent Cell Cycle Reactivation through Transcriptional Regulation of Arabidopsis E2Fa by Lateral Organ Boundary Proteins. *The Plant Cell* 23: 3671–3683

Bernardo-García S, de Lucas M, Martínez C, Espinosa-Ruiz A, Davière J-M & Prat S (2014) BR-dependent phosphorylation modulates PIF4 transcriptional activity and shapes diurnal hypocotyl growth. *Genes & Development* 28: 1681–1694

Borniego MB, Costigliolo-Rojas C & Casal JJ (2022) Shoot thermosensors do not fulfil the same function in the root. *New Phytologist* 236: 9–14

Boter M, Pozas J, Jarillo JA, Piñeiro M & Pernas M (2023) Brassica napus Roots Use Different Strategies to Respond to Warm Temperatures. *International Journal of Molecular Sciences* 24

Boudolf V, Inzé D & De Veylder L (2006) What if higher plants lack a CDC25 phosphatase? *Trends in Plant Science* 11: 474–479

Box MS, Huang BE, Domijan M, Jaeger KE, Khattak AK, Yoo SJ, Sedivy EL, Jones DM, Hearn TJ, Webb AAR, *et al* (2015) ELF3 Controls Thermoresponsive Growth in Arabidopsis. *Current Biology* 25: 194–199

BURSTRÖM H (1953) Studies on Growth and Metabolism of Roots. IX. Cell Elongation and Water Absorption. *Physiologia Plantarum* 6: 262–276

Carmona MJ & Cuadrado A (1986) Analysis of growth components in Allium roots. *Planta* 168: 183–189

Casal JJ & Balasubramanian S (2019) Thermomorphogenesis. *Annu Rev Plant Biol* 70: 321–346

Chae K, Isaacs CG, Reeves PH, Maloney GS, Muday GK, Nagpal P & Reed JW (2012) Arabidopsis SMALL AUXIN UP RNA63 promotes hypocotyl and stamen

filament elongation. *The Plant Journal* 71: 684–697

Challinor AJ, Watson J, Lobell DB, Howden SM, Smith DR & Chhetri N (2014) A meta-analysis of crop yield under climate change and adaptation. *Nature Climate Change* 4: 287–291

Chen M, Tao Y, Lim J, Shaw A & Chory J (2005) Regulation of Phytochrome B Nuclear Localization through Light-Dependent Unmasking of Nuclear-Localization Signals. *Current Biology* 15: 637–642

Chen Q, Dai X, De-Paoli H, Cheng Y, Takebayashi Y, Kasahara H, Kamiya Y & Zhao Y (2014) Auxin Overproduction in Shoots Cannot Rescue Auxin Deficiencies in Arabidopsis Roots. *Plant and Cell Physiology* 55: 1072–1079

Christian Wenzl & Jan U. Lohmann (2023) 3D imaging reveals apical stem cell responses to ambient temperature. *bioRxiv*: 2023.05.04.539361

Chung BYW, Balcerowicz M, Di Antonio M, Jaeger KE, Geng F, Franaszek K, Marriott P, Brierley I, Firth AE & Wigge PA (2020) An RNA thermoswitch regulates daytime growth in Arabidopsis. *Nature Plants* 6: 522–532

Churchman ML, Brown ML, Kato N, Kirik V, Hülskamp M, Inzé D, De Veylder L, Walker JD, Zheng Z, Oppenheimer DG, *et al* (2006) SIAMESE, a Plant-Specific Cell Cycle Regulator, Controls Endoreplication Onset in Arabidopsis thaliana. *The Plant Cell* 18: 3145–3157

Corrêa LDR & Fett-Neto AG (2004) Effects of temperature on adventitious root development in microcuttings of Eucalyptus saligna Smith and Eucalyptus globulus Labill. *Journal of Thermal Biology* 29: 315–324

Covington MF, Panda S, Liu XL, Strayer CA, Wagner DR & Kay SA (2001) ELF3 Modulates Resetting of the Circadian Clock in Arabidopsis. *The Plant Cell* 13: 1305–1316

Crawford AJ, McLachlan DH, Hetherington AM & Franklin KA (2012) High temperature exposure increases plant cooling capacity. *Current Biology* 22: R396–R397

Czechowski T, Stitt M, Altmann T, Udvardi MK & Scheible W-R (2005) Genome-Wide Identification and Testing of Superior Reference Genes for Transcript Normalization in Arabidopsis. *Plant Physiology* 139: 5–17

De Veylder L, Beeckman T & Inzé D (2007) The ins and outs of the plant cell cycle. *Nature Reviews Molecular Cell Biology* 8: 655–665

Delker C, Quint M & Wigge PA (2022) Recent advances in understanding

thermomorphogenesis signaling. *Current Opinion in Plant Biology* 68: 102231

Delker C, Sonntag L, James GV, Janitza P, Ibañez C, Ziermann H, Peterson T, Denk K, Mull S, Ziegler J, *et al* (2014) The DET1-COP1-HY5 Pathway Constitutes a Multipurpose Signaling Module Regulating Plant Photomorphogenesis and Thermomorphogenesis. *Cell Reports* 9: 1983–1989

Delker C, van Zanten M & Quint M (2017) Thermosensing Enlightened. *Trends in Plant Science* 22: 185–187

Domisch T, Finér L & Lehto T (2001) Effects of soil temperature on biomass and carbohydrate allocation in Scots pine (Pinus sylvestris) seedlings at the beginning of the growing season. *Tree Physiology* 21: 465–472

DUDEJA SS & KHURANA AL (1989) The Pigeonpea-Rhizobium Symbiosis as Affected by High Root Temperture: Effect on Nodule Formation. *Journal of Experimental Botany* 40: 469–472

Erickson RO (1959) Integration of Plant Growth Processes. *The American Naturalist* 93: 225–235

Erickson RO & Sax KB (1956) Rates of Cell Division and Cell Elongation in the Growth of the Primary Root of Zea mays. *Proceedings of the American Philosophical Society* 100: 499–514

Fan C, Hou M, Si P, Sun H, Zhang K, Bai Z, Wang G, Li C, Liu L & Zhang Y (2022) Response of root and root hair phenotypes of cotton seedlings under high temperature revealed with RhizoPot. *Frontiers in Plant Science* 13

Fang S, Yan X & Liao H (2009) 3D reconstruction and dynamic modeling of root architecture in situ and its application to crop phosphorus research. *The Plant Journal* 60: 1096–1108

Fei Q, Wei S, Zhou Z, Gao H & Li X (2017) Adaptation of root growth to increased ambient temperature requires auxin and ethylene coordination in Arabidopsis. *Plant Cell Reports* 36: 1507–1518

Fei Q, Zhang J, Zhang Z, Wang Y, Liang L, Wu L, Gao H, Sun Y, Niu B & Li X (2019) Effects of auxin and ethylene on root growth adaptation to different ambient temperatures in Arabidopsis. *Plant Science* 281: 159–172

Feng S, Martinez C, Gusmaroli G, Wang Y, Zhou J, Wang F, Chen L, Yu L, Iglesias-Pedraz JM, Kircher S, *et al* (2008) Coordinated regulation of Arabidopsis thaliana development by light and gibberellins. *Nature* 451: 475–479

Feraru E, Feraru MI, Barbez E, Waidmann S, Sun L, Gaidora A & Kleine-Vehn J (2019) PILS6 is a temperature-sensitive regulator of nuclear auxin input and organ growth in Arabidopsis thaliana. *Proceedings of the National Academy of Sciences* 116: 3893–3898

Fiorucci A-S, Galvão VC, Ince YÇ, Boccaccini A, Goyal A, Allenbach Petrolati L, Trevisan M & Fankhauser C (2020) PHYTOCHROME INTERACTING FACTOR 7 is important for early responses to elevated temperature in Arabidopsis seedlings. *New Phytologist* 226: 50–58

Fonseca de Lima CF, Kleine-Vehn J, De Smet I & Feraru E (2021) Getting to the root of belowground high temperature responses in plants. *Journal of Experimental Botany* 72: 7404–7413

Forbes PJ, Black KE & Hooker JE (1997) Temperature-induced alteration to root longevity in Lolium perenne. *Plant and Soil* 190: 87–90

Fortin M-CA & Poff KL (1990) Temperature Sensing by Primary Roots of Maize 1. *Plant Physiology* 94: 367–369

Franklin KA, Lee SH, Patel D, Kumar SV, Spartz AK, Gu C, Ye S, Yu P, Breen G, Cohen JD, *et al* (2011) PHYTOCHROME-INTERACTING FACTOR 4 (PIF4) regulates auxin biosynthesis at high temperature. *Proceedings of the National Academy of Sciences* 108: 20231–20235

Friml J, Benková E, Blilou I, Wisniewska J, Hamann T, Ljung K, Woody S, Sandberg G, Scheres B, Jürgens G, *et al* (2002) AtPIN4 Mediates Sink-Driven Auxin Gradients and Root Patterning in Arabidopsis. *Cell* 108: 661–673

Gaillochet C, Burko Y, Platre MP, Zhang L, Simura J, Willige BC, Kumar SV, Ljung K, Chory J & Busch W (2020) HY5 and phytochrome activity modulate shoot-to-root coordination during thermomorphogenesis in Arabidopsis. *Development* 147: dev192625

García-Gómez P, Bahaji A, Gámez-Arcas S, Muñoz FJ, Sánchez-López ÁM, Almagro G, Baroja-Fernández E, Ameztoy K, De Diego N, Ugena L, *et al* (2020) Volatiles from the fungal phytopathogen Penicillium aurantiogriseum modulate root metabolism and architecture through proteome resetting. *Plant, Cell & Environment* 43: 2551–2570

Garrido G, Cano EA, Amao MB, Acosta M & Sánchez-Bravo J (1996) Influence of cold storage period and auxin treatment on the subsequent rooting of carnation cuttings. *Scientia horticulturae* 65: 73–84

Gilroy S & Jones DL (2000) Through form to function: root hair development and

nutrient uptake. *Trends in plant science* 5: 56–60

Gladish DK & Rost TL (1993) The effects of temperature on primary root growth dynamics and lateral root distribution in garden pea (Pisum sativum L., cv. "Alaska"). *Environmental and Experimental Botany* 33: 243–258

González-García MP, Conesa CM, Lozano-Enguita A, Baca-González V, Simancas B, Navarro-Neila S, Sánchez-Bermúdez M, Salas-González I, Caro E, Castrillo G, *et al* (2022) Temperature changes in the root ecosystem affect plant functionality. *Plant Communications*: 100514

Grabov A, Ashley MK, Rigas S, Hatzopoulos P, Dolan L & Vicente-Agullo F (2005) Morphometric analysis of root shape. *New Phytologist* 165: 641–652

GRANIER C, MASSONNET C, TURC O, MULLER B, CHENU K & TARDIEU F (2002) Individual Leaf Development in Arabidopsis thaliana: a Stable Thermal‐time‐based Programme. *Annals of Botany* 89: 595–604

Granier C & Tardieu F (1998) Is thermal time adequate for expressing the effects of temperature on sunflower leaf development? *Plant, Cell & Environment* 21: 695–703

Gray WM, Östin A, Sandberg G, Romano CP & Estelle M (1998) High temperature promotes auxin-mediated hypocotyl elongation in Arabidopsis. *Proceedings of the National Academy of Sciences* 95: 7197–7202

Grieneisen VA, Xu J, Marée AFM, Hogeweg P & Scheres B (2007) Auxin transport is sufficient to generate a maximum and gradient guiding root growth. *Nature* 449: 1008–1013

Grif VG, Ivanov VB & Machs EM (2002) Cell cycle and its parameters in flowering plants. *Tsitologiia* 44: 936–980

Grif VG & Valovich EM (1973) mitotic cycle of plant cells at the minimal temperature of mitosis. *TSitologiia*

Guihur A, Rebeaud ME & Goloubinoff P (2022) How do plants feel the heat and survive? *Trends in Biochemical Sciences* 47: 824–838

Gutierrez C (2016) 25 Years of Cell Cycle Research: What's Ahead? *Trends in Plant Science* 21: 823–833

Gutierrez L, Mongelard G, Floková K, Păcurar DI, Novák O, Staswick P, Kowalczyk M, Păcurar M, Demailly H, Geiss G, *et al* (2012) Auxin Controls Arabidopsis Adventitious Root Initiation by Regulating Jasmonic Acid Homeostasis. *The*

Plant Cell 24: 2515–2527

Hanzawa T, Shibasaki K, Numata T, Kawamura Y, Gaude T & Rahman A (2013) Cellular Auxin Homeostasis under High Temperature Is Regulated through a SORTING NEXIN1–Dependent Endosomal Trafficking Pathway. *The Plant Cell* 25: 3424–3433

Hayashi K, Neve J, Hirose M, Kuboki A, Shimada Y, Kepinski S & Nozaki H (2012) Rational Design of an Auxin Antagonist of the SCFTIR1 Auxin Receptor Complex. *ACS Chem Biol* 7: 590–598

He W, Brumos J, Li H, Ji Y, Ke M, Gong X, Zeng Q, Li W, Zhang X, An F, *et al* (2011) A Small-Molecule Screen Identifies l-Kynurenine as a Competitive Inhibitor of TAA1/TAR Activity in Ethylene-Directed Auxin Biosynthesis and Root Growth in Arabidopsis. *The Plant Cell* 23: 3944–3960

Hong S-Y, Seo PJ, Ryu JY, Cho S-H, Woo J-C & Park C-M (2013) A competitive peptide inhibitor KIDARI negatively regulates HFR1 by forming nonfunctional heterodimers in Arabidopsis photomorphogenesis. *Molecules and Cells* 35: 25–31

Ibañez C, Delker C, Martinez C, Bürstenbinder K, Janitza P, Lippmann R, Ludwig W, Sun H, James GV, Klecker M, *et al* (2018) Brassinosteroids Dominate Hormonal Regulation of Plant Thermomorphogenesis via BZR1. *Current Biology* 28: 303-310.e3

Ibañez C, Poeschl Y, Peterson T, Bellstädt J, Denk K, Gogol-Döring A, Quint M & Delker C (2017) Ambient temperature and genotype differentially affect developmental and phenotypic plasticity in Arabidopsis thaliana. *BMC Plant Biology* 17: 114

Inzé D & De Veylder L (2006) Cell Cycle Regulation in Plant Development. *Annu Rev Genet* 40: 77–105

Ito M, Araki S, Matsunaga S, Itoh T, Nishihama R, Machida Y, Doonan JH & Watanabe A (2001) G2/M-Phase-Specific Transcription during the Plant Cell Cycle Is Mediated by c-Myb-Like Transcription Factors. *The Plant Cell* 13: 1891–1905

Ito M, Iwase M, Kodama H, Lavisse P, Komamine A, Nishihama R, Machida Y & Watanabe A (1998) A Novel cis-Acting Element in Promoters of Plant B-Type Cyclin Genes Activates M Phase–Specific Transcription. *The Plant Cell* 10: 331–341

Jung J-H, Barbosa AD, Hutin S, Kumita JR, Gao M, Derwort D, Silva CS, Lai X, Pierre E, Geng F, *et al* (2020) A prion-like domain in ELF3 functions as a thermosensor in Arabidopsis. *Nature* 585: 256–260

Jung J-H, Domijan M, Klose C, Biswas S, Ezer D, Gao M, Khattak AK, Box MS, Charoensawan V, Cortijo S, *et al* (2016) Phytochromes function as thermosensors in Arabidopsis. *Science* 354: 886–889

Kim D, Yang J, Gu F, Park S, Combs J, Adams A, Mayes HB, Jeon SJ, Bahk JD & Nielsen E (2021) A temperature-sensitive FERONIA mutant allele that alters root hair growth. *Plant Physiology* 185: 405–423

Klose C, Venezia F, Hussong A, Kircher S, Schäfer E & Fleck C (2015) Systematic analysis of how phytochrome B dimerization determines its specificity. *Nature Plants* 1: 15090

Koini MA, Alvey L, Allen T, Tilley CA, Harberd NP, Whitelam GC & Franklin KA (2009) High Temperature-Mediated Adaptations in Plant Architecture Require the bHLH Transcription Factor PIF4. *Current Biology* 19: 408–413

Konishi M & Sugiyama M (2003) Genetic analysis of adventitious root formation with a novel series of temperature-sensitive mutants of Arabidopsis thaliana.

Kumar A, Sood A, Palni LMS & Gupta AK (1999) In vitro propagation of Gladiolus hybridus Hort.: Synergistic effect of heat shock and sucrose on morphogenesis. *Plant Cell, Tissue and Organ Culture* 57: 105–112

Kumar SV, Lucyshyn D, Jaeger KE, Alós E, Alvey E, Harberd NP & Wigge PA (2012) Transcription factor PIF4 controls the thermosensory activation of flowering. *Nature* 484: 242–245

Kurihara D, Mizuta Y, Sato Y & Higashiyama T (2015) ClearSee: a rapid optical clearing reagent for whole-plant fluorescence imaging. *Development* 142: 4168–4179

Lee S, Wang W & Huq E (2021) Spatial regulation of thermomorphogenesis by HY5 and PIF4 in Arabidopsis. *Nature Communications* 12: 3656

Legris M, Klose C, Burgie ES, Rojas CCR, Neme M, Hiltbrunner A, Wigge PA, Schäfer E, Vierstra RD & Casal JJ (2016) Phytochrome B integrates light and temperature signals in Arabidopsis. *Science* 354: 897–900

Lincoln C, Britton JH & Estelle M (1990) Growth and development of the axr1 mutants of Arabidopsis. *The Plant Cell* 2: 1071–1080

Lippmann R, Babben S, Menger A, Delker C & Quint M (2019) Development of Wild and Cultivated Plants under Global Warming Conditions. *Current Biology* 29: R1326–R1338

Lobell DB, Bänziger M, Magorokosho C & Vivek B (2011) Nonlinear heat effects on

African maize as evidenced by historical yield trials. *Nature Climate Change* 1: 42–45

Ludwig W, Hayes S, Trenner J, Delker C & Quint M (2021) On the evolution of plant thermomorphogenesis. *Journal of Experimental Botany* 72: 7345–7358

Luo H, Xu H, Chu C, He F & Fang S (2020) High Temperature can Change Root System Architecture and Intensify Root Interactions of Plant Seedlings. *Frontiers in Plant Science* 11

Luschnig C, Gaxiola RA, Grisafi P & Fink GR (1998) EIR1, a root-specific protein involved in auxin transport, is required for gravitropism inArabidopsis thaliana. *Genes & Development* 12: 2175–2187

Macduff JH, Wild A, Hopper MJ & Dhanoa MS (1986) Effects of temperature on parameters of root growth relevant to nutrient uptake: Measurements on oilseed rape and barley grown in flowing nutrient solution. *Plant and Soil* 94: 321–332

Martins S, Montiel-Jorda A, Cayrel A, Huguet S, Roux CP-L, Ljung K & Vert G (2017) Brassinosteroid signaling-dependent root responses to prolonged elevated ambient temperature. *Nature Communications* 8: 309

Melnyk CW (2017) Plant grafting: insights into tissue regeneration. *Regeneration* 4: 3–14

Müller A, Guan C, Gälweiler L, Tänzler P, Huijser P, Marchant A, Parry G, Bennett M, Wisman E & Palme K (1998) AtPIN2 defines a locus of Arabidopsis for root gravitropism control. *The EMBO Journal* 17: 6903–6911

Murashige T & Skoog F (1962) A Revised Medium for Rapid Growth and Bio Assays with Tobacco Tissue Cultures. *Physiologia Plantarum* 15: 473–497

Murín A (1966) The effect of temperature on the mitotic cycle and its time parameters in root tips of Vicia faba. *Naturwissenschaften* 53: 312–313

Murín A (1981) Regulation of the mitotic cycle in seedling roots of Vicia faba by environmental factors. In *Structure and Function of Plant Roots: Proceedings of the 2nd International Symposium, held in Bratislava, Czechoslovakia, September 1–5, 1980* pp 15–18. Springer

Nagel KA, Kastenholz B, Jahnke S, van Dusschoten D, Aach T, Mühlich M, Truhn D, Scharr H, Terjung S, Walter A, *et al* (2009) Temperature responses of roots: impact on growth, root system architecture and implications for phenotyping. *Funct Plant Biol* 36: 947–959

Nakamichi N (2015) Adaptation to the Local Environment by Modifications of the Photoperiod Response in Crops. *Plant and Cell Physiology* 56: 594–604

Nieto C, López-Salmerón V, Davière J-M & Prat S (2015) ELF3-PIF4 Interaction Regulates Plant Growth Independently of the Evening Complex. *Current Biology* 25: 187–193

Nishimura K, Fukagawa T, Takisawa H, Kakimoto T & Kanemaki M (2009) An auxin-based degron system for the rapid depletion of proteins in nonplant cells. *Nature Methods* 6: 917–922

Nishimura T, Hayashi K, Suzuki H, Gyohda A, Takaoka C, Sakaguchi Y, Matsumoto S, Kasahara H, Sakai T, Kato J, *et al* (2014) Yucasin is a potent inhibitor of YUCCA, a key enzyme in auxin biosynthesis. *The Plant Journal* 77: 352–366

Oh E, Zhu J-Y & Wang Z-Y (2012) Interaction between BZR1 and PIF4 integrates brassinosteroid and environmental responses. *Nature Cell Biology* 14: 802–809

Pacheco JM, Mansilla N, Moison M, Lucero L, Gabarain VB, Ariel F & Estevez JM (2021) The lncRNA APOLO and the transcription factor WRKY42 target common cell wall EXTENSIN encoding genes to trigger root hair cell elongation. *Plant Signaling & Behavior* 16: 1920191

Pacheco JM, Ranocha P, Kasulin L, Fusari CM, Servi L, Aptekmann ArielA, Gabarain VB, Peralta JM, Borassi C, Marzol E, *et al* (2022) Apoplastic class III peroxidases PRX62 and PRX69 promote Arabidopsis root hair growth at low temperature. *Nature Communications* 13: 1310

Parent B & Tardieu F (2012) Temperature responses of developmental processes have not been affected by breeding in different ecological areas for 17 crop species. *New Phytologist* 194: 760–774

Park Y-J, Lee H-J, Gil K-E, Kim JY, Lee J-H, Lee H, Cho H-T, Vu LD, De Smet I & Park C-M (2019a) Developmental Programming of Thermonastic Leaf Movement. *Plant Physiology* 180: 1185–1197

Park Y-J, Lee H-J, Gil K-E, Kim JY, Lee J-H, Lee H, Cho H-T, Vu LD, De Smet I & Park C-M (2019b) Developmental Programming of Thermonastic Leaf Movement. *Plant Physiology* 180: 1185–1197

Perrot-Rechenmann C (2010) Cellular Responses to Auxin: Division versus Expansion. *Cold Spring Harbor Perspectives in Biology* 2

POP TI, PAMFIL D & BELLINI C (2011) Auxin Control in the Formation of Adventitious

Roots. *Not Bot Horti Agrobo* 39: 307–316

del Pozo JC, Boniotti MB & Gutierrez C (2002) Arabidopsis E2Fc Functions in Cell Division and Is Degraded by the Ubiquitin-SCFAtSKP2 Pathway in Response to Light[W]. *The Plant Cell* 14: 3057–3071

del Pozo JC & Manzano C (2014) Auxin and the ubiquitin pathway. Two players–one target: the cell cycle in action. *Journal of Experimental Botany* 65: 2617–2632

Quint M, Barkawi LS, Fan K-T, Cohen JD & Gray WM (2009) Arabidopsis IAR4 Modulates Auxin Response by Regulating Auxin Homeostasis. *Plant Physiology* 150: 748–758

Quint M, Delker C, Franklin KA, Wigge PA, Halliday KJ & van Zanten M (2016) Molecular and genetic control of plant thermomorphogenesis. *Nature Plants* 2: 15190

Quint M & Gray WM (2006) Auxin signaling. *Current Opinion in Plant Biology* 9: 448–453

Quint M, Ito H, Zhang W & Gray WM (2005) Characterization of a novel temperature-sensitive allele of the CUL1/AXR6 subunit of SCF ubiquitin-ligases. *The Plant Journal* 43: 371–383

Raschke A, Ibañez C, Ullrich KK, Anwer MU, Becker S, Glöckner A, Trenner J, Denk K, Saal B, Sun X, *et al* (2015) Natural variants of ELF3 affect thermomorphogenesis by transcriptionally modulating PIF4-dependent auxin response genes. *BMC Plant Biology* 15: 197

Reed JW, Nagatani A, Elich TD, Matthew Fagan & Chory J (1994) Phytochrome a and Phytochrome B Have Overlapping but Distinct Functions in Arabidopsis Development. *Plant Physiology* 104: 1139–1149

Rockwell NC, Su Y-S & Lagarias JC (2006) PHYTOCHROME STRUCTURE AND SIGNALING MECHANISMS. *Annu Rev Plant Biol* 57: 837–858

Rogers ED & Benfey PN (2015) Regulation of plant root system architecture: implications for crop advancement. *Current Opinion in Biotechnology* 32: 93–98

Saini K, Dwivedi A & Ranjan A (2022) High temperature restricts cell division and leaf size by coordination of PIF4 and TCP4 transcription factors. *Plant Physiology* 190: 2380–2397

Sauer M, Balla J, Luschnig C, Wiśniewska J, Reinöhl V, Friml J & Benková E (2006)

Canalization of auxin flow by Aux/IAA-ARF-dependent feedback regulation of PIN polarity. *Genes & development* 20: 2902–2911

Scanlon MJ (2003) The Polar Auxin Transport Inhibitor N-1-Naphthylphthalamic Acid Disrupts Leaf Initiation, KNOX Protein Regulation, and Formation of Leaf Margins in Maize. *Plant Physiology* 133: 597–605

Seiler GJ (1998) Influence of temperature on primary and lateral root growth of sunflower seedlings. *Environmental and Experimental Botany* 40: 135–146

Serivichyaswat PT, Bartusch K, Leso M, Musseau C, Iwase A, Chen Y, Sugimoto K, Quint M & Melnyk CW (2022) High temperature perception in leaves promotes vascular regeneration and graft formation in distant tissues. *Development* 149: dev200079

Shaffique S, Khan MA, Wani SH, Pande A, Imran M, Kang S-M, Rahim W, Khan SA, Bhatta D, Kwon E-H, *et al* (2022) A Review on the Role of Endophytes and Plant Growth Promoting Rhizobacteria in Mitigating Heat Stress in Plants. *Microorganisms* 10

Shen H, Zhong X, Zhao F, Wang Y, Yan B, Li Q, Chen G, Mao B, Wang J, Li Y, *et al* (2015) Overexpression of receptor-like kinase ERECTA improves thermotolerance in rice and tomato. *Nature Biotechnology* 33: 996–1003

Silk WK (1992) Steady Form from Changing Cells. *International Journal of Plant Sciences* 153: S49–S58

Silk WK & Erickson RO (1979) Kinematics of plant growth. *Journal of Theoretical Biology* 76: 481–501

Silk WK, Lord EM & Eckard KJ (1989) Growth Patterns Inferred from Anatomical Records 1: Empirical Tests Using Longisections of Roots of Zea mays L. *Plant Physiology* 90: 708–713

Sozzani R, Maggio C, Varotto S, Canova S, Bergounioux C, Albani D & Cella R (2006) Interplay between Arabidopsis Activating Factors E2Fb and E2Fa in Cell Cycle Progression and Development. *Plant Physiology* 140: 1355–1366

Spartz AK, Ren H, Park MY, Grandt KN, Lee SH, Murphy AS, Sussman MR, Overvoorde PJ & Gray WM (2014) SAUR Inhibition of PP2C-D Phosphatases Activates Plasma Membrane H+-ATPases to Promote Cell Expansion in Arabidopsis. *The Plant Cell* 26: 2129–2142

Stavang JA, Gallego-Bartolomé J, Gómez MD, Yoshida S, Asami T, Olsen JE, García-Martínez JL, Alabadí D & Blázquez MA (2009) Hormonal regulation of

temperature-induced growth in Arabidopsis. *The Plant Journal* 60: 589–601

Steffens B & Rasmussen A (2016) The Physiology of Adventitious Roots. *Plant Physiology* 170: 603–617

Stoller EW & Woolley JT (1983) The effects of light and temperature on yellow nutsedge (Cyperus esculentus) basal-bulb formation. *Weed Science* 31: 148–152

Sun J, Qi L, Li Y, Chu J & Li C (2012) PIF4–Mediated Activation of YUCCA8 Expression Integrates Temperature into the Auxin Pathway in Regulating Arabidopsis Hypocotyl Growth. *PLOS Genetics* 8: e1002594

Thuiller W, Lavorel S, Araújo MB, Sykes MT & Prentice IC (2005) Climate change threats to plant diversity in Europe. *Proceedings of the National Academy of Sciences* 102: 8245–8250

Ursache R, Andersen TG, Marhavý P & Geldner N (2018) A protocol for combining fluorescent proteins with histological stains for diverse cell wall components. *The Plant Journal* 93: 399–412

Vandepoele K, Raes J, De Veylder L, Rouzé P, Rombauts S & Inzé D (2002) Genome-Wide Analysis of Core Cell Cycle Genes in Arabidopsis. *The Plant Cell* 14: 903–916

Verkest A, Manes C-L de O, Vercruysse S, Maes S, Van Der Schueren E, Beeckman T, Genschik P, Kuiper M, Inzé D & De Veylder L (2005) The Cyclin-Dependent Kinase Inhibitor KRP2 Controls the Onset of the Endoreduplication Cycle during Arabidopsis Leaf Development through Inhibition of Mitotic CDKA;1 Kinase Complexes. *The Plant Cell* 17: 1723–1736

Wang G, Kong H, Sun Y, Zhang X, Zhang W, Altman N, dePamphilis CW & Ma H (2004) Genome-Wide Analysis of the Cyclin Family in Arabidopsis and Comparative Phylogenetic Analysis of Plant Cyclin-Like Proteins. *Plant Physiology* 135: 1084–1099

Wang R, Zhang Y, Kieffer M, Yu H, Kepinski S & Estelle M (2016) HSP90 regulates temperature-dependent seedling growth in Arabidopsis by stabilizing the auxin co-receptor F-box protein TIR1. *Nature Communications* 7: 10269

von Wangenheim D, Hauschild R, Fendrych M, Barone V, Benková E & Friml J (2017) Live tracking of moving samples in confocal microscopy for vertically grown roots. *eLife* 6: e26792

Weijers D, Schlereth A, Ehrismann JS, Schwank G, Kientz M & Jürgens G (2006) Auxin

Triggers Transient Local Signaling for Cell Specification in Arabidopsis Embryogenesis. *Developmental Cell* 10: 265–270

Weimer AK, Matos JL, Sharma N, Patell F, Murray JAH, Dewitte W & Bergmann DC (2018) Lineage- and stage-specific expressed CYCD7;1 coordinates the single symmetric division that creates stomatal guard cells. *Development* 145: dev160671

Wilson AM (1981) Air and Soil Temperature Effects on Elongation of Adventitious Roots in Blue Grama Seedlings 1. *Agronomy Journal* 73: 693–697

Wu W, Duncan RW & Ma B (2021) The stage sensitivity of short-term heat stress to lodging-resistant traits and yield determination in canola (Brassica napus L.). *Journal of Agronomy and Crop Science* 207: 74–87

Yang X, Dong G, Palaniappan K, Mi G & Baskin TI (2017) Temperature-compensated cell production rate and elongation zone length in the root of Arabidopsis thaliana. *Plant, Cell & Environment* 40: 264–276

Yin K, Ueda M, Takagi H, Kajihara T, Sugamata Aki S, Nobusawa T, Umeda-Hara C & Umeda M (2014) A dual-color marker system for in vivo visualization of cell cycle progression in Arabidopsis. *The Plant Journal* 80: 541–552

Yu H, Chen X, Hong Y-Y, Wang Y, Xu P, Ke S-D, Liu H-Y, Zhu J-K, Oliver DJ & Xiang C-B (2008) Activated Expression of an Arabidopsis HD-START Protein Confers Drought Tolerance with Improved Root System and Reduced Stomatal Density. *The Plant Cell* 20: 1134–1151

Zhang F, DASHTI N, HYNES RK & SMITH DL (1996) Plant Growth Promoting Rhizobacteria and Soybean [Glycine max (L.) Merr.] Nodulation and Nitrogen Fixation at Suboptimal Root Zone Temperatures. *Annals of Botany* 77: 453–460

Zhang F, DASHTI N, HYNES RK & SMITH DL (1997) Plant Growth-promoting Rhizobacteria and Soybean [Glycine max(L.) Merr.] Growth and Physiology at Suboptimal Root Zone Temperatures. *Annals of Botany* 79: 243–249

Zhao Y (2012) Auxin Biosynthesis: A Simple Two-Step Pathway Converts Tryptophan to Indole-3-Acetic Acid in Plants. *Molecular Plant* 5: 334–338

Zhu J, Zhang K-X, Wang W-S, Gong W, Liu W-C, Chen H-G, Xu H-H & Lu Y-T (2015) Low Temperature Inhibits Root Growth by Reducing Auxin Accumulation via ARR1/12. *Plant and Cell Physiology* 56: 727–736

Zhu Z, Esche F, Babben S, Trenner J, Serfling A, Pillen K, Maurer A & Quint M (2022)

An exotic allele of barley EARLY FLOWERING 3 contributes to developmental plasticity at elevated temperatures. *Journal of Experimental Botany*: erac470

Acknowledgements

The reason I came to Prof. Quint's group was the recommendation of my former supervisor Prof. Xu Mingliang (徐明良) from China Agricultural University, both were colleagues at Hohenheim University in the late 1990s. Therefore, first and foremost, I would like to express my deep gratitude to Professor Dr. Xu Mingliang and Professor Dr. Marcel Quint who gave me the opportunity to start my PhD journey. I would like to thank my thesis supervisor Professor Dr. Marcel Quint again, for his invaluable guidance, encouragement and patient support throughout the entire research process. His always insightful feedback and expert knowledge have been crucial in shaping this work.

I would also like to acknowledge the support of Dr. Carolin Delker, Dr. Lennart Eschen Lippold and Dr. Steve Babben, who have provided valuable insights, encouragement, and assistance throughout this journey. I would like to thank the former PhD student Julia Bellstaedt who initiated this project, and to Kai Bartusch for his incredible help in micrografting experiments. I would like to thank Professor Dr. Bettina Hause, Professor Dr. Alain Tissier, Dr. Gerd Balcke, and Dr. Tonni Grube Andersen for the great collaboration in our root thermomorphogenesis project.

I would also like to extend my appreciation to the members of our lab, Kathrin Denk, Jana Trenner, Annette Pahlich, Matthias Reimers, Philipp Janitza, Rebecca Lippmann, Alexander Sandmann, Zihao Zhu and Xin Li for their support and the many stimulating conversations and debates, and for the shared moments of frustration and joy.

I am also grateful for the financial support provided by Chinese Scholarship Council and Deutsche Forschungsgemeinschaft, which has allowed me to undertake this research.

Finally, I would like to thank my family for their unconditional love and unwavering support throughout my academic journey.

Thank you all.

Curriculum Vitae

Personal data

Name Haiyue Ai
Date of birth 25th May 1994
Place of birth Hunan, China
Nationality Chinese
E-mail cauaihaiyue@gmail.com
Tel. +49 (0) 1523 5864533

Education

Since Oct 2019 **PhD student in Plant Physiology**
Martin-Luther-University Halle-Wittenberg, Halle, Germany

Sep 2017 – Sep 2019 **M.Sc. in Agronomy**
China Agricultural University, Beijing, China

Sep 2013 – Sep 2017 **B.Sc. in Agronomy**
Guang Xi University, Nanning, China

List of publications

Ai H, Bellstaedt J, Bartusch KS, Eschen Lippold L, Babben S, Balcke GU, Tissier A, Hause B, Andersen TG, Delker C, et al (2023) Auxin dependent regulation of cell division rates governs root thermomorphogenesis. *The EMBO Journal* 42: e111926.

van Zanten M, **Ai H**, Quint M (2021) Plant thermotropism: an underexplored thermal engagement and avoidance strategy. *Journal of Experimental Botany* 72:7414–7420.

Declaration under Oath

Eidesstattliche Erklärung / Declaration under Oath

Ich erkläre an Eides statt, dass ich die Arbeit selbstständig und ohne fremde Hilfe verfasst, keine anderen als die von mir angegebenen Quellen und Hilfsmittel benutzt und die den benutzten Werken wörtlich oder inhaltlich entnommenen Stellen als solche kenntlich gemacht habe.

I declare under penalty of perjury that this thesis is my own work entirely and has been written without any help from other people. I used only the sources mentioned and included all the citations correctly both in word or content.

_____   _____

Datum / *Date*   Unterschrift des Antragstellers / *Signature of the applicant*